CREWES in 2016

It is a pleasure and a privilege to be able to welcome you to the 2016 CREWES Annual Sponsor's Meeting. We are very much aware that you being here means significant expenditures of time and effort on your part, not just in travel and in the time you spend here, but in making business cases internally to support us. So let me start off with a huge thank-you!

I hope you will find, after seeing our students and researchers discuss their work in the coming days, in both the formal and the informal parts of the meeting, that the investment has been worthwhile. I believe you will. CREWES students and researchers are dedicated, curious, imaginative, and technically highly skilled, and when people like that are supported to work together, remarkable things tend to happen. And remarkable things are happening! In this era of geophysical research, when we as a community are learning how to do practical FWI, quantitative interpretation, and wave-theoretic processing, all on data coming from new types of sensor/acquisition technology, being at a focal point of all four, which we are at CREWES, is tremendously exciting. No week has gone by in 2016 without a student coming in to show me a new first. So, you can understand my pride in being able to showcase these firsts here at our meeting.

It has been a year of changes, starting with Gary's retirement at the end of last year. Fortunately it was not goodbye! Gary has been able to collaborate actively with CREWES in 2016, and he will be rolling out some completely new software in our short courses after the meeting. And we are extremely pleased and excited to welcome Daniel Trad to CREWES as of this past July. Daniel takes on an associate professorship in the Department of Geoscience, as well as the Chair in Exploration Geophysics, and having him join us as an Associate Director of CREWES is wonderful indeed. Daniel's research interests in computation, processing and interpolation, and least-squares migration are powerful complements to our existing research plan, especially in the context of his vision of the bridge between academia and industry.

I became director of this long-standing research group this past January, and many people have asked me how I feel about having "taken the helm" during such challenging times. I certainly see their point: rarely has the scrutiny of investment in geophysics and exploration and monitoring technology been higher. My answer? Indeed – times are very tough… but I relish the opportunity to show the amazing results that make a convincing case for investment in geophysical research. I think I speak for everyone in CREWES when I say that. And given the ideas and new technologies that are exploding in our field right now, with CREWES as a major focal point, I wouldn't trade this start time for any other.

So, welcome! I hope you enjoy the meeting, and that you take lots from it, and perhaps leave us with some feedback and ideas from you as well. And thank you again for the support.

Calgary, Alberta	Kristopher Innanen
November, 2016	CREWES Director

Table of Contents

* Presenter

2016 CREWES Sponsors

Acceleware	BHP Billiton Petroleum (Deepwater) Inc.
CGG	Chevron Corporation
Devon Energy Corporation	Halliburton
INOVA Geophysical	Nexen Energy ULC
Petrobras	Petronas Carigali SDN BHD
Repsol Oil & Gas Canada Inc.	Sinopec
Suncor Energy Inc.	Tullow Oil p.l.c.

Natural Sciences and Engineering Research Council of Canada (NSERC) - Collaborative Research and Development Grant

CREWES Personnel

LEADERSHIP

Kristopher A. Innanen, Director
Associate Professor, Department of Geoscience, University of Calgary

B.Sc. Physics and Earth Science, 1996, York University
M.Sc. Physics, 1998, York University
Ph.D. Geophysics, 2003, University of British Columbia

- Work Experience: University of Houston

Don C. Lawton, Associate Director
Professor, Department of Geoscience, University of Calgary

B.Sc. (Hons. Class I) Geology, 1973, University of Auckland
Ph.D. Geophysics, 1979, University of Auckland

- Work Experience: New Zealand Steel Mining Ltd., Amoco Minerals (N.Z.) Ltd., Carbon Management Canada

Daniel Trad, Associate Director
Associate Professor, Department of Geoscience, University of Calgary

Licenciatura in Geophysics, 1994, Universidad Nacional de San Juan, Argentina
Ph.D Geophysics, 2001, University of British Columbia

- Work Experience: Electromagnetic Methods (Argentina and Brazil), Seismic Research and development (Veritas, CGG, Techco, in Calgary and France).

Gary F. Margrave, Emeritus Director
Emeritus Professor, Faculty Professor, Department of Geoscience, University of Calgary

B.Sc. Physics, 1975, University of Utah
M.Sc. Physics, 1977, University of Utah
Ph.D. Geophysics, 1981, University of Alberta

- Work Experience: Chevron Canada Resources, Chevron Geoscience Company, Devon Canada

Laura A. Baird, Program Manager

BA, History, 1992, University of Calgary

- Work Experience: Alberta Cancer Board, Department of Geoscience at the University of Calgary

Kevin W. Hall, Technical Manager

B.Sc. Geophysics, 1992, University of Calgary
M.Sc. Geophysics, 1996, University of Calgary

- Work Experience: Lithoprobe Seismic Processing Facility at the University of Calgary

ADJUNCT DIRECTOR

Laurence R. Lines
Professor and Interim Head, Department of Geoscience, University of Calgary

B.Sc. Physics, 1971, University of Alberta
M.Sc. Geophysics, 1973, University of Alberta
Ph.D. Geophysics, 1976, University of B.C.

- Work Experience: Amoco Production Research, Tulsa University, Memorial University of Newfoundland

RESEARCH STAFF, POST DOCS and VISITING SCHOLARS

Kevin L. Bertram

Electronics Technician Certificate, 2005, Southern Alberta Institute of Technology

- Work Experience: Aram Systems Ltd.

Malcolm B. Bertram

B.Sc. Geology, Auckland, New Zealand

- Work Experience: GSI (Western Australia), Western Geophysics (Western Australia), Auckland University, University of Calgary.

Huaizhen Chen

B.Sc., Geophysics, 2010, China University of Petroleum
Ph.D., Geophysics, 2015, China University of Petroleum

Patrick F. Daley

B.Sc. Mathematics, 1974, University of Alberta
M.Sc. Physics 1976, University of Alberta
Ph.D. Geophysics, 1979, University of Alberta

- Work Experience: Independent contractor associated with research centres of major oil companies

Yu Geng

B.Sc. Information Engineering, 2005, Xi'an Jiaotong University
Ph.D. Information and Communication System, 2014, Xi'an Jiaotong University

- Work Experience: MILAB, IGPP, Department of Earth and Planetary Sciences, University of California, Santa Cruz

David C. Henley

B.Sc. Physics, 1967, Colorado State University
M.Sc. Physics, 1968, University of Michigan

- Work Experience: Shell Oil Co., Shell Canada Ltd

Helen Isaac

B.Sc. Mathematics, 1973, Imperial College, London
M.Sc. Geophysics, 1974, Imperial College, London
Ph.D. Geophysics, 1996, University of Calgary

- Work Experience: Phillips Petroleum Company, Hudson's Bay Oil and Gas, Canterra Energy, Husky, Fold-Fault Research Project at the University of Calgary

Marie Macquet

B.Sc. Earth Science, 2009, University of Nantes (France)
M.Sc. Planetology, 2011, University of Nantes (France)
Ph.D. Geophysics, 2014, Isterre, University of Grenoble (France)

Joe Wong

B.Sc. Physics/Mathematics, 1971, Queen's University
M.Sc. Applied Geophysics, 1973, University of Toronto
Ph.D. Applied Geophysics, 1979, University of Toronto

- Work Experience: Ontario Ministry of the Environment, University of Toronto, JODEX Applied Geoscience Limited

Huixing Zhang

B.Sc. Geophysics, 1997, China University of Mining and Technology (Xuzhou)
B.Ma. Management Engineering (International Trade), 1999, China University of Mining and Technology (Xuzhou)
Ph. D Geophysics, 2004, China University of Mining and Technology (Beijing)

- Work experience: Ocean University of China

ASSOCIATED FACULTY and SCIENTISTS

Andreas Cordsen
Technical Advisor, CREWES, University of Calgary

M.Sc. Geology, 1975, Queen's University, Kingston
M.Sc. Geophysics, 1980, Dalhousie University, Halifax

- Work Experience: BEB, Esso Resources, Norcen Energy, GEDCO, Schlumberger

Sam Gray
Technical Advisor, CREWES, University of Calgary

B.S. Math, 1970, Georgetown University
Ph.D., Math, 1978, University of Denver

- Work experience: U.S. Naval Research Lab, General Motors Institute, Amoco, BP, Veritas, CGG

Hassan Khaniani

B.Sc. Petroleum Exploration Engineering, 2002, Petroleum University of Technology (PUT)-Iran
M.Sc. Petroleum Exploration Engineering, 2006, University of Calgary / PUT
Ph.D. Geophysics, 2015, University of Calgary

- Work Experience: National Iranian Oil Co. (NIOC), Nexen, Suncor Energy, Reservoir Waveform Solution Ltd (RWS)

Michael P. Lamoureux
Professor, Department of Mathematics and Statistics, University of Calgary
Adjunct Professor, Department of Geoscience, University of Calgary

B.Sc. Mathematics, 1982, University of Alberta
M.Sc. Mathematics, 1983, Stanford University
Ph.D. Mathematics, 1988, University of California, Berkeley

- Work Experience: Farallon Computing, NSERC Canada

Roy O. Lindseth MC., FRSC
Technical Advisor, CREWES, University of Calgary

Doctor of Laws, Honoris Causa, 1978, University of Calgary

- Work Experience: Chevron; NSERC, Teknica Corporation; TCPL

Faranak Mahmoudian
Technical Advisor, CREWES, University of Calgary

B.Sc., Applied Physics, 2000, K. N. Toosi University of Technology, Iran
M.Sc., Geophysics, 2006, University of Calgary
Ph.D., Geophysics, 2013, University of Calgary

- Work Experience: Shell Canada

Claude Ribordy
Technical Advisor, CREWES, University of Calgary

Dipl. Physics, 1960, Eidgenossische Technische Hochschule ETH, Zurich
Ph. D. Nuclear Physics, University of Fribourg

- Work Experience: Aquitaine Canada, Petro-Canada, BP, Hampson-Russell Software Ltd, CGG

Brian H. Russell
Adjunct Professor, Department of Geoscience, University of Calgary

B.Sc. Physics, 1972, University of Saskatchewan
Honours Certificate in Geophysics, 1975, University of Saskatchewan
M.Sc. Geophysics, 1978, University of Durham
Ph.D. Geophysics, 2004, University of Calgary

- Work Experience: Chevron Geoscience Company, Teknica Resource Development, Veritas Software Ltd., Hampson-Russell Software Ltd.

Robert R. Stewart
Cullen Chair in Exploration Geophysics, University of Houston
Adjunct Professor, Department of Geoscience, University of Calgary

B.Sc. Physics and Mathematics, 1978, University of Toronto
Ph.D. Geophysics, 1983, Massachusetts Institute of Technology

- Work Experience: Veritas Software Ltd., Gennix Technology Corp., University of Calgary

Xiucheng Wei
Technical Advisor, CREWES, University of Calgary

B.Sc. Geophysics, 1982, China University of Petroleum
M.Sc. Geophysics, 1992, China University of Petroleum
Ph.D. Geophysics, 1995, China University of Petroleum

- Work Experience: China National Petroleum Company (CNPC), China University of Petroleum (CUP), British Geological Survey (BGS), China Petroleum & Chemical Corporation (Sinopec), International Research Coordinator with the Faculty of Science at the University of Calgary

Matt Yedlin
Associate Professor, Department of Electrical and Computer Engineering, University of British Columbia

B.Sc. Honors Physics, 1971, University of Alberta
M.Sc. Physiology, 1973, University of Toronto
Ph.D. Geophysics, 1978, University of British Columbia

- Work Experience: Conoco

GRADUATE STUDENTS

Winnie Ajiduah

B.Sc. Physics, University of Benin, Nigeria
M.Sc. Geophysics, University of Port Harcourt, Nigeria

- Work Experience: Shell Petroleum Development Company of Nigeria

Khaled Al Dulaijan

B.Sc. Geosciences, 2003, University of Tulsa, Oklahoma
M.Sc. Geophysics, 2008, University of Calgary

- Work Experience: Saudi Aramco

Khalid Almuteri

B.Sc. Geophysics, 2012, University of Houston

- Work Experience: Saudi Aramco

Tim Cary

BA in Physics University of Oxford 2012
BSc in Geophysics with distinction, University of Calgary 2016

- Work experience: Imperial Oil

Raúl Cova

B.Sc. Geophysical Engineering, 2004. Simon Bolivar University, Venezuela.
Graduate Diploma in Petroleum Studies, 2011. IFP School. Venezuela

- Work experience: PDVSA Intevep. Venezuela, Shell Canada

Matt Eaid

BSc. (First Class Honours) Geophysics, University of Calgary, 2015

- Work experience: Shell Canada Ltd.

Dennis Ellison

BSc Geophysics, 2013, University of Calgary.

- Work experience: Thrust Belt Imaging

Ali Fathalian

B.Sc. Applied Physics, 2001, University of Razi, Iran
M.Sc. Condensed Matter Physics, 2003, University of Razi, Iran
Ph.D. Condensed Matter Physics, 2007, University of Razi, Iran

Adriana Gordon

B.Sc. Geophysics 2015, Simon Bolivar University, Venezuela

Marcelo Guarido de Andrade

B.Sc. Physics, 2006, University of São Paulo, Brazil
M.Sc. Geophysics, 2008, University of São Paulo, Brazil

- Work Experience: Orthogonal Geophysics, Husky Energy

Saul Guevara

B.Eng. Civil Engineering, 1984, National University of Colombia
M.Sc. Geophysics, 2001, University of Calgary

- Work Experience: Ecopetrol ICP

Bobby Gunning

B.Sc. Geophysics (first class honours), 2014, University of Calgary

- Work Experience: MEG Energy, Devon Energy, Canadian Natural Resources Limited

Heather Hardeman

B.Sc. Mathematics (summa cum laude), 2012, University of Montevallo, AL, USA.
M.A. Mathematics, 2014, Wake Forest University, NC, USA.

- Work Experience: Fotech Solutions

Nadine Igonin

B.Sc. Geophysics (first class honours), 2016, University of Calgary

- Work Experience: Microseismic Industry Consortium at the University of Calgary

Andy Iverson

B.Sc. Geophysics (First Class Honours), 2012, University of Calgary

- Work Experience: Apache Canada Ltd

Scott Keating

B.Sc. Honours Physics 2014, University of Alberta

Oliver Lahr

B.Sc. Pure and Applied Mathematics, 1988, University of Calgary

- Work Experience: Hampson-Russell Software Ltd.

Bernie Law

B.Sc. Geological Engineering (Geophysics), 1982, University of Saskatchewan

- Work Experience: Key Seismic Solutions Ltd.

Junxiao Li

B.Sc. Science of Information and Computing (Geophysics), 2009, China University of Petroleum (Beijing)
Bachelor of Arts. English, 2009, China University of Petroleum (Beijing)
M.Sc. Geophysics, 2012, China University of Petroleum (Beijing)

Siming (Emma) Lv

B.Sc. Geophysics, 2015, China University of Petroleum (East China)

Andrew Mills

BSc Geophysics, 2014, University of Calgary

- Work experience: Nexen Energy

Michelle Montano

B.Sc. Geophysics 2008, Simon Bolivar University, Venezuela

- Work experience: PDVSA Sismica Bielovenezolana, Daqing de Venezuela

Shahpoor Moradi

B.Sc. Applied Physics, 2000, University of Razi, Iran
M.Sc. Theoretical Physics, 2002, University of Razi, Iran
Ph.D. Theoretical Physics, 2006, University of Razi, Iran

Evan Mutual

B. Sc Geophysics, 2015, University of Calgary

- Work experience: Qeye Labs

Davood Nowroozi

B.Sc. Mining engineering, University of Tehran, 1996
M.Sc. Mining engineering, University of Tehran, 1999

- Work Experience: Geophysicist at National Iranian Oil Company

Wenyong Pan

B.Sc. Computer and Software Engineering, 2009, China University of Geosciences (Beijing)
M.Sc. Geophysics, 2012, China University of Geosciences (Beijing)

Sergio Jorge Romahn Reynoso

B. Eng. Geophysics, 2004, National University of Mexico
M.Sc. Exploration Geophysics, 2012, University of Leeds. U.K.

- Work Experience: PEMEX

Eric Rops

B.Sc. Honors Geophysics, 2014, The University of Western Ontario

- Work experience: Sander Geophysics Ltd., Husky Energy, Nexen-CNOOC, Chevron

Tyler Spackman

BSc Geophysics 2014, University of Calgary

- Work Experience: Tourmaline Oil Corp., Husky Energy, Shell Canada

Jian Sun

B.Sc. Geophysics, 2009, Shandong University of Science and Technology, China
M.Sc. Geophysics, 2012, Shandong University of Science and Technology, China

Todor Todorov

B.Sc. Applied Geophysics, 1996, University of Mining and Geology, Bulgaria
M.Sc. Geophysics, 2002, University of Calgary

- Work Experience: Petro-Canada / SUNCOR Energy

Ron Weir

B.Sc. Geophysics, 1978, University of Alberta

- Work Experience: Harvest Operations Corp/KNOC

Kiki Xu

M.Sc. Computer Science, 2008, University of Calgary

- Work experience: Hampson-Russell Software Ltd.

Student Theses

The following theses are included with the CREWES 2016 Research Report:

M.Sc.	Rafael Asuaje	Sensitivity of interval Vp/Vs analysis of seismic data
M.Sc.	Tianci Cui	Improving Seismic-to-well Ties
M.Sc.	Jessica Marie Dongas	Development and Characterization of a Geostatic Model for Monitoring Shallow CO2 Injection
M.Sc.	Sina Esmaeili	Influence of Low Frequencies on Seismic Impedance Inversion
Ph.D.	Shahin Jabbari	A Theoretical Framework for Seismic Time-lapse Difference AVO Analysis with Validation on Physical Modelling and Field Data
Ph.D.	Shahin Moradi	Time-Lapse Numerical Modeling for a Carbon Capture and Storage (CCS) Project in Alberta, Using a Poroelastic Velocity-Stress Staggered-Grid Finite-Difference Method
M.Sc.	Bona Wu	A Multicomponent Walkaway Vertical Seismic Profile Experiment in a Heavy Oil Reservoir

Azimuthal anisotropy in elastic and equivalent media

Sitamai W. Ajiduah*, Gary F. Margrave and P. F. Daley

ABSTRACT

A seismic numerical modeling experiment has been conducted to acquire a wide azimuth 3D-3C seismic data from an isotropic heterogeneous elastic model and an anisotropic homogeneous equivalent model in order to verify the suitability of these two modeling approaches for anisotropic studies. This study focuses on reflection amplitude and traveltime comparison of the two models. Although, geophysicists often prefer to use anisotropic homogeneous equivalent models for various seismic modeling and imaging tasks, there are however some benefits of heterogeneous models over anisotropic homogeneous equivalent models. We show that the anisotropic equivalent modeling predicts strong interbed multiples and multimodes which are much weaker in the heterogeneous elastic model. This is because a heterogeneous medium will cause irregular scattering of the multiple and multimode events, thus diminishing these events. Both modeling results reveals AVAZ signatures which shows more significant azimuthal variations in the elastic model than in the equivalent model because of the strong multimode conversions which tend to obscure primary reflections at far offsets.

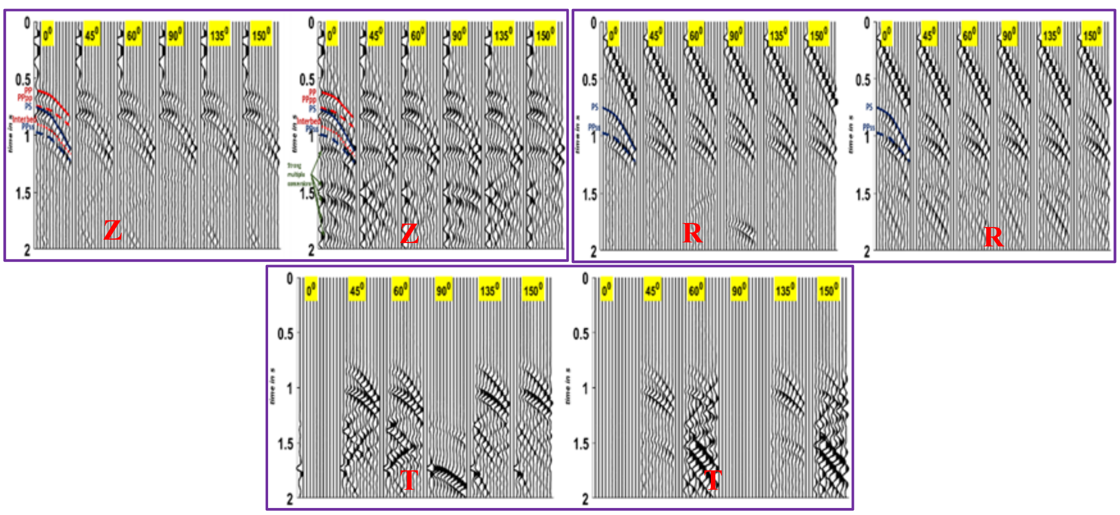

FIG. 1. Z, R and T seismogram of isotropic heterogeneous elastic model (left) and homogenous equivalent model (right).

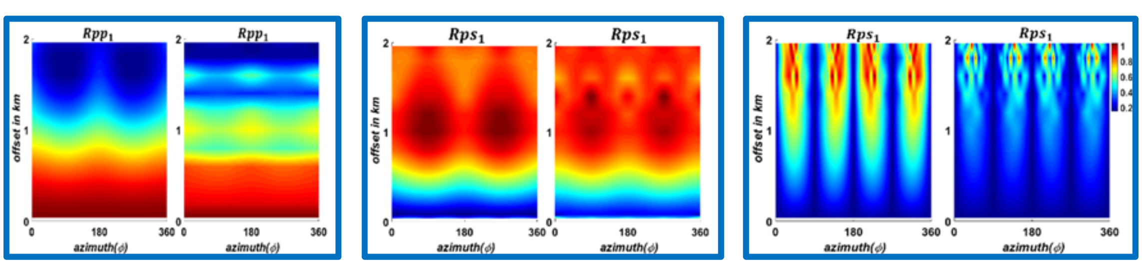

FIG. 2a. PP refl. from HTI top, elastic (left), equivalent. (right)

FIG. 2b. PS -Radial refl. from HTI top, elastic (left), equivalent. (right)

FIG. 2c. PS-Transverse refl. from HTI top, elastic (left), equivalent. (right)

Interval VVAZ analysis of 3D pre-stack seismic data in Altamont-Bluebell field

Khaled Al Dulaijan*, and Gary F. Margrave

ABSTRACT

The 3D seismic data was acquired within Bluebell Field, the eastern portion of Altamont-Bluebell field in northeastern Utah. Altamont-Bluebell field is within the Uinta Basin, and is considered an unconventional reservoir in the sense that natural fractures act as fluid storage and conduits in the tight sandstones and carbonates. Information related to fracture orientation and intensity is vital for the development of such reservoirs. Therefore, this paper utilizes Velocity Variations with Azimuth (VVAZ) to estimate the direction and intensity of fractured-induced anisotropy within the three main reservoirs.

VVAZ inversion method is applied based on the non-hyperbolic NMO equation for TI media that was derived by Grechka and Tsvankin (1998). Our code has been tested on a 3D physical modeling dataset and results are shown in another report. Isotropic NMO velocities are used along with azimuthally variant time residuals to estimate fast and slow NMO velocities and their direction. Dix-type interval properties are calculated to estimate interval anisotropy for each reservoir interval.

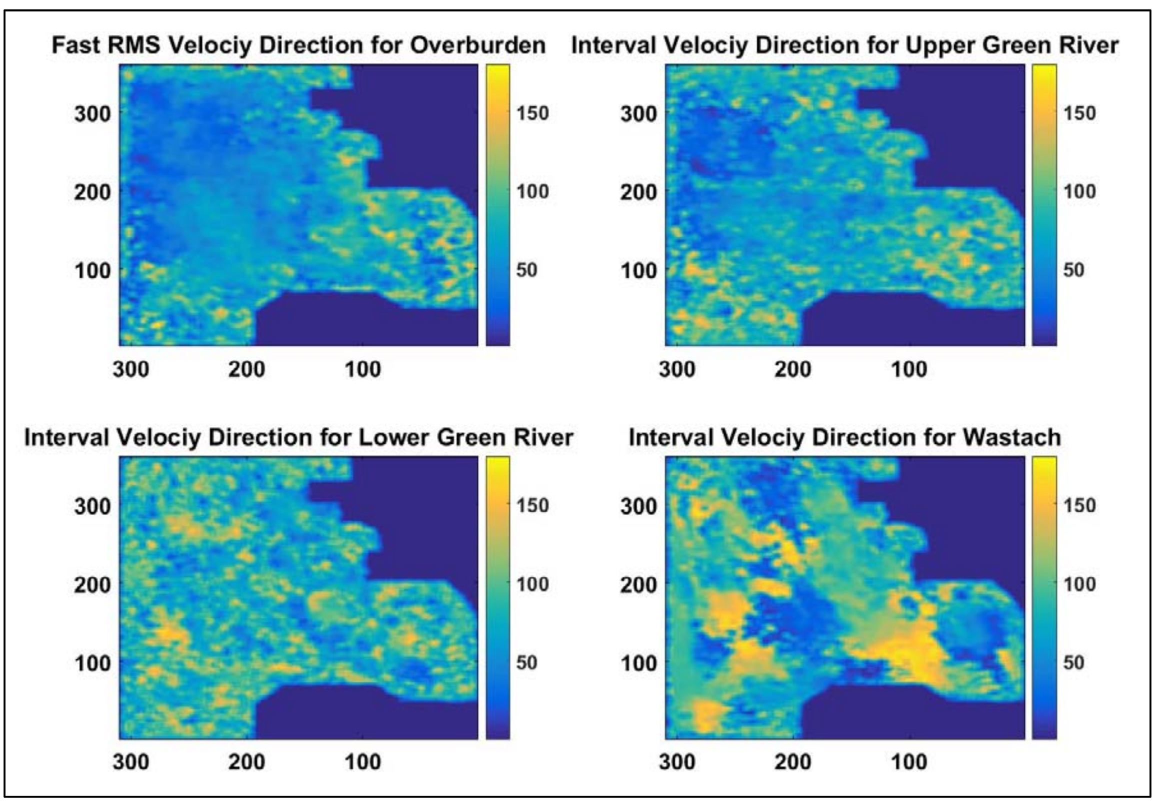

FIG. 1. VVAZ Results: Velocity Anisotropy Direction for overburden and the three main reservoirs.

S-wave splitting analysis of 4-C VSP in Altamont-Bluebell field

Khaled Al Dulaijan, and Gary F. Margrave

ABSTRACT

The 4-C VSP was acquired within Bluebell Field, the eastern portion of Altamont-Bluebell field in northeastern Utah. Altamont-Bluebell field is within the Uinta Basin, and is considered an unconventional reservoir in the sense that natural fractures act as fluid storage and conduits in the tight sandstones and carbonates. Information related to fracture orientation and intensity is vital for the development of such reservoirs. S-wave splitting can be useful for fracture-induced anisotropy. Therefore, this paper utilizes S-wave splitting to estimate the direction and intensity of fractured-induced anisotropy within the three main reservoirs using 4-C VSP data.

S-wave analysis is carried using Alford (1986) 4-C rotation to separate fast and slow modes. This method assumes that the symmetry axis is vertically invariant. In order to overcome this assumption, layer stripping was applied using Winterstien and Meadows (1991).

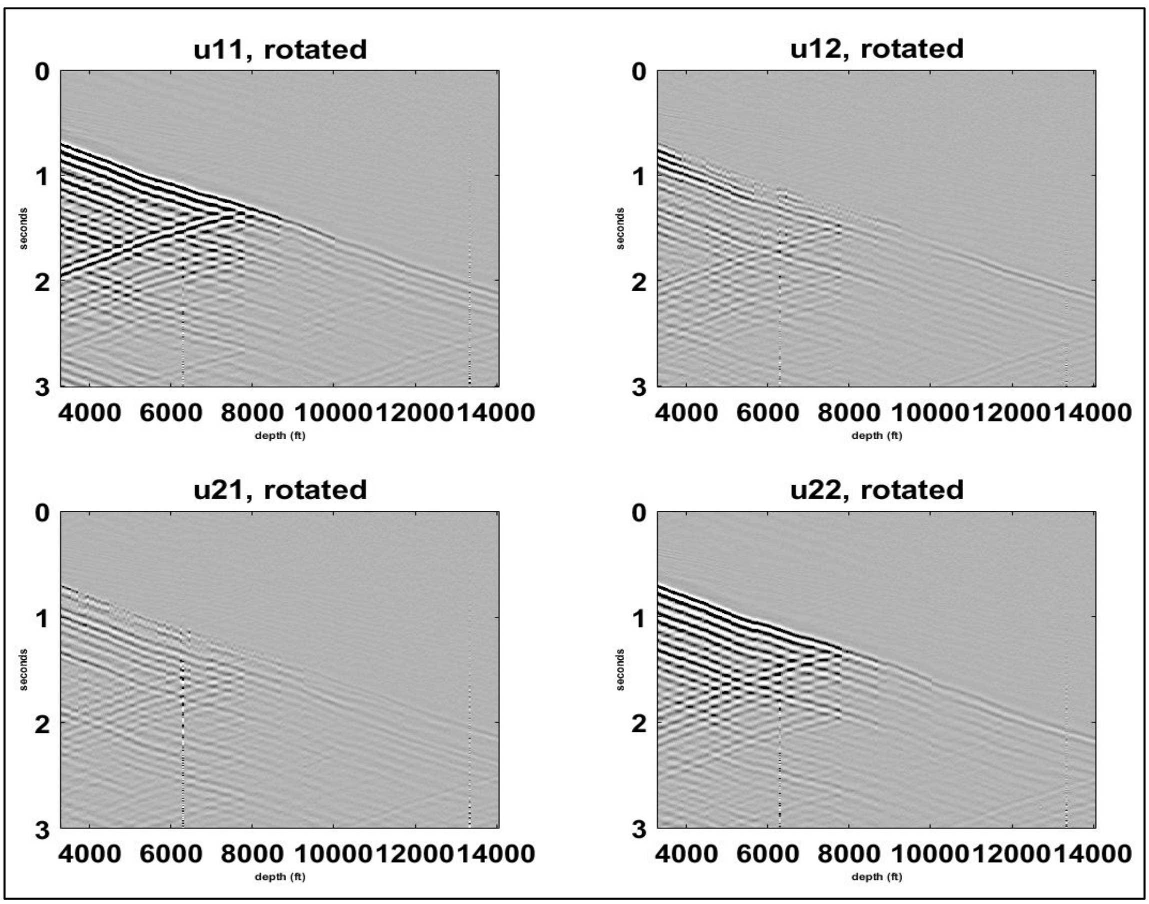

FIG. 1.VSP after 4-C rotation and layer stripping: ***u11*** (fast S-wave), ***u12***, ***u21***, and ***u22*** (slow S-wave).

VVAZ analysis of offset VSPs in Altamont-Bluebell field

Khaled Al Dulaijan, and Gary F. Margrave

ABSTRACT

The offset VSPs, used for this paper, were acquired within Bluebell Field, the eastern portion of Altamont-Bluebell field in northeastern Utah. Altamont-Bluebell field is within the Uinta Basin, and is considered an unconventional reservoir in the sense that natural fractures act as fluid storage and conduits in the tight sandstones and carbonates. Information related to fracture orientation and intensity is vital for the development of such reservoirs. Azimuthal variations of P-wave velocities can be a valuable tool for fracture information. Therefore, this paper utilizes Velocity Variations with Azimuth (VVAZ) to estimate the direction and intensity of fractured-induced anisotropy within the three main reservoirs using offset VSPs seismic data.

VVAZ inversion method is applied based on the elliptical NMO equation for TI media that was derived by Grechka and Tsvankin (1998). Here, a VVAZ workflow is developed for offset, workaround, or walkaway VSPs using a method for surface seismic. Interval anisotropy properties are calculated within each reservoir.

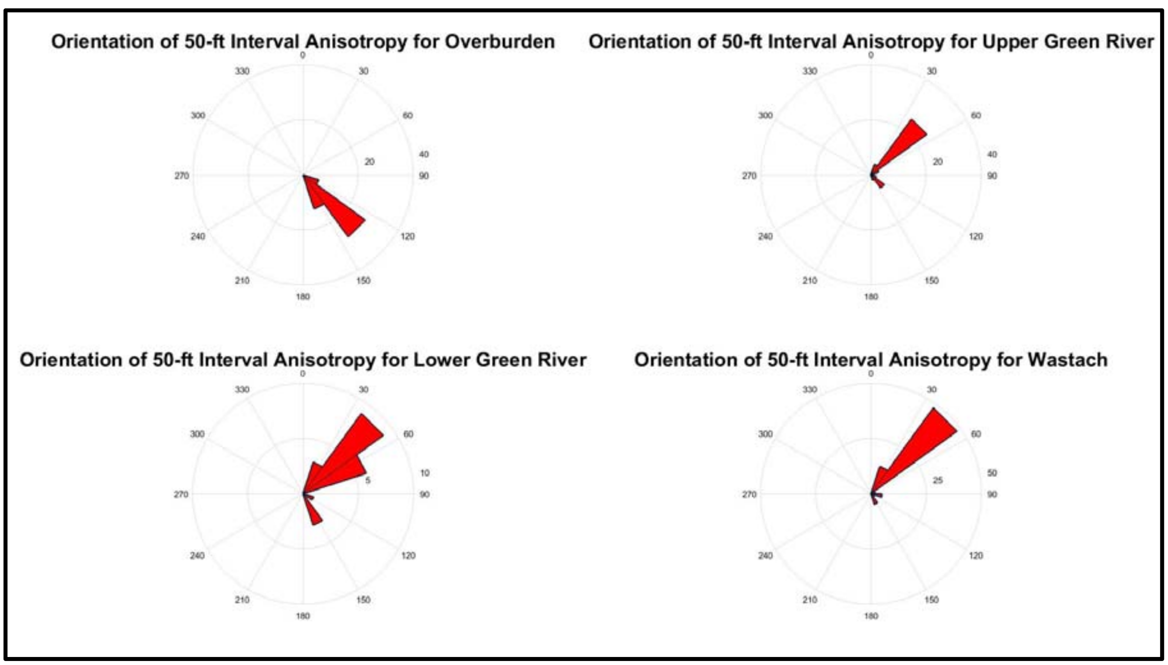

FIG. 1. Circular histogram showing the orientation of 50’ interval anisotropy of: overburden, Upper Green River, Lower Green River, and Wasatch.

Evaluating the potential of reflection-based waveform inversion

Khalid Almuteri*, Yu Geng and Kris Innanen

ABSTRACT

Full waveform inversion (FWI) is a powerful tool to build high-resolution velocity models, from recorded seismic data. However, a major issue with FWI is that it fails at reconstructing the low-wavenumber components in the absence of low-frequency information in the data. Generally, for a limited-offset acquisition geometry, deep targets are only sampled by reflected waves with narrow scattering angles, which makes such failure inevitable. In this paper, we point out the limitation of conventional FWI when applied to reflection data, and review an alternative approach to overcome this limitation. The new waveform inversion formalism relies on decomposing the subsurface model into a background part that we seek to resolve, and a reflectivity part that we assume to be known. We show that separating the decoupled velocity model into long-wavelength and short-wavelength components permit us to extract the contribution of the reflected data to the background part of the velocity model.

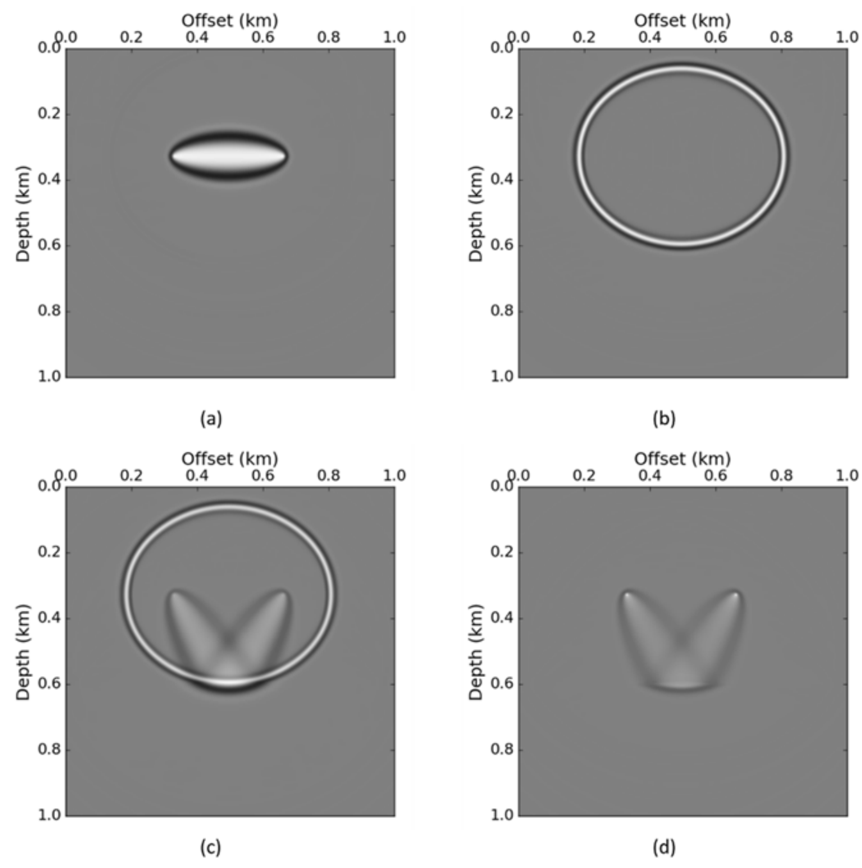

FIG. 1. FWI and RWI sensitivity kernels. (a) FWI direct wave sub-kernel. (b) Migration ellipse. This is the FWI reflected wave sub-kernel when model is smooth and does not contain reflectivity information. (c) FWI reflected wave sub-kernel. (d) RWI sensitivity kernel. We use a Ricker wavelet as a source function and the full bandwidth in generating the sensitivity kernels.

Tutorial: acoustic full waveform inversion in time domain

Khalid Almuteri and Kris Innanen

ABSTRACT

Full waveform inversion (FWI) is an optimization problem that aims at extracting the earth's physical parameters, from recorded seismic data, through an iterative inversion process. This paper reviews the concept of FWI and provides an environment where a single-parameter acoustic FWI problem can be solved in time domain. We cover the wave equation discretization, using a second-order finite difference approximation, Clayton-Engquist absorbing boundary conditions, modeling stability and grid dispersion, and we derive the gradient needed to solve this optimization problem.

Full waveform inversion (FWI) is an optimization problem that aims at extracting the earth's physical parameters, from recorded seismic data, through an iterative inversion process. This paper reviews the concept of FWI and provides an environment where a single-parameter acoustic FWI problem can be solved in time domain. We cover the wave equation discretization, using a second-order finite difference approximation, Clayton-Engquist absorbing boundary conditions, modeling stability and grid dispersion, and we derive the gradient needed to solve this optimization problem.

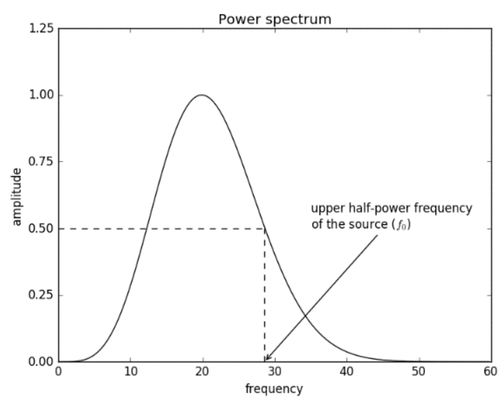

FIG. 1. Power spectrum of source wavelet [figure 3a of (Alford et al., 1974)].

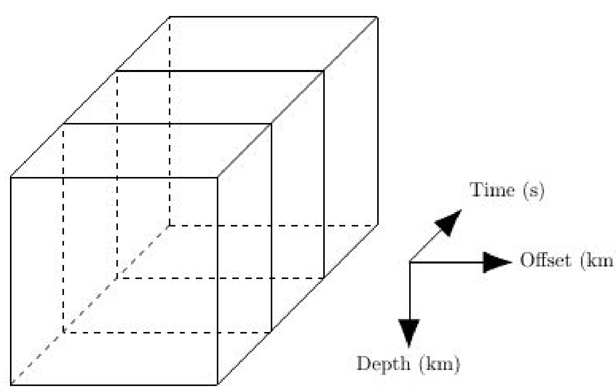

FIG. 2. Wavefield cube.

CREWES in the field 2016, a brief overview

Kevin L. Bertram, Kristopher A.H. Innanen, Don C. Lawton, Kevin W. Hall and Malcolm B. Bertram

ABSTRACT

CREWES has the distinction of being one of the very few research consortiums that has year round access to industry acquisition equipment. This allows acquisition research to be carried out by CREWES as well as giving students the opportunity to witness in field data acquisition. This benefits the students greatly in that it shows them what is possible as well as some of the limitations of data gathering.

Acquisition projects that CREWES has been a part of in 2016 include: a) two collaborative seismic projects in New Zealand; b) a seismic acquisition test at the Priddis Test Site using both downhole 3C receivers and two different types of surface 3C receivers; c) the 2016 undergraduate field school which performed a 1C 2D line near Pincher Creek, Alberta; d) a return to Priddis to use a shear wave source to record a 3C 2D surface line and downhole 3C.

FIG. 1. CREWES testing equipment and acquiring data in the field.

New wireless thumper controller

Kevin Bertram

ABSTRACT

CREWES has access to a shear wave accelerated weight drop thumper source. A mass is raised using hydraulics against pressurized nitrogen (~1000psi) and then releases it to strike an aluminum foot to generate seismic energy. This thumper has the ability to drive energy straight down or to be tilted forty five degrees to either side to generate shear waves.

The thumper control system is simplistic in that it is a set of single pole double throw switches that control the hydraulic valves. Currently the operator has to stand near the thumper, specifically near the engine, to run it. This exposes the operator to high pressure hydraulics and nitrogen as well as the heat and noise of the engine.

To make it safer and more comfortable for the operator a wireless controller for the thumper has been built. This device has a fairly large range but is expected to only be used a few metres from the thumper. With cold weather in mind, this is designed to be used from within the vehicle that is towing the thumper.

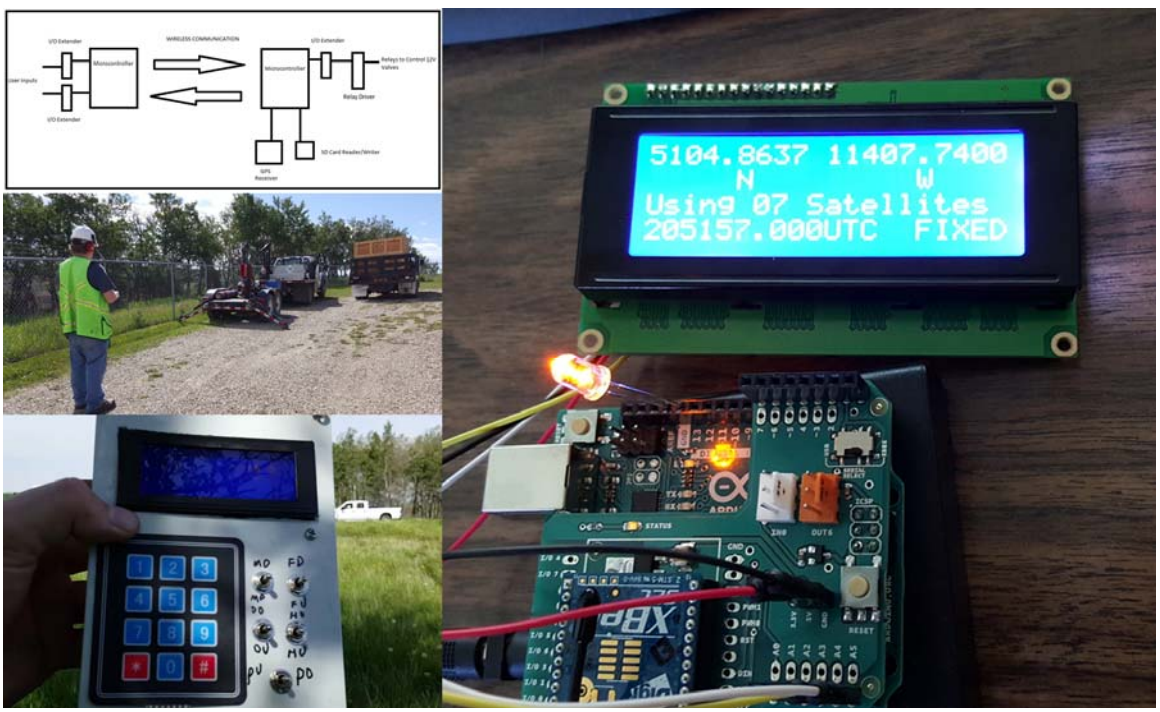

FIG. 1. From the drawing board to the proof of concept.

Priddis experiment

Kevin L. Bertram, J. Helen Isaac, Kevin W. Hall and Malcolm B. Bertram

ABSTRACT

A 3C seismic experiment was conducted at the Priddis test site in June of 2016. 3C geophones down test hole Number One were used for recording along with surface receivers. Two receiver lines (Lines 1 and 3) were laid out with one towards the North and one towards the East with a receiver spacing of five metres. A grid of nodal seismic receivers was laid out between the two lines. All nodal receivers had a spacing of twenty metres.

Several source lines were used with this experiment. Two lines coincided with the two receiver lines that were laid out to the North and East from the test hole while a third was shot in between these two, all with a spacing of five metres. There were also three source lines laid out in a quarter circle between receiver lines one and three with radii of ten metres, twenty metres and thirty metres.

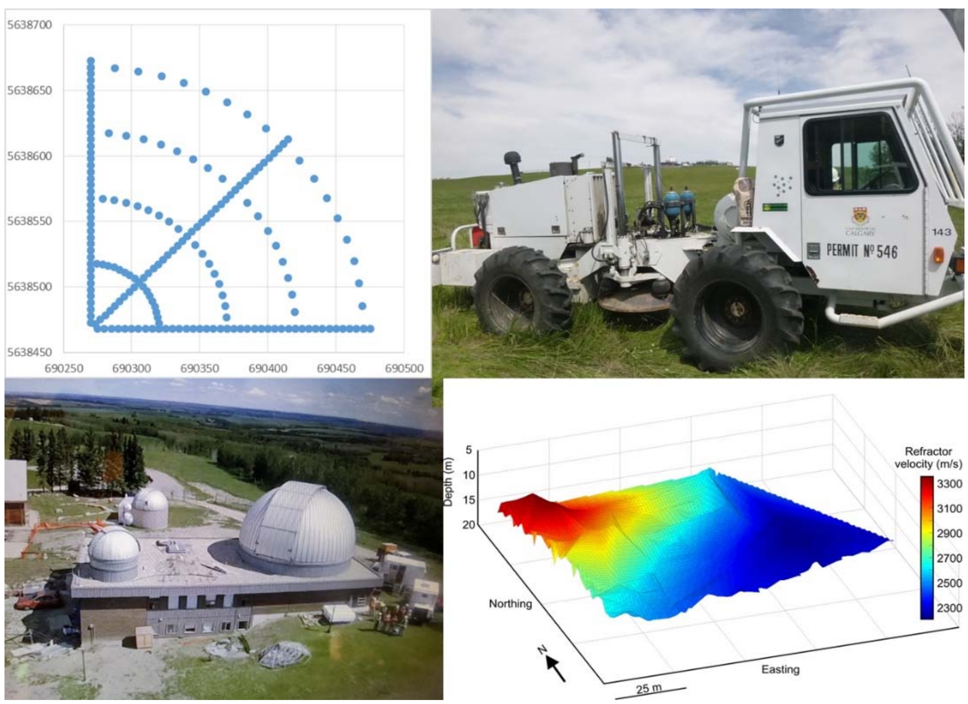

FIG. 1. Acquisition and results from the Priddis Test Site.

Azimuthal elastic impedance inversion for fluid term and fracture weakness

Huaizhen Chen*, Kristopher Innanen, Yuxin Ji (SINOPEC), Xiucheng Wei

ABSTRACT

Fracture weaknesses and fluid factor are important parameters to identify the location of underground fractures and the type of fluids. In this report, we demonstrate a direct method to estimate Lamé constants and fracture weaknesses of the dry fractured rock, and fluid term from partially incident-angle-stack seismic data, based on azimuthal elastic impedance (EI). We first derive a linearized PP- wave reflection coefficient for the case of an interface separating two horizontal transverse isotropic (HTI) media, which can isolate the effects of fractures and fluids. Using the derived reflection coefficient, we propose the expression of azimuthal EI. Estimation of fluid term and fracture weaknesses is implemented as a two-step inversion, which includes inversion of partially-incident-stack seismic data for EI at different azimuths, and the estimation of fluid term and fracture weaknesses from the inverted results of azimuthal EI using a Bayesian Markov- chain Monte Carlo (MCMC) method. Tests on synthetic and real data can confirm the stability of the proposed inversion method.

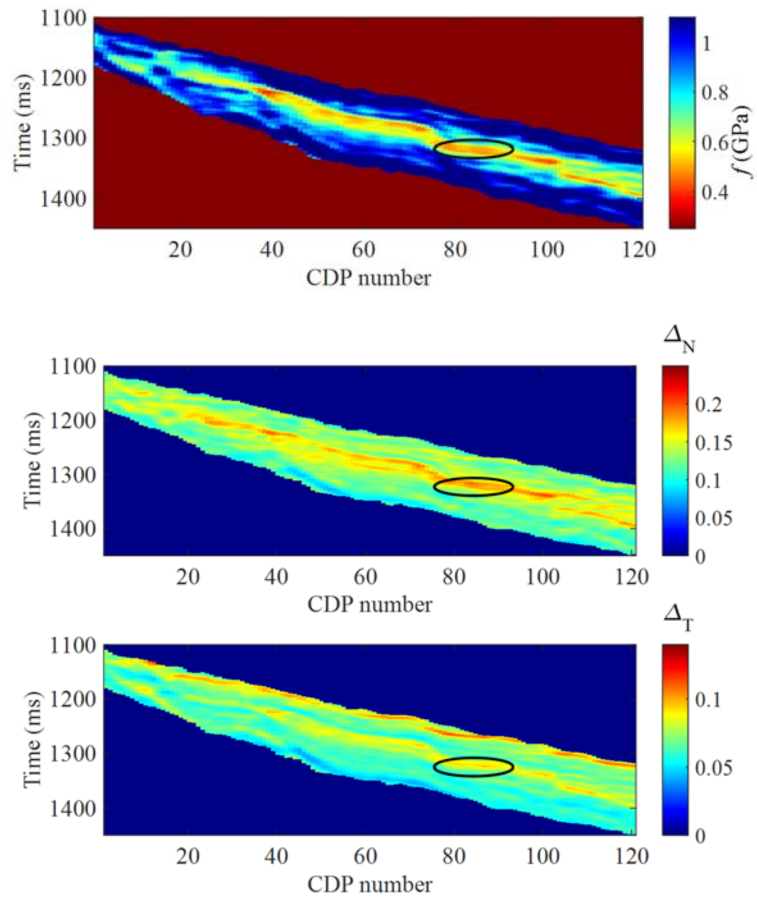

FIG. 1: Inversion results of fluid term and fracture weaknesses

Joint inversion of PP- wave and PSV- wave data for P- wave and S- wave inverse quality factors at different frequencies — Synthetic test

Huaizhen Chen, Kristopher Innanen, Yuxin Ji (SINOPEC), Xiucheng Wei

ABSTRACT

In this report, we demonstrate a method to estimate P-wave and S-wave velocities, density, and inverse quality factors from PP- wave and PSV- wave seismic data at different frequencies. We first employ the extension of Mavko- Jizba squirt relations for all frequencies to calculate P- wave and S- wave velocities and quality factors to find how the velocity and quality factor change with frequency in seismic frequency range, and then we derive the approximate expressions of PP- wave and PSV- wave reflection coefficients in terms of P-wave and S-wave impedances, density, and inversion quality factors to discuss how the real and imaginary parts of PP-wave and PSV- wave reflection coefficients vary with frequency and the angle of incidence. Base on the derived approximate reflection coefficients, we propose a method to use seismic data to predict elastic properties (P- wave and S- wave impedances, and density) and inverse quality factors. Singular value decomposition (SVD) algorithm is used to solve the inversion problem, and initial models are utilized to constraint the inversion. We illustrate the inversion method with synthetic data, and we also test the robustness of the inversion method.

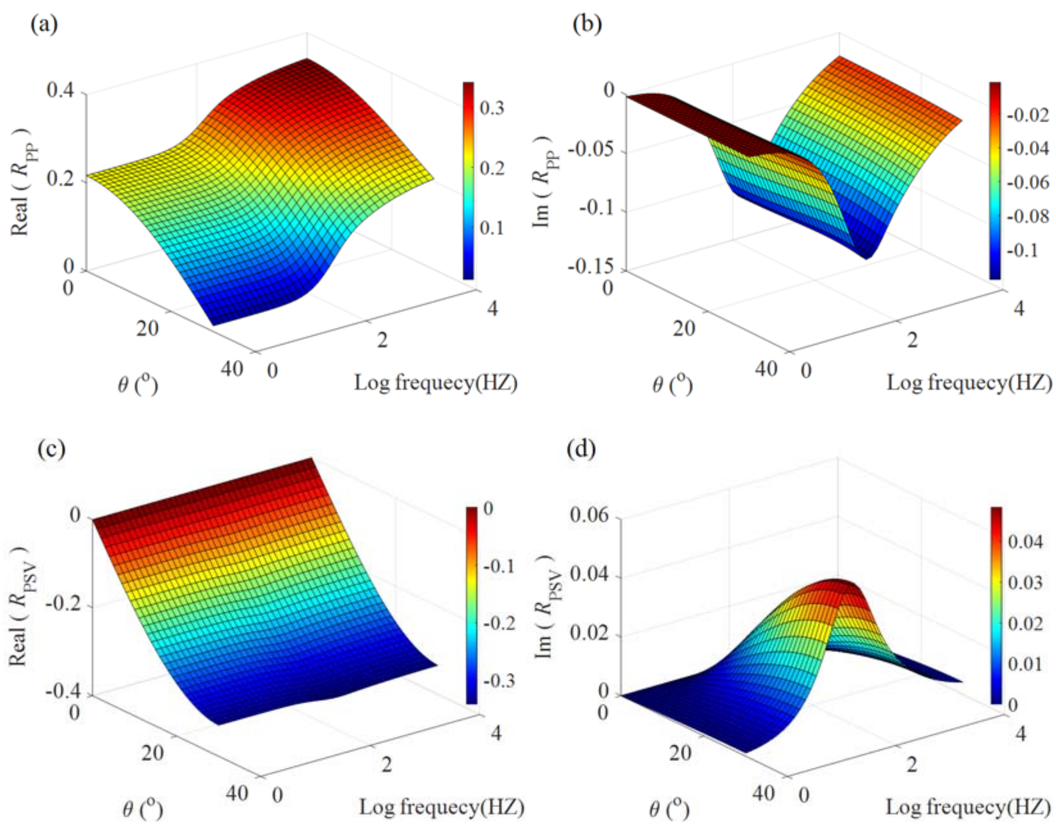

FIG. 1. Complex PP- wave and PSV- wave reflection coefficients

Multiantenna GPR data acquisition design

Raul Cova*, Mathew Yedlin[1], Dave Henley, Jean-Yves Dauvignac[2], Nicolas Fortino[2], Kevin Hall, Christian Pichot and Stéphane Gaffet[3]

ABSTRACT

Detailed characterization of shallow sediments requires the use of very high frequency signals able to resolve fine changes in rock properties. For this reason Ground Penetrating Radar (GPR) has been chosen by the Matter-wave laser Interferometric Gravitation Antenna (MIGA) project to provide the information needed to apply near-surface corrections. Given the similitude of the physics of electromagnetic waves and seismic waves we used seismic modelling software to simulate GPR signals. The goal was to study two acquisition setups designed for the data acquisition. The original setup consisted of eight GPR transceivers, five of them spaced at 0.2m and the rest at 1m, for a maximum offset of 3.8m. This setup, despite providing a regular offset sampling was not able to provide the data needed for accurate velocity picking. For the second design the separation between the first and second group of transceivers was increased from 1m to 4m to provide a maximum offset of 6.8m. This setup provided better data for velocity picking, especially for deep events. However, under this configuration not all offsets could be sampled. The time images obtained confirm that a depth migration is needed to properly map the dip of the interfaces, especially in areas with significant lateral velocity changes. Performance of depth migration and inversion algorithms on the modelled GPR data remains to be explored.

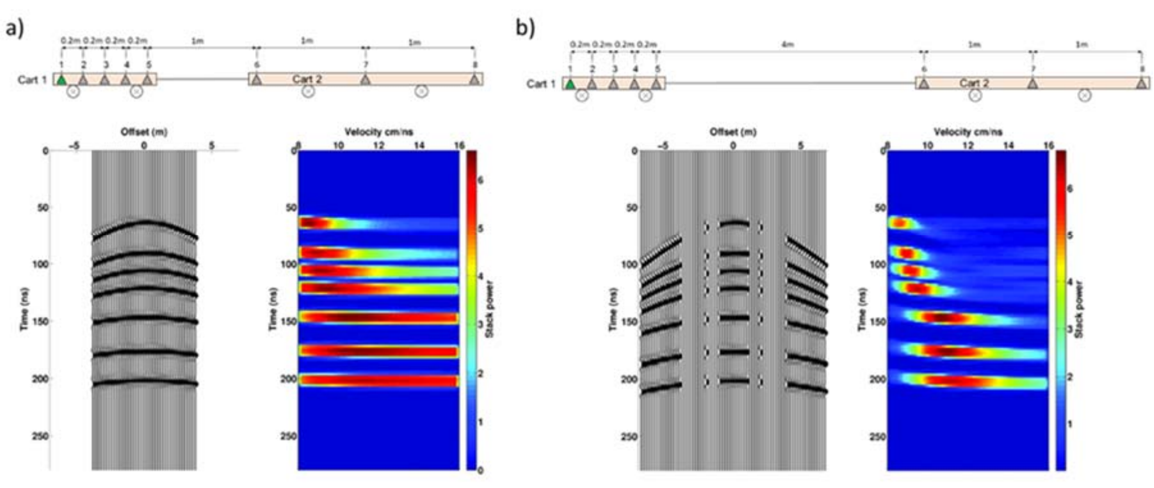

FIG. 1. a) Original and b) extended multiantenna acquisition setups. The original setup provides regular offset sampling but the data is not suitable for accurate velocity picking. The extended setup provides better velocity definition at the expense of an irregular offset sampling.

[1] Department of Electrical and Computer Engineering, University of British Columbia
[2] Laboratoire d'Electronique, Antennes et Télécommunications (LEAT), Université Nice-Sophia Antipolis
[3] Low Background Noise Inter-disciplinary Underground Science and Technology, LSBB Underground Research Laboratory

PS-wave traveltime difference inversion for S-wave near-surface characterization in the tau-p domain

Raul Cova* and Kris Innanen

ABSTRACT

In the processing of P-wave data one important product of computing static corrections is a P-wave near-surface velocity model. This model is usually inverted from the traveltimes of the refracted waves. In the case of converted-wave data, for which S-wave near-surface corrections must be used on the receiver locations, refracted S-waves are usually not available or hard to identify. Here, we propose an inversion approach based on the τ differences obtained by crosscorrelating τ-p receiver gathers from different locations. For this, the structure of the near-surface at a given location must be know. Then, the τ-p receiver gathers are crosscorrelated with the gather obtained at the reference location, and the time lag of the maximum of the crosscorrelation function is picked. These picks along with an initial guess of the depth of the near-surface layer, its S-wave velocity, local dip and velocity of the medium underneath (replacement velocity) are the input to initialize the inversion. An iterative quasi-Newton inversion approach is used in this study. Different data conditions are used to study the robustness of the inversion. Results show that the inversion of the depth of the near-surface layer is very sensitive to the presence of noise in the picks and the lack of large rayparameter values (p>0.5ms/m). Although to a lesser degree, inverted velocities were also affected by these conditions. However, inverted dips displayed very stable results under different data conditions. Alternative inversion approaches able to exploit the robustness of the inverted dips must be considered to improve the results provided in this study.

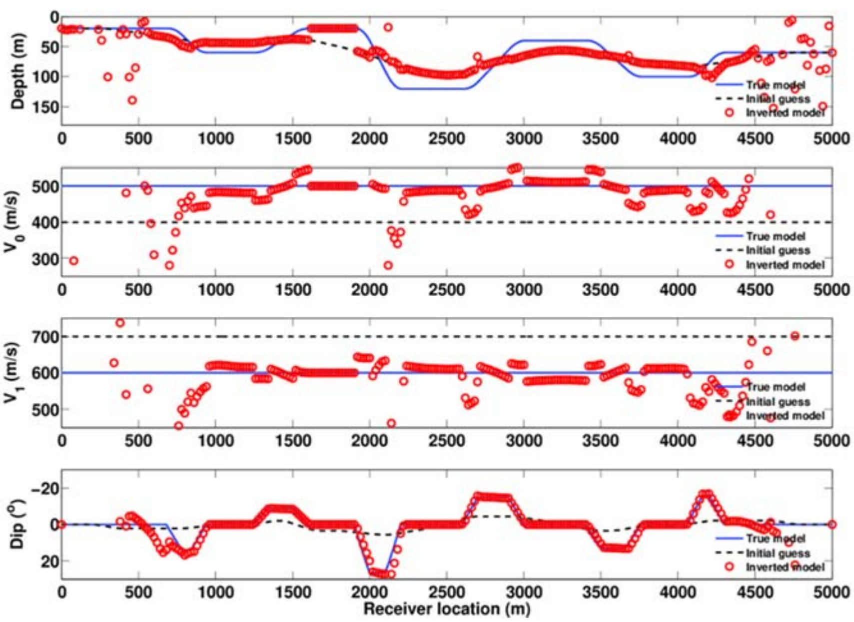

FIG. 1. Inversion results after processing raytraced PS-data. Inverted velocities are slightly unstable but around the true values in the model. In contrast, depth results seem strongly constrained by the initial velocity values. Inverted dips successfully recovered the true dips in the model and showed stable results.

Comments on the paper of Clayton and Engquist (1977) – absorbing boundary conditions

P.F. Daley and E.S. Krebes

ABSTRACT

The paper by Clayton and Engquist (1977) is often quoted in the literature, almost exclusively when problems involving finite difference methods are being discussed when dealing with acoustic wave propagation and coupled P-S_V wave propagation in an elastic medium using finite differences or related methods. With the recent interest in perfectly matched layers (PML) methods it is often used as a bench mark with which to determine the numerical accuracy of this relatively new method (for example, Zhu and McMechan, 1991). This attention is for the most part based on one page of the 1977 paper. There are some cursory instructions on how to proceed to obtain paraxial approximations for the wave equations in the vicinity of finite, usually perfectly reflecting, boundaries and how to employ them. As the single page is followed by an appendix for its implementation, little thought has been paid to what has been said on that page. Here we would like to expand on that page for the information of others who wish to use this method for similar, usually more complex, problems and for its possible use in hybrid methods, where one or more of the spatial derivatives have been removed by integral transform methods. As others have questioned the authors on this topic, it was thought that this mild tutorial could be useful.

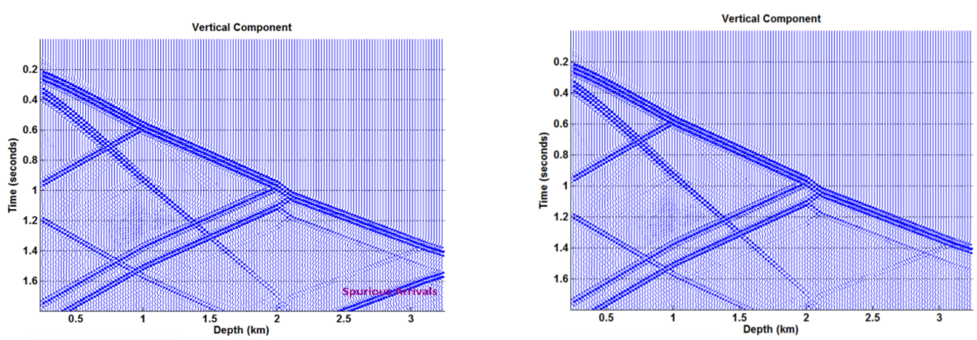

FIG. 1. The vertical component of the VSP synthetic of the model used here. In the upper panel the *spurious reflections* from the model bottom are present. In the lower panel these have been removed using the method described here.

REFERENCES

Clayton, R. and Engquist, B., 1977, Absorbing boundary conditions for acoustic and elastic wave equations, Bulletin of the Seismological Society of America, 67, 1529-1540.

Zhu, X. and McMechan, G.A., 1991. Finite-difference modeling of the seismic response of fluid saturated, porous, elastic media using Biot theory. Geophysics, 56, 424-435.

Higher order approximate expressions for qP, qS_1 and qS_2 phase velocities in a weakly anisotropic orthorhombic medium

P.F. Daley and E.S. Krebes

ABSTRACT

Higher order linearized approximations of the phase velocities for the quasi – compressional (qP) and two quasi – shear wave types, qS_1 and qS_2, in a *weakly anisotropic* orthorhombic medium are presented. Some manipulation of the formulae obtained by standard linearization techniques is done so that the phase velocities are in the form consisting of the most degenerate cases of phase velocities (ellipsoids) in an orthorhombic medium plus correction terms to compensate for the deviation from the degenerate orthorhombic case. This is analogous to the ellipsoidal case in a transversely isotropic medium. The quantities in the formulae for the phase velocities all have physical interpretations, that is, they can all be associated with some physically realizable quantity. Further, obtaining the related approximations for group velocities of the three wave propagation types is considerably simplified.

PP and PS reflection and transmission coefficients in anelastic media: the anomalous case

P.F. Daley and E.S. Krebes

ABSTRACT

Using the derivation of reflection and transmission coefficients at the interface between two elastic given in Aki and Richards (1980) as a starting point, modified coefficients may be obtained for the case of two anelastic media in welded contact at a similar (plane) boundary. The anelastic equivalents of two elastic velocity distributions are considered for $P-$wave incidence on the plane boundary separating the two medium. Figures showing the plots of amplitude and phase of the four coefficients P_1P_1, P_1P_2, P_1S_1 and P_1S_2 are produced with the results from the elastic case included in all of the plots

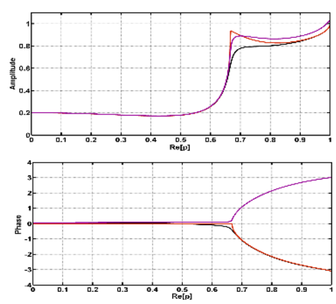

FIG.1. P_1P_1 reflection coefficient for P – wave incidence from the upper medium onto the plane interface separating the upper and lower media. Amplitude and phase of the generally complex valued reflection coefficient are plotted versus the real part of the horizontal slowness vector $(0 \le \mathrm{Re}[p_1] \le 1/\alpha_1)$.**(Red indicates reference elastic case.) (Purple indicates the anomalous case before corrections.)**

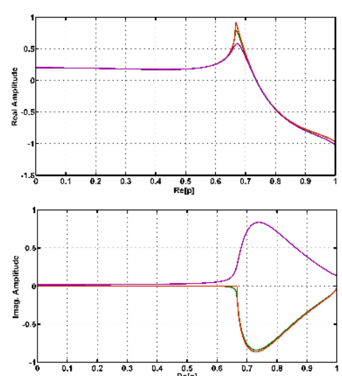

FIG. 2. ***P_1P_1*** reflection coefficient for P – wave incidence from the upper medium onto the plane interface separating the upper and lower media. **Real and imaginary** parts of the generally complex valued reflection coefficient are plotted versus the real part of the horizontal slowness vector $(0 \le \mathrm{Re}[p_1] \le 1/\alpha_1)$. **(Red indicates reference elastic case.) (Purple indicates the anomalous case before corrections.)**

REFERENCES

Aki, K. and Richards, P.G., 1980. Quantitative Seismology, Freeman, San Francisco, CA.

P-S_V wave propagation in a radially symmetric vertically inhomogeneous TI medium with absorbing boundary conditions

P.F. Daley and E.S. Krebes

ABSTRACT

Finite integral transforms, which are a specific subset of pseudo – spectral methods are used to reduce the spatial dimensionality of the coupled $qP-qS_V$ wave propagation problem in a transversely isotropic (TI) medium to that in one spatial dimension, usually depth, and time. The introduction of an absorbing boundaries, at least at the model bottom is useful in the removal of spurious arrivals. The top model boundary is usually wanted in the numerical calculations and reflections from the model sides may be removed by a judicious choice of model parameters, which does not significantly increase the run time.

In this paper, a method based on that presented in Clayton and Engquist (1977) and is employed for the coupled $P-S_V$ wave propagation problem in a transversely isotropic medium at the model bottom. The medium considered here is assumed to be radially symmetric and finite Hankel transforms are used to remove the radial coordinate (r). The problem that remains is a coupled problem in depth (z) and time (t). The anisotropic parameters may arbitrarily vary with depth.

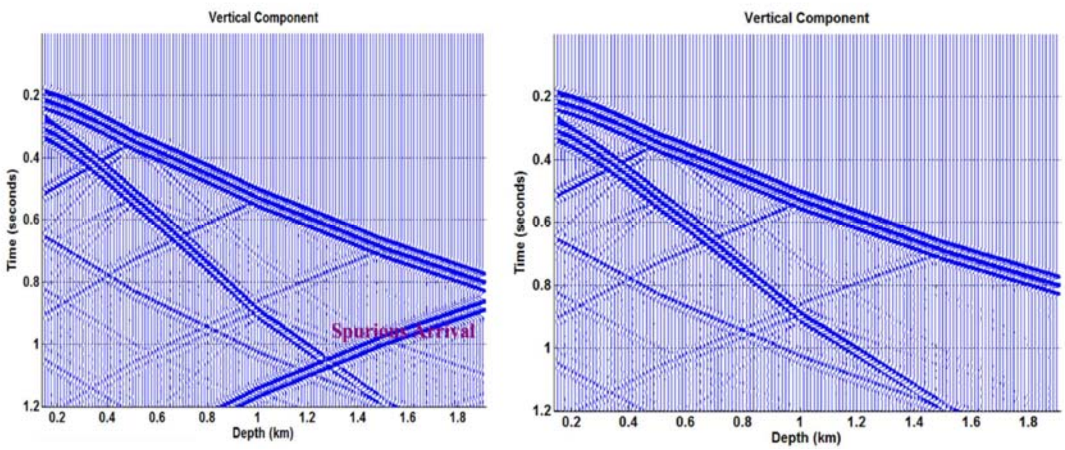

FIG. 1. The vertical component of the *VSP* synthetic of the transversely isotropic (*TI*) model used here. In the upper panel the *spurious reflections* from the model bottom are present. In the lower panel these have been removed using the method described here.

REFERENCE

Clayton, R. and Engquist, B., 1977, Absorbing boundary conditions for acoustic and elastic wave equations, Bulletin of the Seismological Society of America, 67, 1529-1540.

1.5D internal multiple prediction in the wavenumber-time domain with implementation in Python

Matthew Eaid and Kris Innanen

ABSTRACT

Most seismic interpretation and processing algorithms treat primaries as signal and multiples as noise. Multiple reflections are separated into two major categories. Multiples which have at least one down going reflection at the earth's surface are called surface related internal multiples. Multiple reflections where all downward reflections are contained to the subsurface are referred to as internal multiples. While the prediction and subsequent removal of surface related internal multiples is a fairly well understood problem, the prediction of internal multiples is not. Historically internal multiples have been predicted by exploiting assumptions about the multiples that the primaries do not obey. However, when these assumptions are not met by the internal multiples the prediction algorithms fail to properly predict the internal multiples. Weglein et al., (1997) proposed a fully data driven, wave equation method of predicting internal multiples based on the inverse scattering series. The algorithm derived by Weglein et. al, performs the prediction in the frequency-wavenumber domain, and then converts the prediction back to the offset-time domain. In recent years The CREWES project has adapted the original algorithm into many different domains in order to investigate the optimal domain in which to predict internal multiples; one such domain is the wavenumber time domain. We will present the wavenumber-time algorithm, provide pseudocode examples of how to implement it in the Python programming language, and will show a synthetic prediction example.

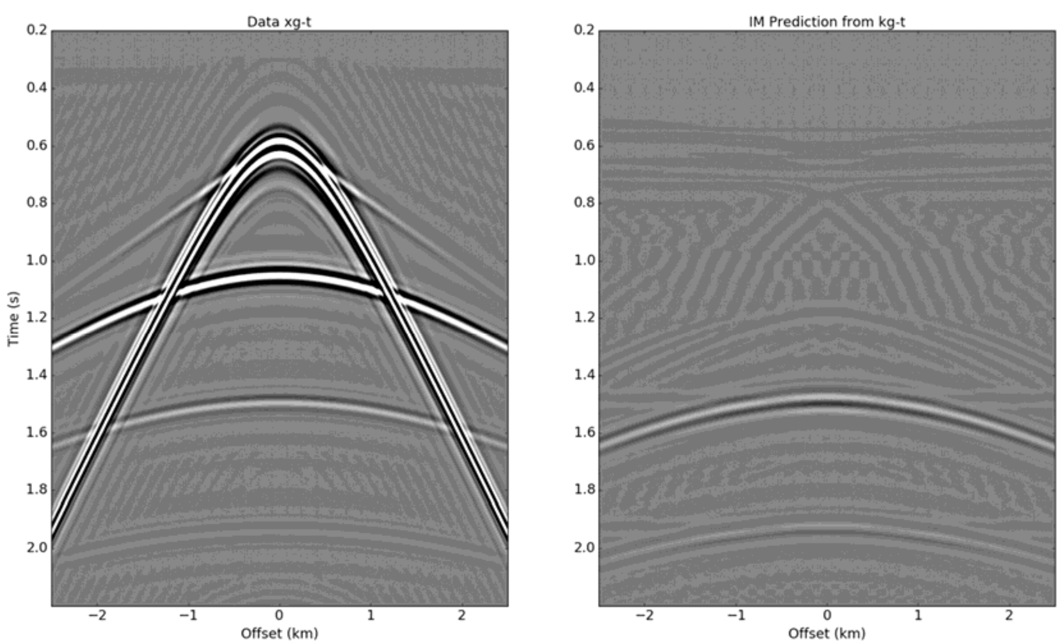

FIG. 1. Data (left), and the resulting internal multiple prediction (right).

1D and 1.5D internal multiple prediction in MatLab

Matthew Eaid, Jian Sun, Scott Keating, and Kris Innanen

ABSTRACT

An inverse scattering series approach to internal multiple prediction was developed by Weglein et al. in the late 1990's. Their method exploited the idea that all multiples can be constructed from a combination of primary events and other multiples, in a fully data driven manner (Weglein et al., 1997). Innanen (2015) presented the mathematics behind the inverse scattering series approach in the time domain. Sun and Innanen (2014) show the prediction algorithm in the planewave domain, while Pan and Innanen (2013) explore the prediction in the frequency-wavenumber domain. This paper is meant as a companion to the 2016 CREWES MatLab toolbox release, it will summarize the key ideas behind an inverse scattering series approach to internal multiple prediction in each domain listed above. The implementation of each algorithm will be reviewed and synthetic examples will be provided. Adaptive subtraction is also reviewed with synthetic examples.

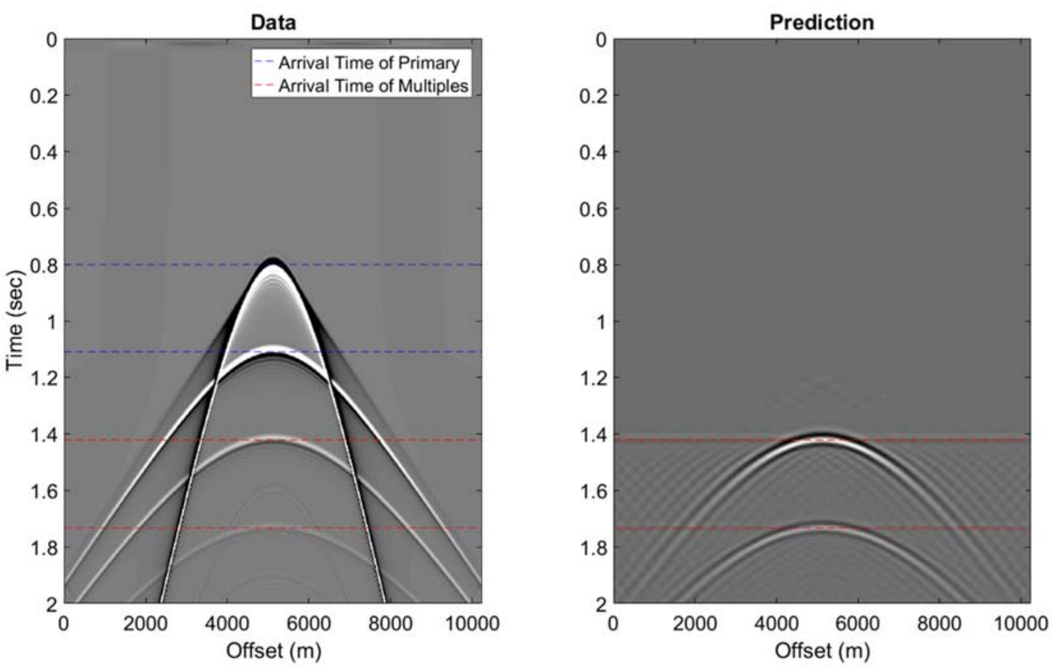

FIG. 1. Input data (left), the result of the prediction (right). The blue dashed lines indicate the zero offset travel time of the two primary events. The red dashed lines indicate the zero offset travel time of a first order internal multiple, and a second order internal multiple.

Time domain internal multiple prediction on synthetic, and field VSP data

Matthew Eaid and Kris Innanen

ABSTRACT

Surface seismic methods represent the only technology capable of large scale 3D characterization of conventional and unconventional oil and gas reservoirs, monitoring of enhanced oil recovery, and water and CO2 injection. When seismic energy is injected into the earth, and the earth response recorded, two main type of events are seen, primaries and multiples. Primary energy arises from waves that have reflected once and returned to the surface to be recorded; multiples arise from waves that reflect more than once. Most seismic interpretation and processing workflows treat primary events as signal and multiples as undesirable noise. It is for this reason that the prediction and subsequent removal of multiple energy has become a popular research topic.

Multiple energy is classified into two main types, surface related or free surface multiples, and internal multiples. Free surface multiples are multiples in which at least one of the downward reflections occurs at the free surface of the earth. Internal multiples are multiples in which all downward reflections are restricted to the subsurface. Many successful schemes have been investigated to accurately predict and remove free surface multiples. The same cannot be said for internal multiples, although some important strides have been made in recent years. Weglein et al. (1997) proposed a wave equation based method of internal multiple prediction that is fully data driven, based on the inverse scattering series. The algorithm proposed by Weglein et al. was originally derived in the frequency-wavenumber domain. This paper reviews the time domain algorithm proposed by Innanen (2015) and then applies it to both synthetic and land zero offset VSP datasets. We also introduce a method of improving our predictions by converting the VSP data into zero offset sections.

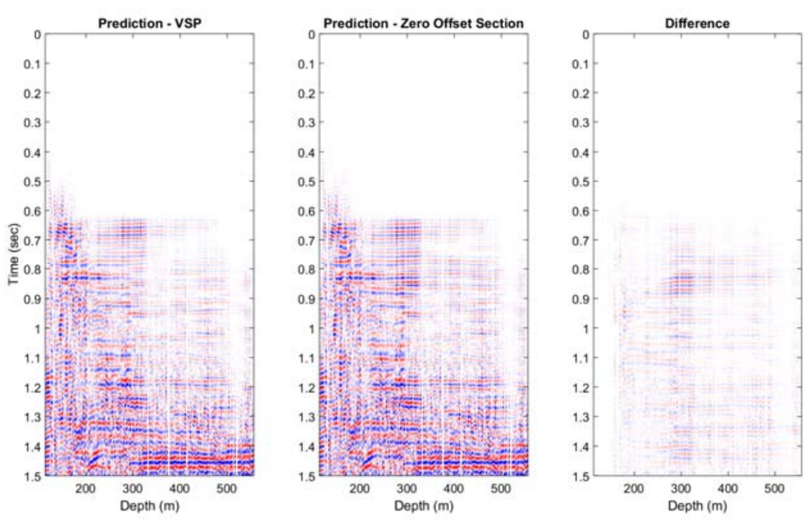

FIG. 1. Internal multiple prediction from VSP (left), zero offset section (middle), and the difference section (right).

Improved resolution in depth imaging through reflection static corrections derived from model-based moveout

Dennis K. Ellison*, Kris Innanen

ABSTRACT

When seismic data are used to image the subsurface, assumptions (Figure 1a) and calculations are made about the near-surface to overcome the uncertainty of the velocities of the low velocity layer.

Reflection statics are calculated because often the lack of detailed near-surface information leads to inaccuracies. A normal moveout (NMO) velocity field is picked and applied to stack the data in preparation for the reflection statics calculations. NMO is a correction based on the assumption that the moveout can be approximated by a hyperbola (Figure 1c). However, the accuracy of this assumption is valid when the moveout on data is near-hyperbolic, and deviates when the moveout is more complicated due to complex geology (Figure 1d). Scenarios of non-hyperbolic moveout are when high velocities are near the surface and when there are variations in the seismic weathering thickness and velocities (Figure 1b).

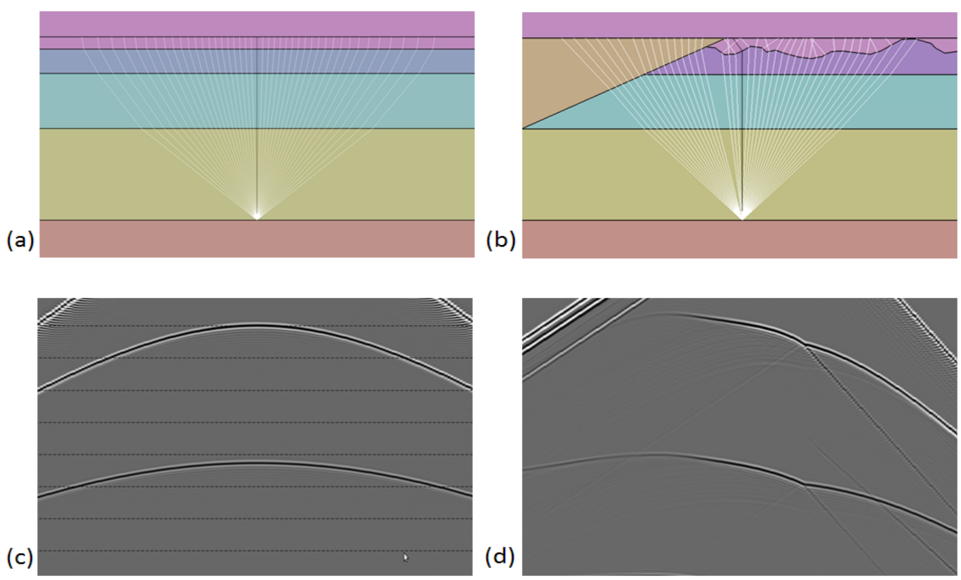

FIG. 1. Ray fan showing (a) near-vertical rays at the near-surface when velocities are slower in the near surface and when seismic weathering is flat and geology is horizontally homogeneous, (b) non-vertical rays in the near-surface when velocities are faster than the layer below and when seismic weathering is complicated. (c) The expected hyperbolic moveout for flat geology, (d) moveout that deviates from the hyperbolic assumption given a complex geology.

Raytracing in depth migration has overcome many of the issues with the assumptions in time migration. Foothills datasets and other geologically complex environments compel us to look for ways to overcome these assumptions as they are violated. Using the depth migration velocity model we apply the zero-offset traveltimes as the moveout correction for reflection static calculations in depth imaging.

2D finite-difference modeling and imaging of viscoacoustic wave propagation using a PML absorbing boundary condition

Ali Fathalian* and Kris Innanen

ABSTRACT

The constant-Q wave propagation by series of standard linear solid mechanisms using perfectly matched layers absorbing boundary condition (PML) are investigated. An PML with an unsplit field is derived for the viscoacoustic wave equation by introducing the auxiliary variables and their associated partial differential equations. The unsplit PML are tested on a homogeneous velocity and Marmousi velocity models by applying the 2-4 staggered grid finite-difference scheme. When the wave propagating in the subsurface the amplitude and phase of seismic wave distort due to attenuation. The acoustic reverse time migration (RTM) can not explain this distortion, so we used an unsplit viscoacoustic wave equation with constant Q-model. Comparing the numerical tests on synthetic data for unsplit viscoacoustic reverse time migration and acoustic reverse time migration show the advantages of our approch over acoustic RTM when the recorded data had strong attenuation effects.

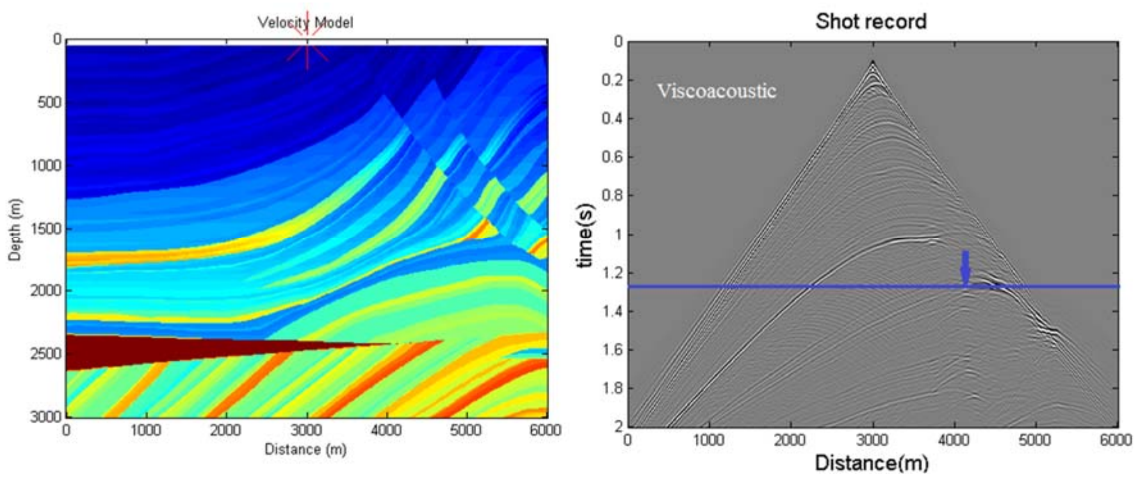

FIG. 1. Show shot record from viscoacoustic simulation using PML absorbing boundary condition

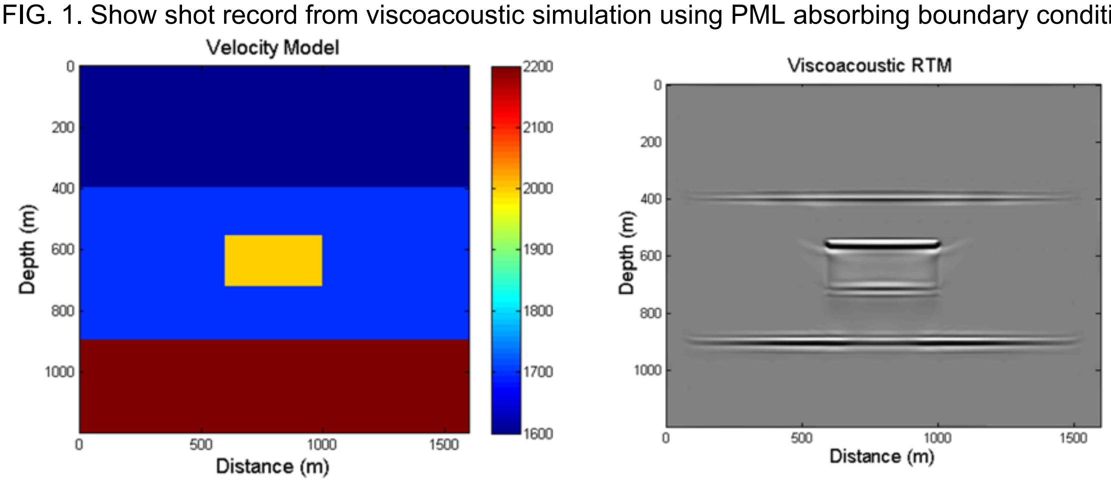

FIG. 2. The viscoacoustic RTM images of the layered model.

The relationship between scattering theory and the reflection coefficient for elastic media: Forward scattering series

Ali Fathalian and Kris Innanen

ABSTRACT

The scattering theory can be used as a powerful theoretic approach to understand and process seismic data. Exploring inverse scattering series, which have been used to remove multiples from seismic data, depends on understanding how these series generate primaries and multiples. The inverse scattering methods depend on an understanding of how the forward scattering series generates primaries and multiples. In this work, we study the forward scattering series for elastic media in order to identify on which terms in inverse scattering series are important for imaging and inversion. Primary reflections are described by all of the terms in the series excluding the first term.

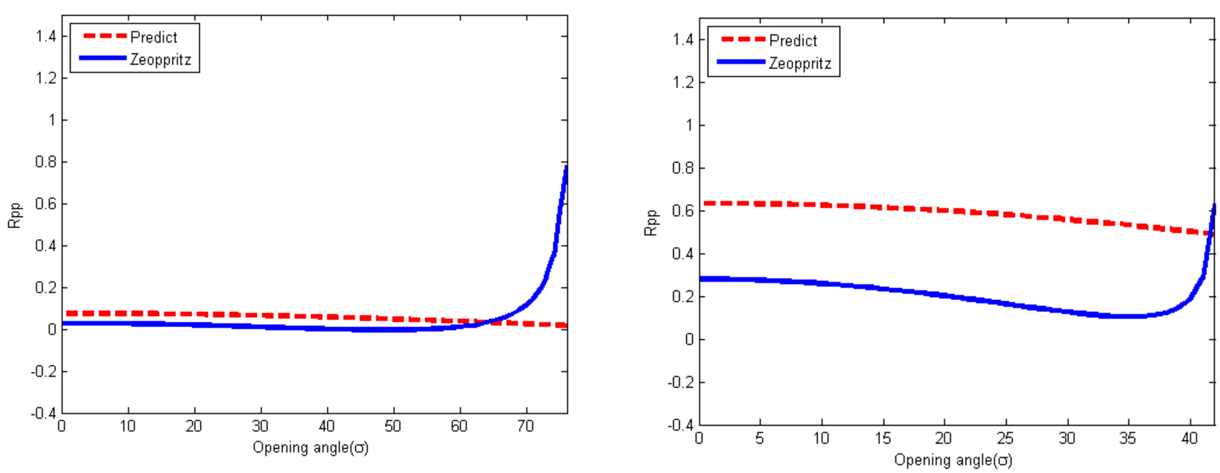

FIG. 3: The comparison between the synthesized and the actual values of Rpp for small and large layer contrast models.

Frequency domain nonlinear full-waveform inversion

Yu Geng*, Kris Innanen

ABSTRACT

Based on a data-fitting procedure, full waveform inversion (FWI) aims to build high resolution subsurface structures using full waveform information. Although FWI is a highly nonlinear inverse problem, it is usually solved as a local optimization problem under a linear approximation. Recently applications of FWI show that FWI can successfully build high resolution models in shallow regions, where long-to-intermediate wavelength structures can be reconstructed from diving waves and post-critical reflections. When first order scattering is considered during the construction of sensitivity kernel, recently developed reflection waveform inversion (RWI) provides the possibility to retrieve long-to-intermediate wavelengths in deeper regions from pre-critical reflections. In this study, we first present the construction of nonlinear sensitivities under the scattering theory. Extending the sensitivity kernel to higher order can help reduce the nonlinearity and improve the convergence of FWI. We then present a two-iteration approach to perform nonlinear FWI in the frequency domain. Finally, we apply this nonlinear FWI on the Marmousi velocity model. The inverted models with different frequency ranges and different initial models show that this nonlinear FWI can build a reliable high resolution model in both shallow and deeper regions.

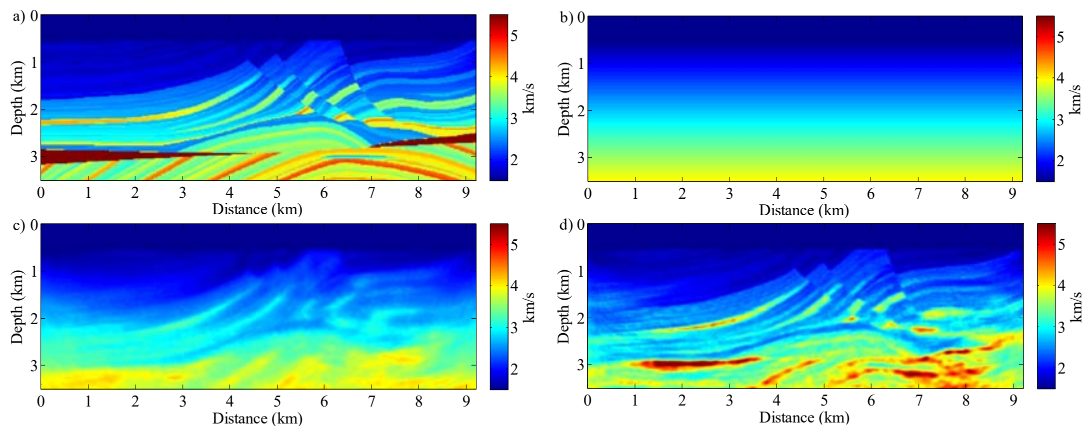

FIG. 1. Inversion of Marmousi model. a) True Marmousi model, b) initial model, inverted model using c) FWI and d) nonlinear FWI with 10 iterations for 5 frequencies starting from 2Hz to 15Hz.

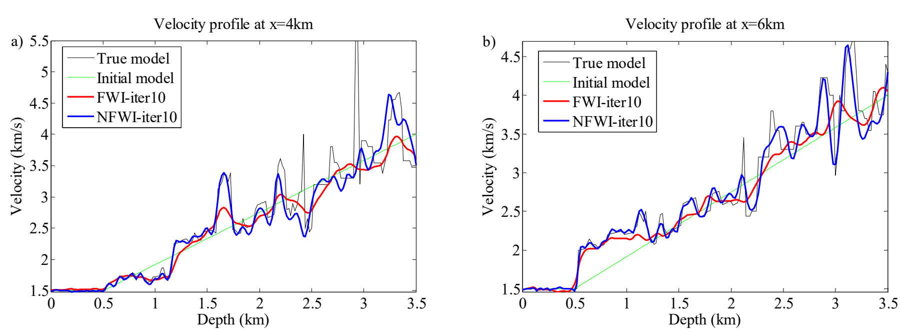

FIG. 2. Velocity profiles of the inversion results along a) x=4km, b) x=6km.

VSP azimuthal travel time analysis at the Field Research Station near Brooks, AB.

Adriana Gordon*, Don C. Lawton and David W. Eaton

ABSTRACT

As part of the Containment and Monitoring Institute (CaMI) CO_2 injection project, Vertical Seismic Profile data (VSP) were acquired at the Field Research Station in May 2015. A half walk-around VSP survey was acquired and processed for an azimuthal analysis. Obtaining the first break traveltime variations with azimuth, was the first step. Statics corrections and median filters were applied to help differentiate a sinusoidal trend in the data. The fast direction, estimated from the trend, is at approximately 40 degrees, which is similar to the Western Canada stress orientation (NE-SW). An estimation of the anisotropy parameter epsilon (ε) yield a value of 0.02, indicative of weak anisotropy. The data was rotated as a starting point of the processing flow by using with different approaches, in order to obtain imaging results in the future work.

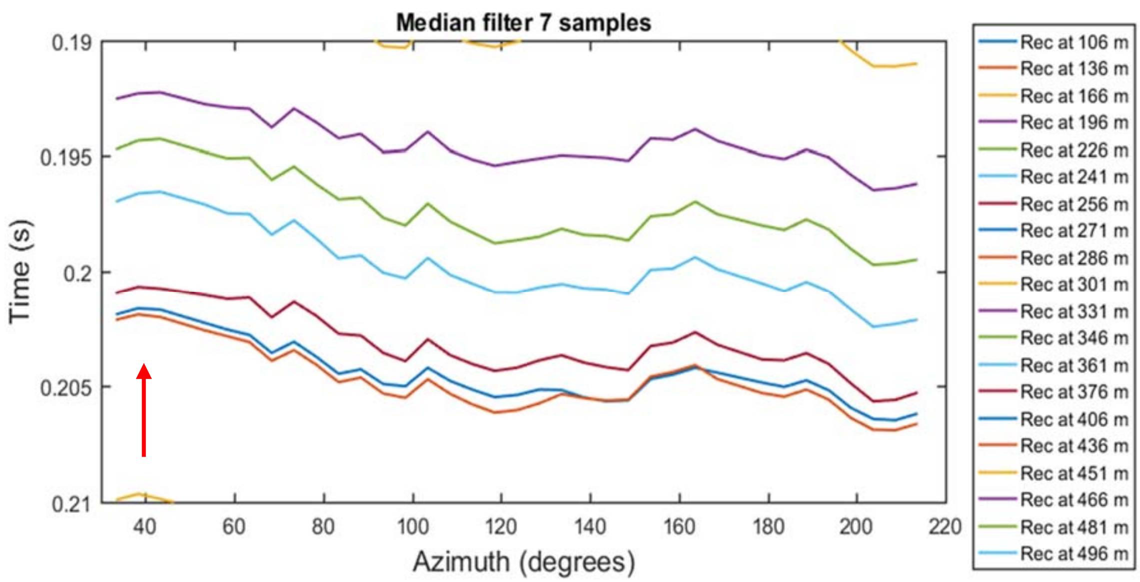

FIG. 1. Traveltime variations observed from the first break picks versus azimuth for each receiver of shot line 204 after static corrections and median filter of 7 samples using a larger scale. Each colored curve represents a receiver depth. The fast direction estimated from the figure is approximately 40 degrees indicated by the red arrow.

FWI without tears: a forward modeling free gradient

Marcelo Guarido, Laurence Lines, Robert Ferguson

ABSTRACT

Full waveform inversion (FWI), a machine learning algorithm, has the goal to find the Earth's model parameters that minimize the difference of acquired and synthetic shots. We did a simulation of the methodology on 2D data at the Marmousi model. The report is divided in two parts. On the first part, we applied a band-limited impedance inversion on the migrated residuals to estimate a gradient cheaper and leading to a with higher resolution at deeper areas and more continuity of the geologic features when compared to previous works. On the second part, we introduce a new interpretation of the gradient as a residual impedance inversion of the acquired data. Its estimation is forward modeling and wavelet free, reducing its costs drastically, as the inverted model was obtained on a personal laptop without parallel processing. The new method was successfully applied on the acoustic Marmousi simulation. The inverted model, when using the same starting point, is comparable to the results of using the migrated residuals. A preliminarily test was done by inversion the order of migration and stack and using a post-stack depth migration to estimate the gradient with promising outputs. In the end, we are proposing a new FWI approximation that is cheap and stable and could be used on real data in the same processing center that has enough computer power to run a PSDM or even just a post-stack depth migration.

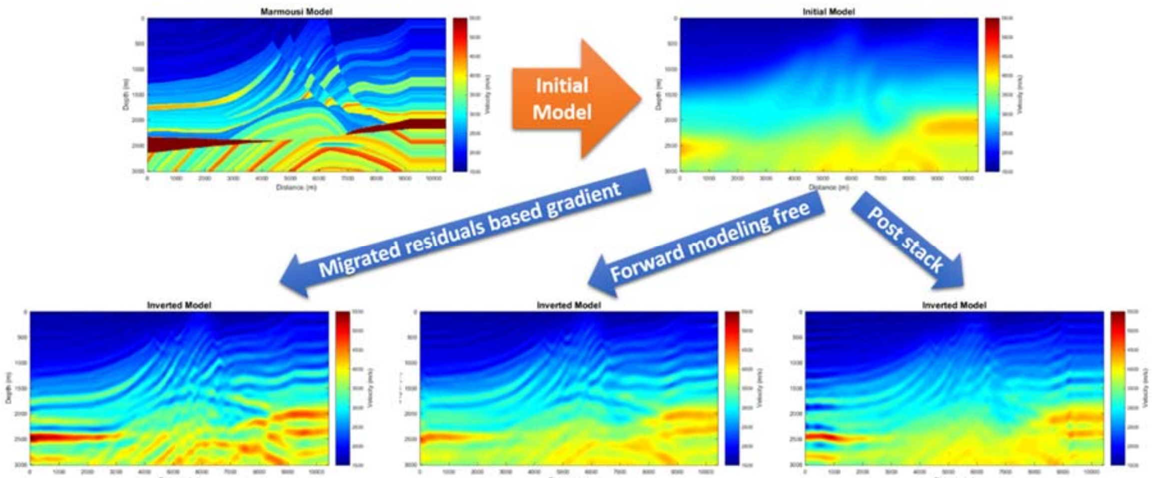

FIG. 1: Comparing the outputs of different approximations of the FWI: the classic, the forward modeling free gradient and the post stack forward modeling free gradient.

Wave mode separation and prestack depth migration of multicomponent data in the presence of topography

Saul E. Guevara and Gary F. Margrave

Scalar methods for multicomponent data processing require separate wave modes in principle. A method for wave mode separation in the presence of topography is tested on synthetic seismic data, generated on a complex geology model with a 2D elastic FD method. The resulting data are migrated using two preSDM approaches, Kirchhoff and PSPI, and also taking into account the rough topography. The seismic images obtained show the challenging characteristics of these data; however the methods provide insights into approaches that can be rewarding for elastic wave processing in complex settings.

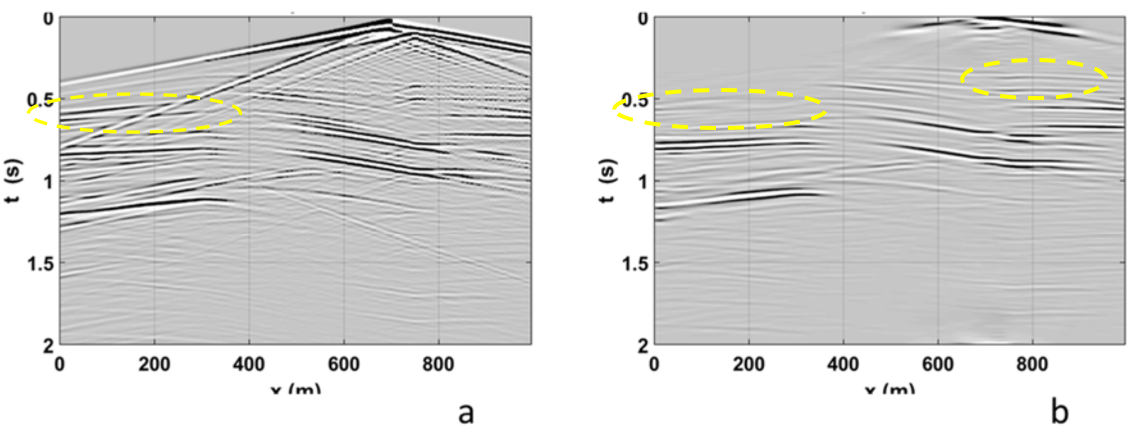

FIG. 1. Wave mode separation with topography. (a) Horizontal component of a synthetic shot record obtained in a model with complex geology and topography. (b) *S*-wave resulting of wave-mode separation for the same shot. Notice that events corresponding to *P*-waves are attenuated (yellow oval at the left-hand side), although there are also traces of P wave reflections (top oval).

The promise of 3D 3C seismic data for improved imaging and reservoir characterization in the Alberta oil sands

Bobby J. Gunning*, Don C. Lawton and Helen Isaac

ABSTRACT

A 3D 3C seismic data set from the Athabasca Oil Sands region was processed and interpreted. The vertical and radial geophone components were processed as the PP and PS seismic data. PP and PS seismic data were processed to stack using Vista and ProMAX processing software. Prestack PP gathers were generated for analysis. Stacked datasets were correlated with regional well control and pervasive reflection horizons were picked. The main hydrocarbon reservoir, the McMurray formation was studied based on the PP and PS seismic datasets. A large Upper McMurray aged channel feature was found running through the seismic volume. Truncations of regional seismic character were found at the McMurray channel location. A model-based post stack impedance inversion is performed on the PP seismic data. Interval RMS amplitude and impedance reveal in-situ natural gas and potential improved reservoir; these findings are correlated with geological control. Prestack inversion outputs bound the geological interpretation even further.

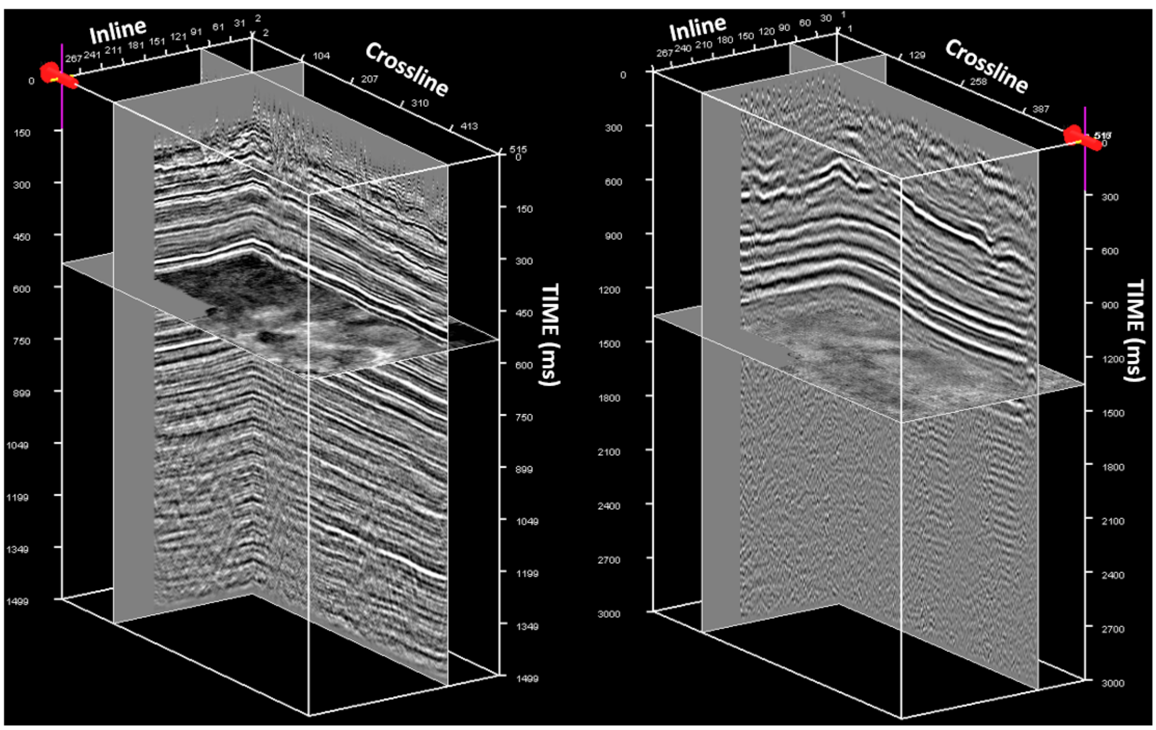

FIG. 1. Fully processed PP and PS volumes.

Always finding faults: New Zealand 2016

Kevin W. Hall*[1], Helen Isaac[1], Malcolm Bertram[1], Kevin Bertram[1], Don Lawton[1], Alexis Constantinou [2], Doug Schmitt[3], Randy Kofman[3], Jennifer Eccles[4], Vera Lay[5], Stefan Buske[5], John Townend[6], Martha Savage[6], Andrew Gorman[7] and Richard Kellett[8]

ABSTRACT

CREWES participated in two collaborative seismic programs that were conducted on the North and South Islands of New Zealand in early 2016. The South Island survey was conducted in the Whataroa Valley, primarily on unconsolidated glacial and river sediments, and consisted of a variety of geophone and distributed acoustic sensing (DAS) vertical seismic profile (VSP) surveys in the DFDP-2b borehole, as well as surface 1C-2D, 1C-3D and 3C-3D surveys on the surface. The purpose of this survey was to better understand the Alpine Fault, which runs along the west coast of the South Island and has potential to produce M8+ earthquakes (Figure 1a). The North Island survey was conducted along the top of a stop-bank over unconsolidated river and marine sediments in the Hauraki Rift, and consisted of a single 1C-2D crooked-line. One of the goals of this project was to test the viability of seismic reflection surveying to image faults using a Vibe in this area. This seismic line crosses the northern Kerepehi fault, which has previously been inferred from gravity data. The Kerepehi fault is considered to be active, and is thought to have produced M6+ earthquakes in the past (Figure 1b).

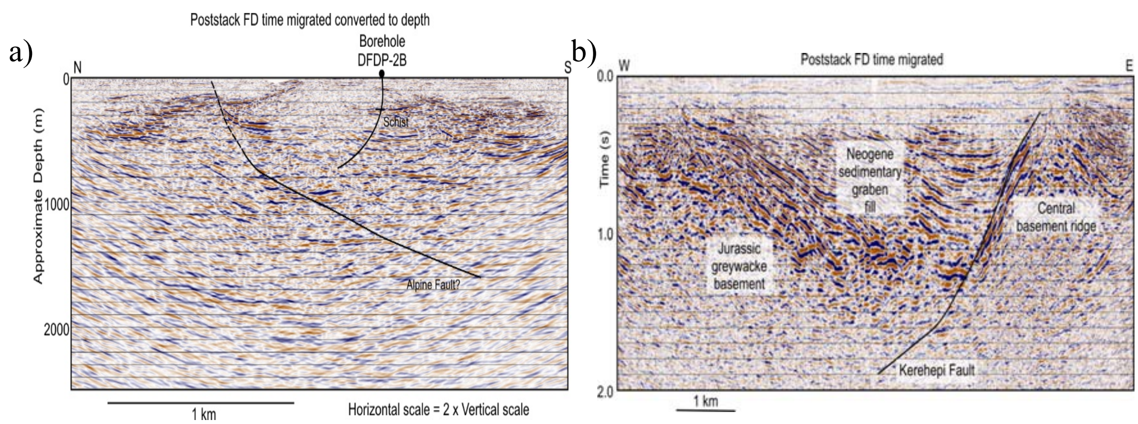

FIG. 1. Depth-converted post-stack time migrated section with the location of the DFDP-2B borehole and our interpretation of the Alpine Fault (a), and our interpretation of the Kerepehi fault on a post-stack time migrated section (b).

[1] CREWES, University of Calgary, Calgary, Alberta, Canada
[2] Schlumberger Fiber Optics Technology Center, Romsey, England
[3] University of Alberta, Edmonton, Alberta, Canada
[4] University of Auckland, Auckland, New Zealand
[5] Technical University Bergakadamie Freiberg (TUBAF), Freiberg, Germany
[6] Victoria University of Wellington, Wellington, New Zealand
[7] University of Otago, Dunedin, New Zealand
[8] GNS Science, Lower Hutt, New Zealand

Exact Solutions for Reflection Coefficients, in 1D and 2D

Heather K. Hardeman, Michael P. Lamoureux

ABSTRACT

In this paper, we solve the 1D and 2D elastic wave equation using two different velocity fields: a velocity jump and a velocity ramp. We require the density and modulus satisfy the relation established in (Lamoureux et al., 2012) and (Lamoureux et al., 2013) using some parameter α. We find the reflection coefficient for the 1D case of a velocity jump given general α. Extending these velocities to the two dimensions, we compute the analytic solutions to the 2D elastic wave equation and find the reflection coefficients for a plane wave hitting the jump and ramp at normal incidence. Finally, we conclude with discussion of the case where the plane wave hits the transition zone of the 2D velocity ramp at non-normal incidence given varying density. The motivation for this paper is to extend the work of the authors in (Lamoureux et al., 2012) and (Lamoureux et al., 2013) and to demonstrate explicit reflection coefficients in a continuously varying velocity field.

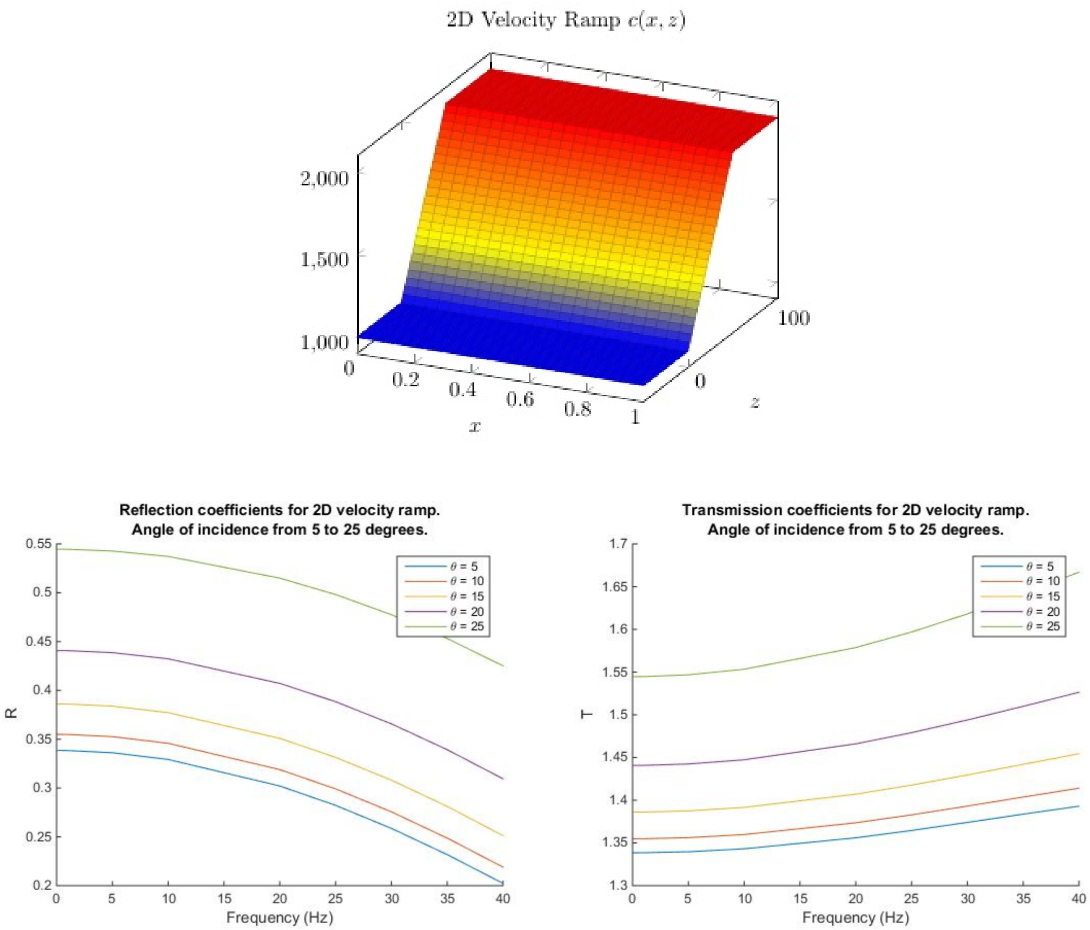

FIG. 1: The 2D velocity ramp (top). The reflection coefficients for incident angles 5, 10, 15, 20, 25 degrees (bottom left). The transmission coefficients for incident angles 5, 10, 15, 20, 25 degrees (bottom right).

To boldly go into the next dimension: 3D raypath interferometry issues

David C. Henley

ABSTRACT

The technique known as raypath interferometry was developed to correct seismic reflection data for difficult near-surface conditions by generalizing and relaxing the assumptions used by conventional surface-correction algorithms (statics corrections). We have demonstrated the success of the technique on model data as well as on several sets of 2D field data, both PP and PS. The method improves not only the alignment and coherence of reflection events, but also their waveform consistency.

We are now extending raypath interferometry to 3D. In previous work, we introduced the source-receiver azimuth as a third dimension for grouping 3D traces for analysis. This approach allows us to use a 2D trace transform (initially the RT, or radial trace transform) to move the data to a common-raypath domain for applying interferometry. We showed the success of this approach by applying it to the vertical component of the Blackfoot 3D-3C field data, and showing improved event coherence.

Here, we apply raypath interferometry to the radial horizontal (PS) component of the same Blackfoot data set. As with the PP component, we demonstrate improved event coherence on the common-ray-parameter ensembles (Figure 1). Because of limitations in our RT transform algorithm preventing proper inversion to the X-T domain, we determined that a promising alternative is to replace this RT Transform with a Tau-P Transform, which avoids the shortcomings of our RT algorithm. The principal limitation of the Tau-P approach appears to be the large amount of storage required by Tau-P transforms when performed at sufficient resolution to invert X-T data with good fidelity. Ultimately, with proper data storage management, full comparison of CMP and CCP stack traces of corrected and uncorrected 3D data will be possible.

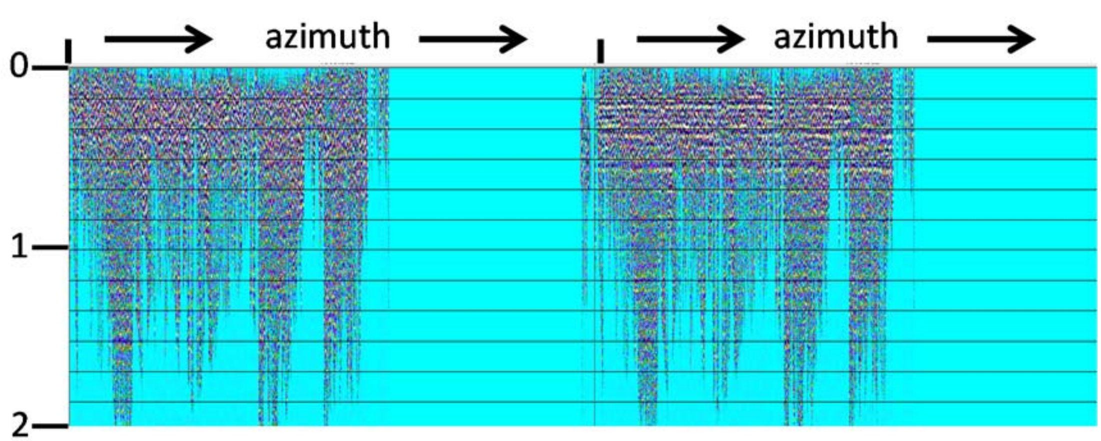

FIG. 1. Common-ray-parameter PS trace ensemble before and after 3D raypath interferometry, using the RT transform. Ray parameter is -1500m/s for both ensembles. Dead traces indicate no data for this particular ray parameter over the azimuth range indicated; raypaths associated with any given ray parameter will typically occupy only about half the available azimuth range.

A geometrical model of DAS fibre response

Kris Innanen*

ABSTRACT

A geometrical model of the shape and response of a buried DAS fibre, which allows for both a helical wind and arbitrary curvature of the cable, is a tool for analysis and appraisal of DAS experiments. The model takes as input vectors describing the cable shape and (optionally) the parameters of the helix. As output, the model generates arc-length, fibre positioning, and tangent information, with (optionally) a gauge length imposed. Five example applications of the model are presented: (1) the fibre may be embedded in modelled 3D elastic wave field and its response computed; (2) the 3C vector wave is reconstructed along the fibre within defined reconsruction windows; (3) the six components of tensor strain are reconstructed similarly; (4) the cosine theta directionality rule for P-wave displacement is generalized to the arbitrarily curved fibre; and (5) the cosine squared theta directionality rule for P-wave strain is similarly generalized.

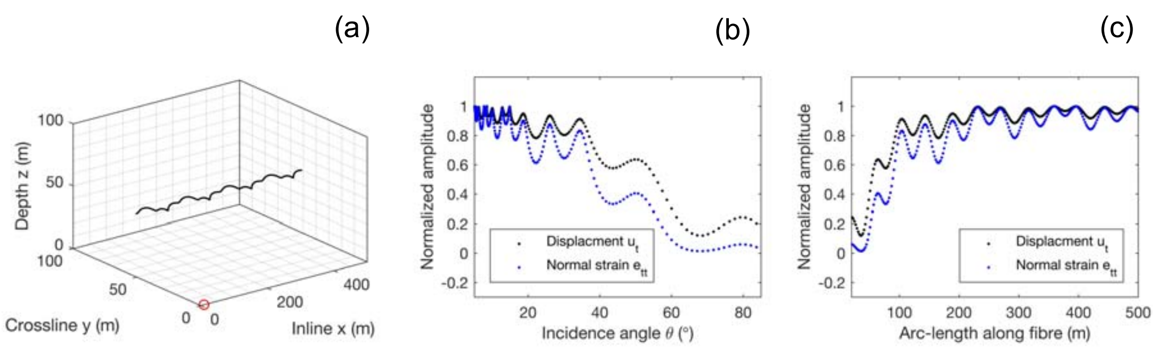

FIG. 1. (a) Three vectors describing the positioning of all points along the cable axis are given, as are the parameters of the helical wind; the resulting shape and its geometrical characteristics are computed. Auxiliary information (e.g., the source position in red) is incorporated. (b) The generalized relationship between the component of vector displacement caused by a P-wave originating at the source point (black) and the angle of incidence with which the P-wave impinges on the fibre, and the tensor strain likewise (blue) are computed. (c) The variation of these same quantities can be plotted with respect to the arc-length along the fibre. Angle of incidence and arc-length are derived features of the geometrical model.

Brooks Revisited

J. Helen Isaac and Don C. Lawton

ABSTRACT

The first CO_2 injection well was drilled in 2015 at the Containment and Monitoring Institute's Field Research Station near Brooks, Alberta. We used well logs from the new CO_2 injection well, 10-22-017-16W4M, to compare our pre-drill depth estimates of formation tops with those encountered in the well. Our estimate of the depth of the target Basal Belly River Formation, which we had derived from the mapped well tops and the 3D seismic data interpretation, was about 3.5 m high. Our estimate of the top of a 2-m thick sand in the Medicine Hat Formation was 3 m high. Our predictions of the shale content in the Belly River Formation above the target injection zone are supported by gamma ray log and lithology data from the new well.

We created synthetic seismograms from the dipole logs acquired in the new well and tied the seismic data. Figure 1 shows the P-wave, S-wave and Vp/Vs logs from the well correlated to the PP and PS seismic data with synthetic seismograms, and the lithology (courtesy Schlumberger). The PP synthetic seismogram shown here is a stacked multi-offset synthetic seismogram. The PP and PS data show good character matches between the seismic data and the synthetic seismograms. Although the seismic data did not require re-interpreting, we used the formation tops from the new well to revise the depth structure maps. We also updated the post-stack joint PP-PS inversion to 550 m depth by using the dipole logs from the new well.

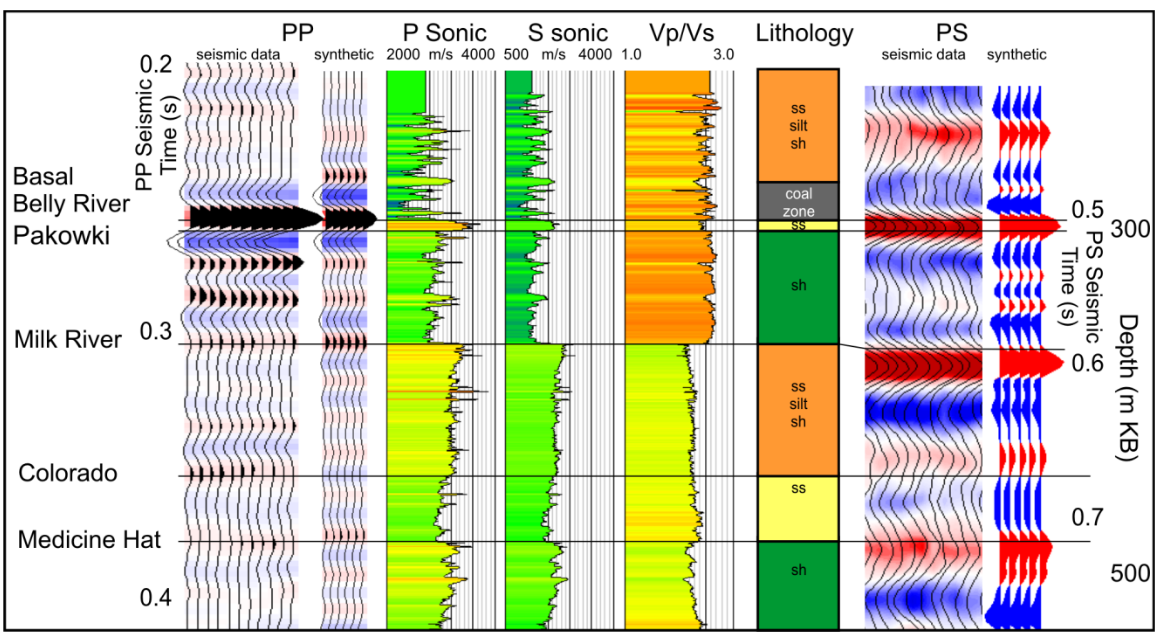

FIG. 1. Logs from the new injection well, which was drilled to 550 m, correlated to the PP and PS seismic data with synthetic seismograms. The logs and seismic data are displayed in PP time.

Anacoustic FWI: Implementation and challenges

Scott Keating and Kris Innanen

ABSTRACT

Full-waveform inversion (FWI) estimates subsurface properties by minimizing differences between synthetic and observed data. It is important for the success of FWI that the synthetic modeling can reproduce the physical mechanisms which give rise to the observed data. Attenuation plays a prominent role in wave propagation, and thus its inclusion in FWI is desirable. An anacoustic FWI is not a trivial extension of FWI however, and problems arise when incautiously applying the same optimization, regularization, and frequency band updating strategies. Specific problems like these and some of their solutions are outlined in this report.

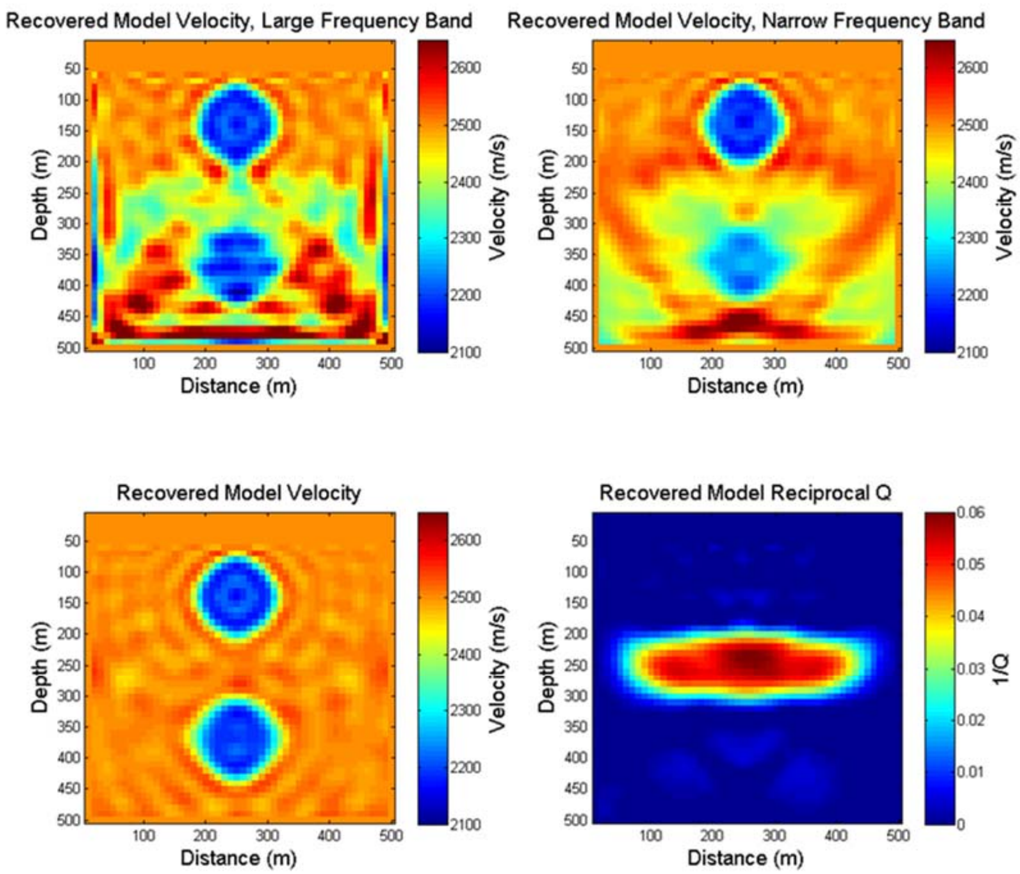

FIG. 1. Top: Recovered velocity model applying acoustic FWI to anacoustic data, inverting a broad (left) or narrow (right) frequency band at each iteration. Bottom: Recovered velocity (left) and Q (right) model applying anacoustic FWI. Velocity estimate is considerably improved using anacoustic FWI.

Applying the truncated Newton method in anacoustic full waveform inversion

Scott Keating and Kris Innanen

ABSTRACT

In this report, the truncated Newton (TN) method and its application to anacoustic FWI is investigated. Larger problems are shown to be efficiently solvable when using TN FWI instead of full Newton FWI. It is also found that stricter forcing terms are required in anacoustic FWI to achieve results comparable to acoustic TN FWI, due mostly to cross-talk effects. This additional cost can partly mitigated by using effective preconditioning and a CG inner solver, or better mitigated using a BFGS inner solver. Even with these strategies, significant cost is incurred to accurately recover Q. If only velocity is desired, it can be effectively recovered with a lower cost.

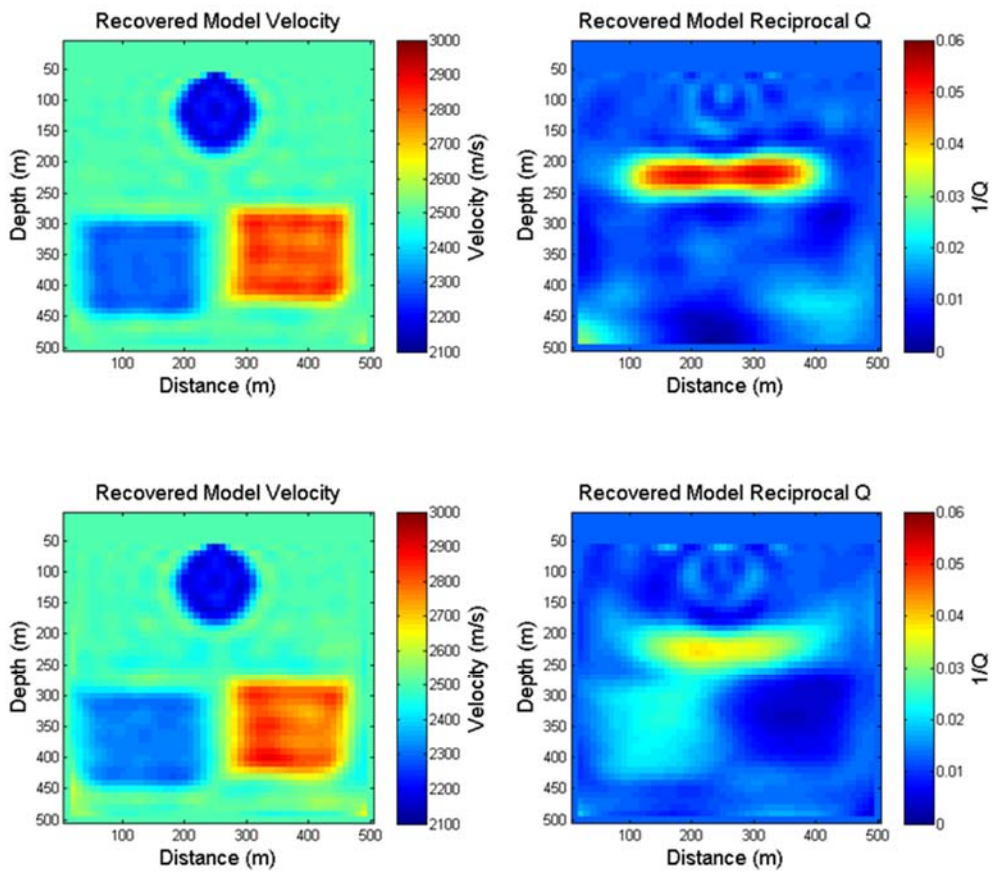

FIG. 1. Recovered velocity (left) and Q (right) models for Gauss-Newton FWI (top) and truncated Newton FWI (bottom), with a forcing factor of 10^{-2}. The same forcing factor applied in the acoustic case yields a TN result similar to the Gauss Newton one. Here, the velocity model still benefits from considerable Q compensation, but the recovered Q model is very poor in the TN method with this forcing. This forcing factor is appropriate if Q compensation is the priority, but a more demanding (and thus expensive) forcing must be chosen if Q recovery is desired.

Effects of discrepancies between modeled and true physics in anacoustic FWI

Scott Keating* and Kris Innanen

ABSTRACT

In this report, anacoustic FWI with an unknown attenuation model type is investigated. Numerical experiments are performed using a SLS true model type. Assuming a known Q model type which differs from the true Q model type led to very poor results, arguably worse than the results of an acoustic FWI. By relaxing the requirement of known model type and recovering anacoustic parameters over small frequency bands, results were dramatically improved. This recovery of model parameters of a known attenuation model type locally in frequency is a promising approach for coping with unknown attenuation model type.

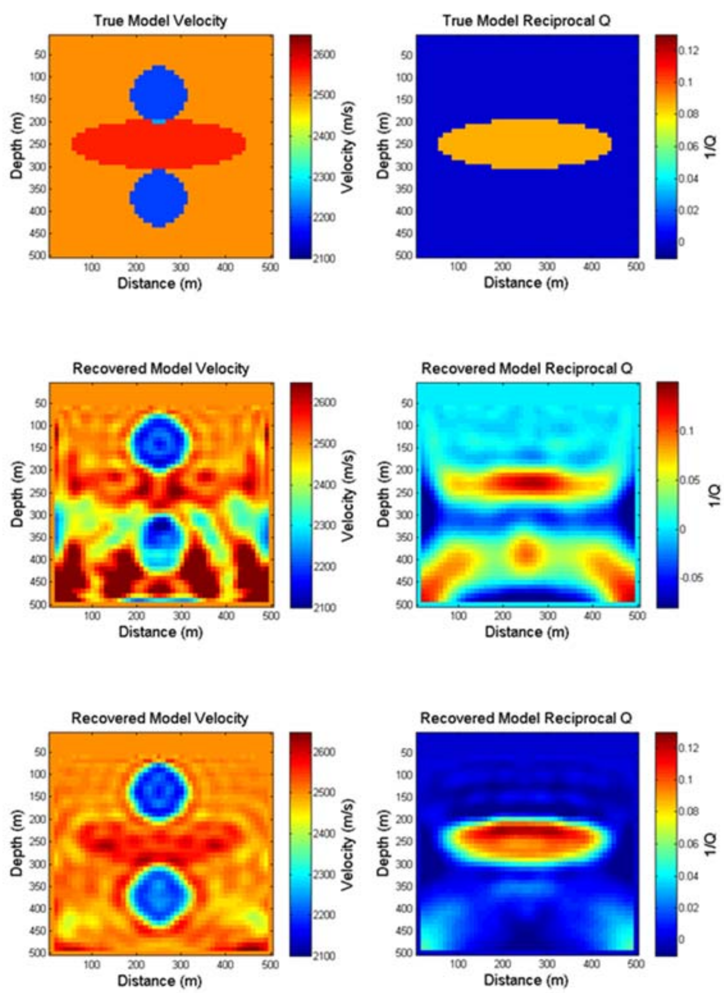

FIG. 1. Velocity (left) and reciprocal Q (right) of true SLS model at 15Hz (top), nearly constant Q FWI result (middle), and flexible nearly constant Q FWI result (bottom). By allowing anacoustic parameters to vary with frequency, the flexible anacoustic FWI approach is better able to match the true behaviour.

Preliminary processing of the Chaparral-Farnsworth VSP data set with focus on attenuation

Scott Keating, Kris Innanen, Scott Leaney

ABSTRACT

In this report the Chaparral Farnsworth VSP data was investigated, with the aims of establishing an attenuation profile and identifying difficulties that may arise if anacoustic FWI were applied to the data. Q estimates were generated using both the spectral ratio method and the centroid frequency shift method. These yielded consistent results, prominently featuring nonphysical negative Q. Scattering effects were investigated as a potential cause for this error. Synthetic VSP data generated using the well logs demonstrated that scattering effects do provide effective negative Q forcing in the Q estimation methods, but not in the correct locations or to the necessary extent to cause the apparent negative Q in the measured data. Scattering effects on a smaller scale than the well log sampling could not be discarded as a potential cause for this behaviour however. A capacity to be able to account for both Q induced frequency shifts and sub seismic resolution scattering induced shifts is identified as a desirable property in any anacoustic FWI to be applied to this data.

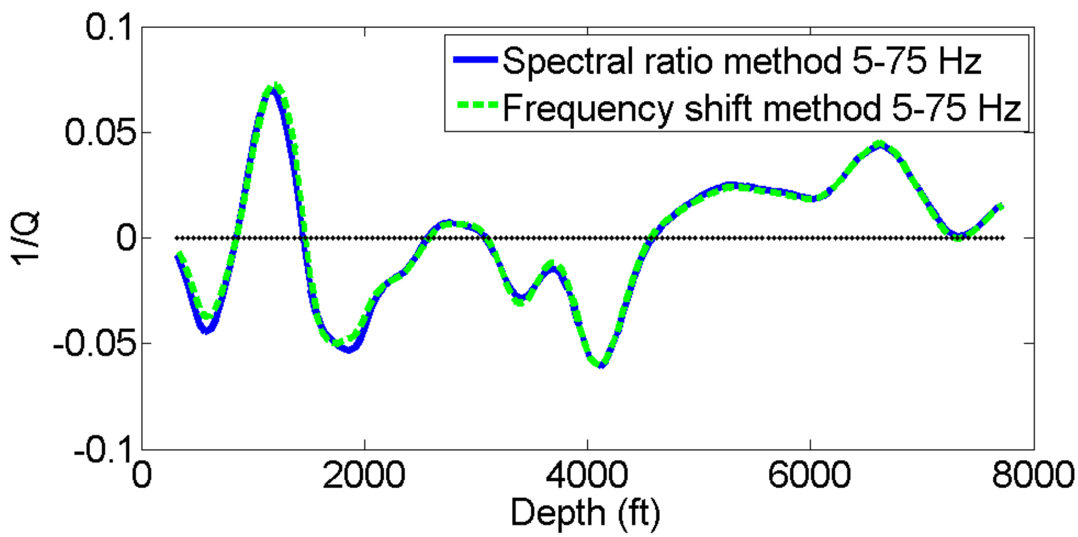

FIG. 1. Comparison of recovered Q for the spectral ratio and centroid frequency shift methods for the Chaparral Farnsworth VSP data. The agreement of the two methods on the presence of non-physical negative Q strongly implies that there is a significant failing in the common assumptions of these methods.

Radiation patterns in anisotropic models by Kirchhoff modelling/migration and AVO/AZ inversion

Hassan Khaniani and Daniel Trad

ABSTRACT

We use the Kirchhoff approximation to implement Full Waveform Inversion (FWI) method on a 3D synthetic dataset. The waveform characteristics in terms of traveltime and amplitude are approximated by the Double Square Root (DSR) equation and the linearized Amplitude Variation with Offset method (AVO). This approach considers pre-critical reflection data for both modeling and inversion. For inversion of a model with a horizontal axis of symmetry, i.e. horizontal transverse isotropy (HTI) media, the azimuthal dependant amplitude variation with azimuth (AVO/AZ) is used, while for analysis of a model with a vertical axis of symmetry, i.e. vertical transverse isotropy (VTI) media, amplitude variation with offset (AVO) is used. To analyse these AVO/AZ patterns, we migrate a shot record with 3D PSTM with dense acquisition size to compensate for poor sampling artefacts . The time slices of the target zone are shown in FIG. 2. These acquisition artefacts have more effect on the results of migration than on the amplitude of the AVO/AZ patterns. We study the performance of AVO/AZ inversion using the amplitudes sampled along the black dashed lines in FIG. 2, namely, AB, AC, AD, AE and AF with azimuth of 0 º, 30 º, 45 º,60 º and 90º. By describing the numerical aspects of FWI by PSTM and AVO/AZ, we hope to provide an efficient tool that other scientists can use to visualize the radiation patterns of an isotropic and anisotropic media. The FWI framework is applied here only to synthetic data, but application to real seismic reflection data is left for future research.

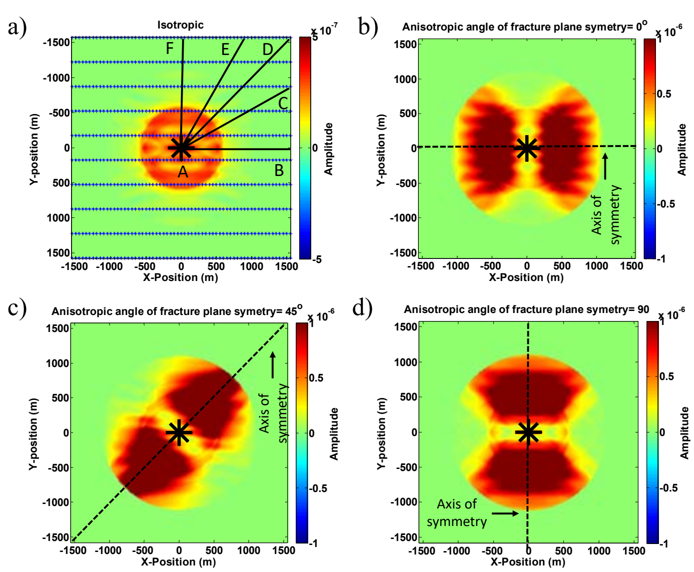

FIG. 2. Evaluation of AVO/AZ formulation for different azimuth of axis of symmetry. The scenarios are implemented for a) Isotropic media, b) HTI #1 media with axes of symmetry of $\phi_{ref} = 0$, c) HTI#2 media with axes of symmetry of $\phi_{ref} = 45$ and d) HTI #3 media with axes of symmetry of $\phi_{ref} = 90$. The solid line in a) correspond to AVO/AZ curves sampling azimuth of AB, AC, AD, AE, AF, 0º, 30 º, 45 º, 60º and 90. The blue dots in figure (1a) is geophone positions.

Amplitude Migration in v(z) Media

Oliver Lahr and Gary F. Margrave

ABSTRACT

This report is meant to investigate the notion that amplitude migration in a v(z) medium must be treated differently than migration in a constant velocity medium. It is based on findings that migrated shot gathers near edges do not show even remotely close correct amplitudes. Reasons seem to deal with the fact that geometrical, both in-phase and out of phase, must be dealt with. To prove this, a ray based analysis was undertaken to account for spreading of both kinds. Based on that, it will be shown here that accounting for a v(z) medium will result in migrations that restore amplitudes more correctly than simply assuming a constant velocity medium. In particular, we will use a flat reflector model and a simple AVO 3 model. Also, several cost-saving measures that come with this improved migration will be pointed out.

Slices and amplitude plots highlighting the success of the v(z) migration vs. the constant velocity migration for a simple AVO 3 reflector are shown in *Figure 1*.

This data model consists of a 1000x1000 m survey, with a depth of 2500 m. There is a background layer down to 150 m, at which the data takes the form of an AVO 3 anomaly. The data was extracted from Zhang and Brown(2001). For other details, such as the creation of 3D shots, please refer to our accompanying CREWES report.

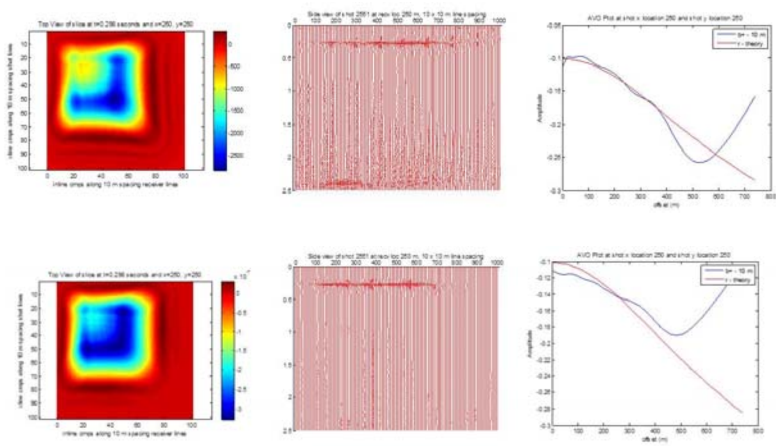

FIG. 1. Results of migration for Simple AVO 3 reflector at shot location x=y =250 m. Top Row: using v(z) algorithm Bottom Row: Using constant Kirchhoff

It is easily seen that the migrated amplitudes (blue) more closely agree with the expected amplitudes(red) after v(z) migration(top) than after v(constant) migration.

References:

Zhang, H and Brown R.J., 2001, A review of AVO analysis: CREWES Research Report, 13, 357-380.

Grid algebra in finite difference methods

Michael P. Lamoureux*, Heather K. Hardeman

ABSTRACT

Large, sparse matrices often appear in numerical methods for solving partial differential equations, particularly in finite difference solutions to the wave equation in two and three dimensions. We demonstrate a technique to represent these operators directly on a grid and develop linear algebraic methods to simplify or factor the operator into a form that is easy to solve using back-substitution. We apply the technique to implement an implicit solver for a finite difference algorithm applied to the wave equation in two dimensions.

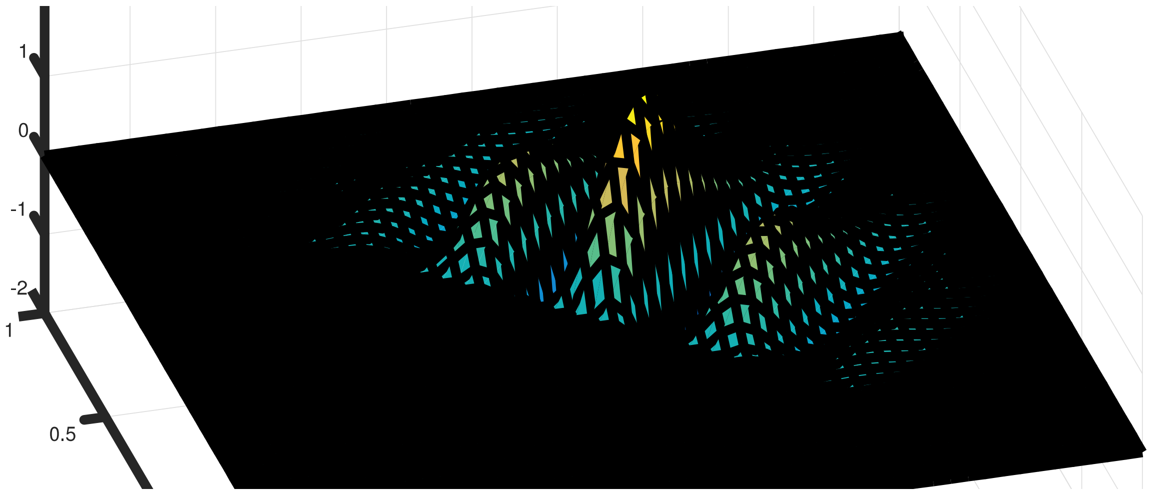

FIG. 1. Wave propagation in 2D, using grid algebra technique.

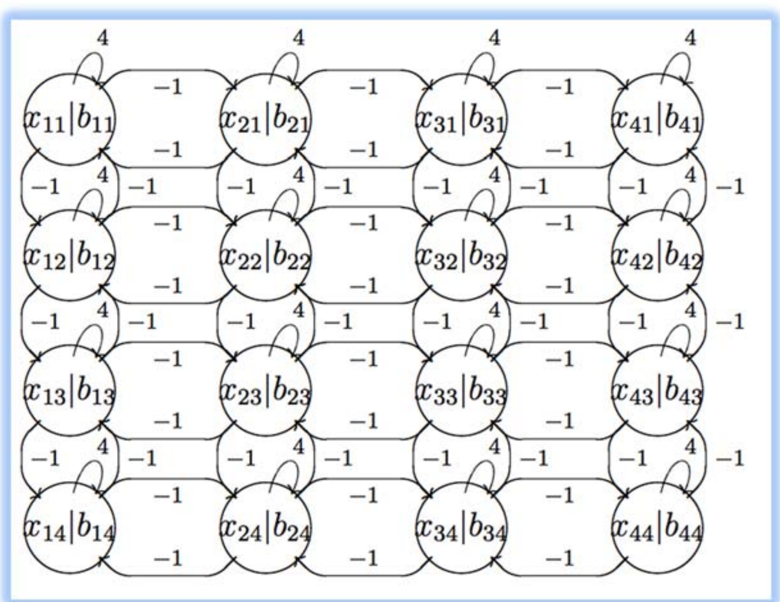

FIG. 2. A grid representation of a linear operator in 2D.

Incorporating reflection data into refraction statics solution

Bernie Law and Daniel Trad

ABSTRACT

Near surface models from refraction inversion contain several types of errors, which are partially compensated later in the data flow by reflection residual statics. In this work, we modify the dataflow to automatically include feedback information from reflection statics from stack-power maximization. We modify GLI by adding model and data weights computed from the long wavelength components of surface consistent residual statics. By using an iterative inversion, these weights allow us to update the near surface velocity model and to reject first arrival picks that do not fit the updated model. In this non-linear optimization work flow the refraction model is derived from maximizing the coherence of the reflection energy and minimizing the misfit between model arrival times and the recorded first arrival times. This approach can alleviate inherent limitations in shallow refraction data by using coherent reflection data.

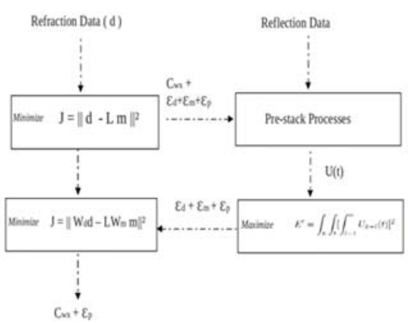

FIG. 1. Inversion work flow.

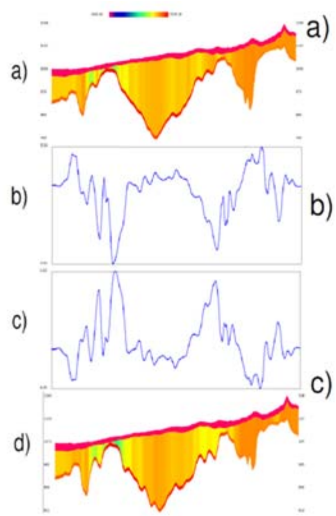

FIG. 2. a) Refraction model, b)Wm for velocity and c) thickness, d) updated refraction model

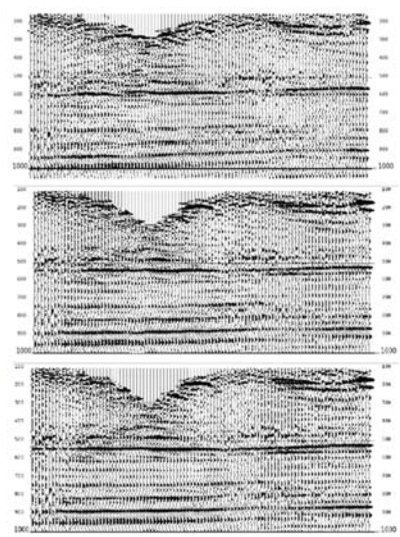

FIG. 3. a) CDP stack with datum statics correction b) CDP stack with refraction statics correction c) CDP stack with stack-power maximization and refraction statics using updated refraction model

Near-surface velocity characterization at Priddis and installation of fibre-optic cables at Brooks, Alberta

Don C. Lawton*, Malcolm B. Bertram, Kevin W. Hall, Kevin L. Bertram

ABSTRACT

CREWES operates a shear-wave seismic source for multicomponent near-surface seismic studies. The source component of the system is a model A200 weight drop device with a 100 kg hammer accelerated by compressed nitrogen operating at 1000 psi. In 2016, we recorded a multicomponent walk-away vertical seismic profile at the Priddis Geophysical Observatory in to characterize the near-surface P-wave and S-wave velocity structure to a depth of 141m. P-wave data were collected with the source operating in a vertical force orientation. A pivot system enables the source to generate both P-wave and S-waves. The source mast can be operated in a vertical mode for generating P-waves and it can rotate ± 45 degrees transverse to the longitudinal axis of the trailer, in order to generate down-going P-wave and S-waves simultaneously. Pure-mode down-going S-waves are generated by subtracting records taken with the mast rotated in the positive and negative tilt modes. Figure 1a shows good-quality zero-offset P-wave and S-wave VSP data recorded into the CREWES well with a 3C receiver spacing of 3.06 m. Two layers are interpreted from the first arrival P-wave and S-wave travel times, with the first layer thickness of 46 m. P-wave velocities are 2450 m/s and 3260 m/s and S-wave velocities are 796 m/s and 1346 m/s respectively. This yields Vp/Vs values of 3.08 in the first layer, and 2.42 in the second layer.

At the Brooks Field Research Station, being developed by the Containment and Monitoring Institutes, both straight and helical optical fibres have been installed in a 350 m deep well and in a 1.1 km trench, to assess optical fibre recording for VSP and surface seismic surveys. The installation schematic is shown in Figure 1b. Recording into the fibre will be undertaken in 2017.

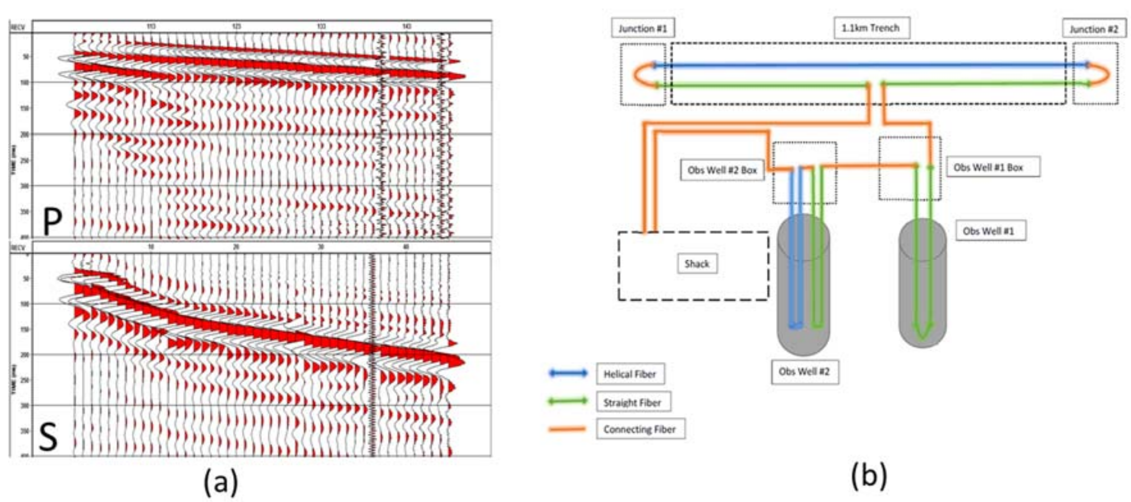

FIG. 1. (a) Near-surface P-wave and S-wave VSP data at Priddis, and (b) layout of linear and helical optical fibre at the Brooks Field Research Station

A 3D pseudospectral method for order reduced SH wave simulation

Junxiao Li, Kris Innanen, Guo Tao, Laurence R. Lines and Kuo Zhang

ABSTRACT

In this paper, the order reduced velocity-displacement SH-wave equations in VTI media are first proposed. During SH-wave simulation, the spatial derivatives of the new SH wave equations are transformed into wavenumber domain and a staggered-grid Fourier pseudospectral time-domain (PSTD) method is used to obtain discretized forms of these wavenumber operators, which in turn, effectively eliminates the Gibbs phenomenon that arises when Fourier transforming a discontinuous function in heterogeneous media. The order reduced velocity-displacement SH-wave equations also make it possible to set hybrid perfectly matched layers around computational boundaries to mitigate artificial reflections. Finally, this new scheme is applied for wavefield modeling in two-layer heterogeneous media. Comparisons of simulation results with PSTD using second-order SH-wave equation further verify its accuracy.

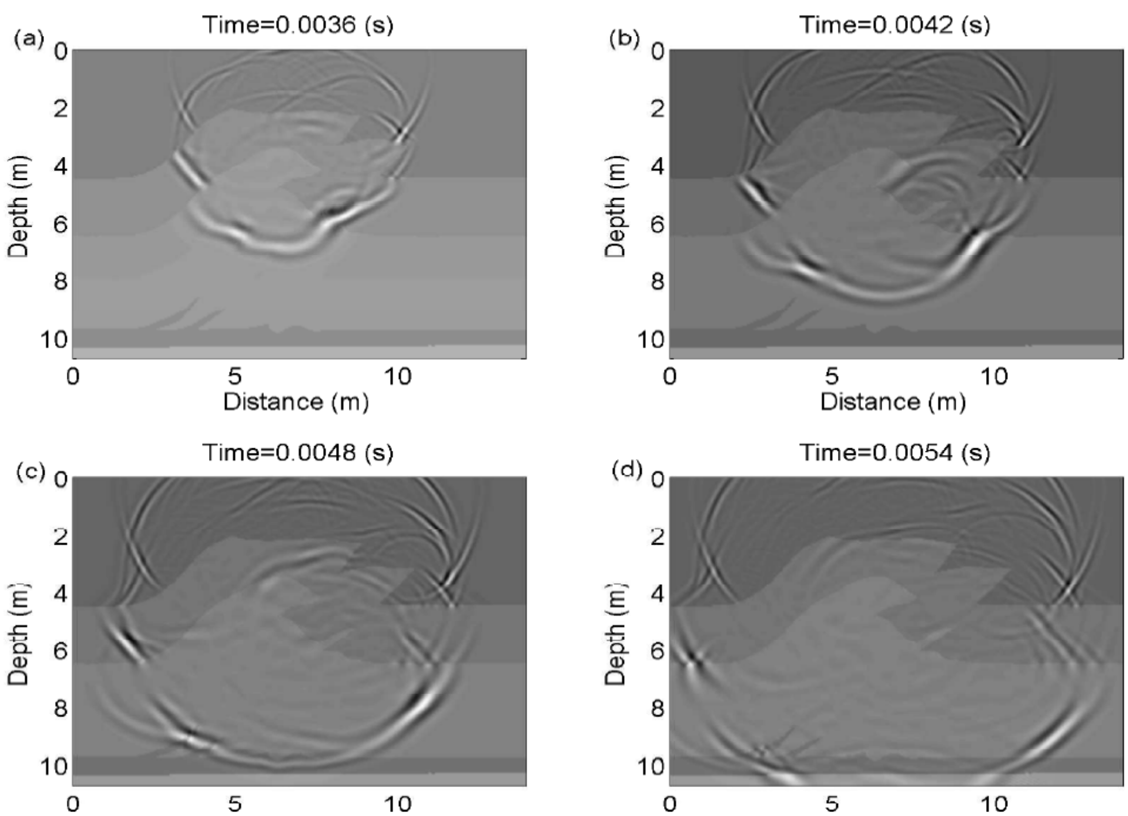

FIG. 1. Snapshots for SH propagation in thrust fault model (x-z plane)

Elastic wave-vector decomposition using wave vector rotation in anisotropic media

Junxiao Li, Kris Innanen, Guo Tao and Laurence R. Lines

ABSTRACT

Elastic wave propagating in anisotropic media can be treated as a polarization deviation of wave vector in terms of isotropic media. The deviation angle between the wave normal and qP-wave's polarization direction can be estimated based on the phase angle and elastic constants (or Thomsen parameters). The anisotropic polarization vectors' components are thus determined according to the rotation matrix calculated by the deviation angle. The anisotropic wavefield-separation operators are constructed at each point using the calculated polarization vectors. Finally, the vector wavefield decomposition based on the Helmholtz theory are then used to decompose coupled qP- and SV- modes.

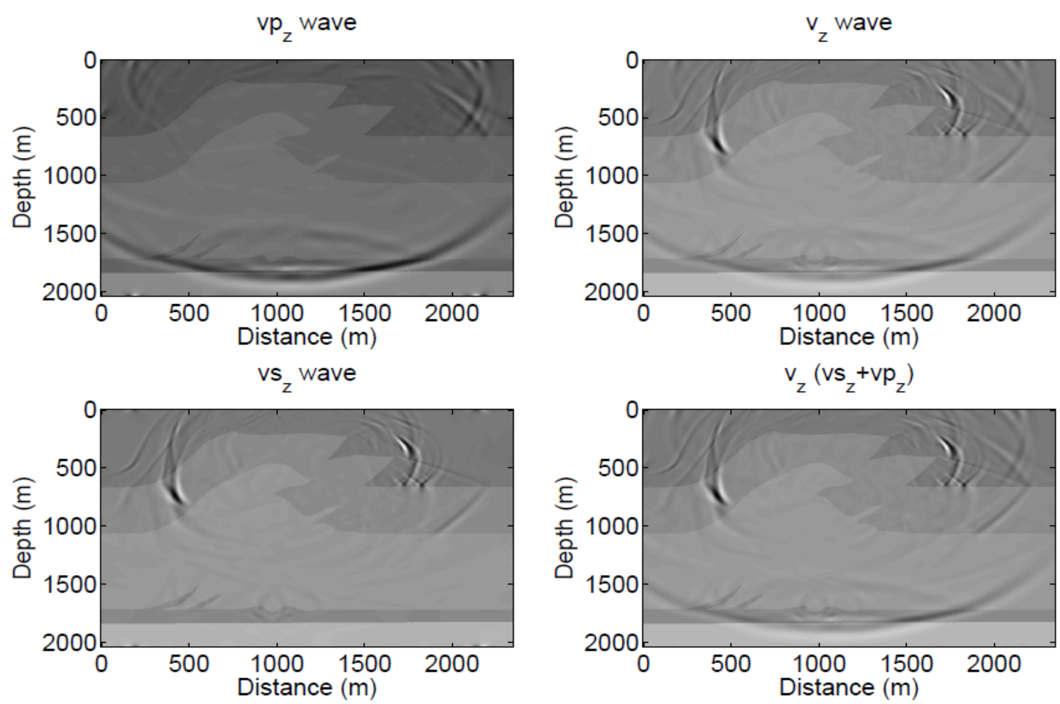

FIG. 1. The decomposed P- and S-wave components and original wave.

Gradient calculation for anisotropic FWI

Junxiao Li*, Wenyong Pan and Kris Innanen

ABSTRACT

The 3-D TTI medium can be characterized as eight parameters (5 independent elastic moduli in constitutive coordinate system, density, and tilt as well as azimuth angle) at each spatial point. One of the key issues in implementing FWI for parameter characterizing TTI media is efficient gradient calculation of objective function with respect to each model parameter. To calculate the gradient of each independent parameter involves the synthetic and adjoint data, as well as the derivatives of elastic moduli with respect to the independent parameters of the model. In this paper, the synthetic and adjoint wavefields are simulated with a staggered-grid finite-difference algorithm in anisotropic media. The derivatives of the elastic modulus tensor for TTI media are also analyzed in this paper. Numerical examples of the gradients calculation are thus illustrated in a three-layer TTI model. One of the issues addressed in the discussion is that the synthetic data at each time step should be stored on the disk so as to perform cross-correlation with the adjoint wavefields to generate the gradient for FWI in time domain. The huge dataset storage during synthetic wavefield simulation and loading when calculating the gradient is highly memory cost and time consuming. The use of random boundary layer allows us to compute both the adjoint and synthetic wavefield simultaneously without the necessity of storing total synthetic data. In this paper, cubic grains are implemented as random boundary layers. The randomized elastic moduli instead of velocities are thus added in elastic wave equations in TTI medium. The synthetic waveforms with random boundary layers are finally illustrated.

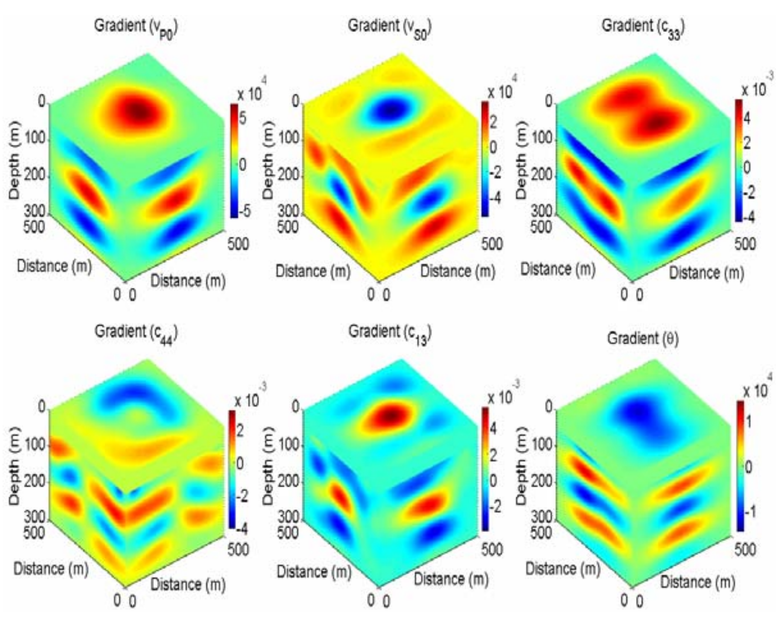

Fig. 1. Gradients of each parameters in a 3-layer TTI media

SH Waves, Rays, and Full Waveform Inversion

Laurence R. Lines*, Edward S. Krebes and P. F. Daley

ABSTRACT

With the continuous advances in high performance computing and multicomponent seismic recording, there continues to be increased interest in full waveform inversion (FWI) of seismic data. The SH-wave mode is appealing since unlike P-wave and SV-wave modes, this seismic mode does not undergo mode conversions at a boundary. SH-waves have a viscoelastic reflection response that can be modeled by finite-difference modeling, ray tracing or analytic methods. Since these modeling methods could be used in the full waveform inversion of real shear-wave data, it is important to know the differences and similarities of these methods. For pre-critical arrivals, the finite-difference (FD) viscoelastic wave modeling agrees with the viscoelastic reflection coefficients from analytic expressions even though the 2-D FD method assumes a cylindrical wave source and the reflection coefficient expression is derived for plane wave reflections. It is shown that the plane waves can be constructed from a sum of cylindrical waves with varying time delays. Near the critical angle, the plane wave method breaks down, and the 2-D FD expression would seem to be favored For real data of recorded SH-waves, full waveform inversion should take into account these amplitude differences due to 3-D spreading when using FD models. Given these considerations and the need for methods that are computationally faster than 3-D finite-difference methods, it is recommended that the 2.5D hybrid scalar wave equation of Daley et al. (2009) be used for full waveform inversion of P-wave reflection data from flat interfaces.

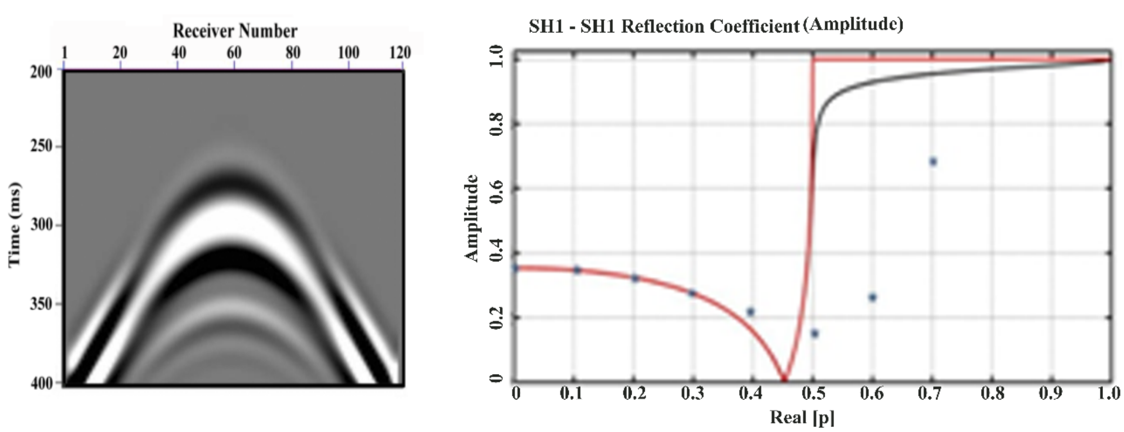

FIG. 1. (top) The SH- wave FD wave equation reflection response for a 2-layer model after removal of the direct wave. (bottom) A comparison of the SH reflection coefficients for the elastic (red curve) and viscoelastic (black curve). Agreement between FD and ray reflection response is good until near the critical angle.

Implementation of Hagedoorn's Plus-Minus method in Matlab GUI

Siming Lv

ABSTRACT

The basic theory of seismic refraction and one of the most popular refraction methods---plus-minus are elaborated. Despite of the limitations of plus-minus method, such as can only deal with single interface model with inclination angle smaller than 10° in "analyze window", researchers benefit by its convenience to roughly explore the subsurface structure and acquire significant information of layers. This pragmatic method is realized in Matlab as a graphical user interface (GUI), as a more approachable tool for beginners. From finite difference model and field data tests, usability of the tool is proved.

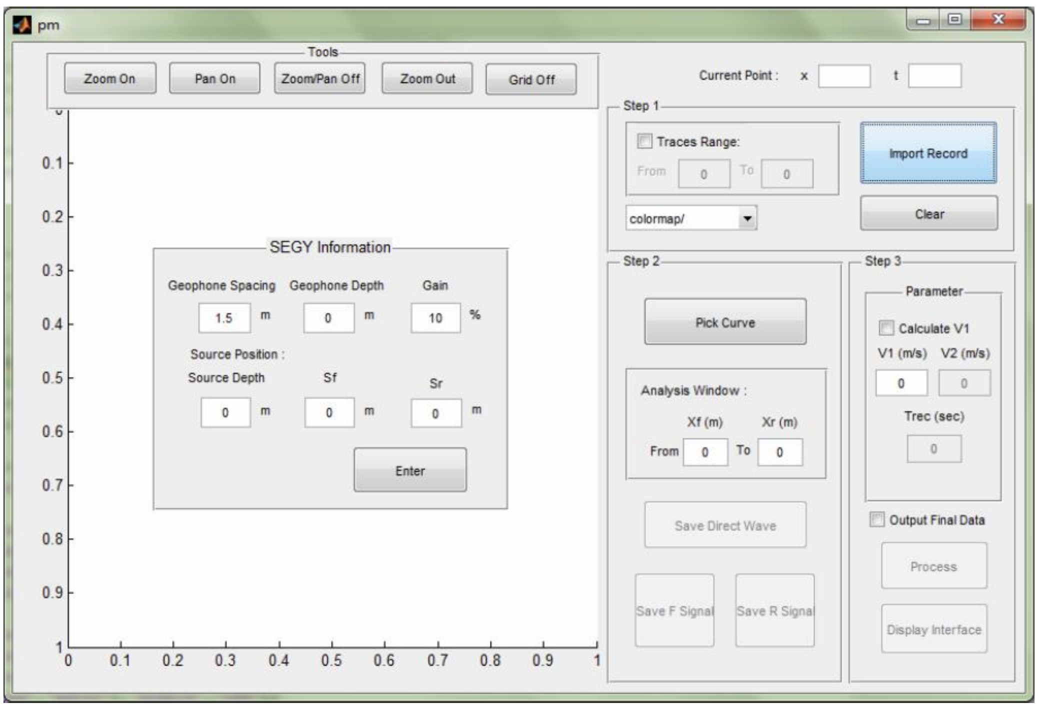

FIG. 3. Layout of "pm"

Towards characterization of intrinsic and stratigraphic Q in VSP data with information measures

Siming Lv* and Kris Innanen

ABSTRACT

The problem of distinguishing between intrinsic Q and stratigraphic filtering is a classical example of non-uniqueness in seismic data analysis. Two very different mechanisms affecting propagating waves – reverberations between thin layers and transformation of mechanical energy to heat – produce almost identical effects. A version of the Shannon entropy, defined on snapshots of a VSP wave field, has been proposed to discuss these two influences, but it so far has been used to argue that the distinction is not as meaningful as we might think. In this project the entropy calculation is extended in time domain and also to frequency domain, aiming to locate what can be separated between these two effects. Conditional probabilities in which correlation of wave field values with neighbouring values is incorporated, rather than a statistical PDF histograms of single instances of particular wave field values. 1D VSP modelling codes and a range of well logs are used to investigate the separability of intrinsic/extrinsic sources of attenuation and dispersion. Progress of this kind will have significant impact on reservoir characterization where viscosity changes are expected: such changes can be tied to intrinsic Q but not extrinsic Q. The results, in which the various processes produce noticeable differences in entropy, indicate that this is a promising line of inquiry. Parameters like bin size have a large effect on the entropy, especially at late times, so that the footprint of bin size is studied in detail.

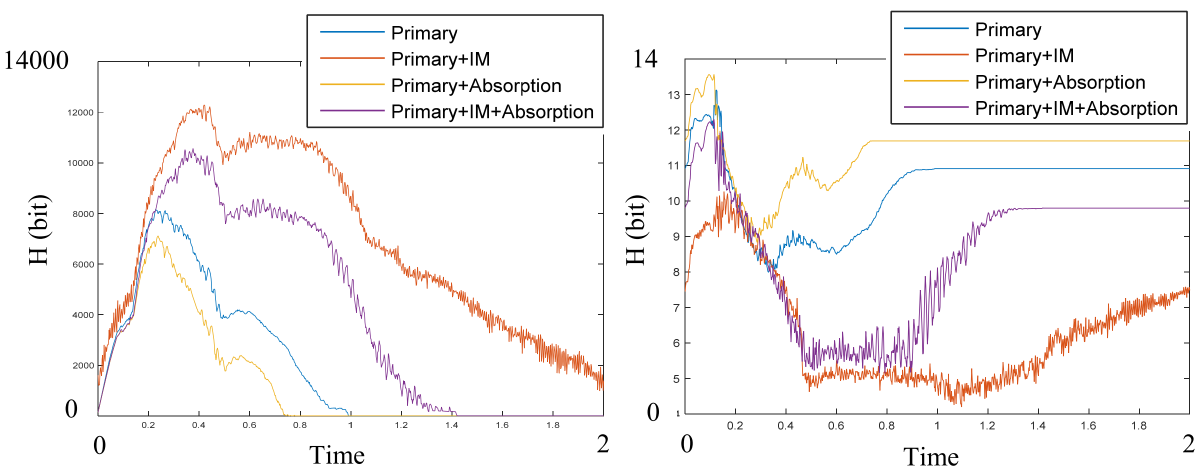

FIG. 1. The initial (left) and conditional (right) amplitude entropy variation comparison of wave fields built from well Blackfoot 1227

Feasibility study of time-lapse seismic monitoring of CO_2 sequestration.

Marie Macquet*, Don C. Lawton, Jessica Dongas and Jacky Barraza

Geological sequestration is one way to reduce our CO2 emissions in the atmosphere. Background studies are made prior to the beginning of the injection to ensure the security of this method. In the CaMI.FRS project near Brooks, Alberta, numerous wells give us information about the lithology, the porosity, the permeability, the velocities (and many others parameters) of the medium. Beside these direct data, seismic studies were conducted in order to characterize the subsurface.

After this prior work is done, numerical simulations were done in order to characterize the feasibility of the time-lapse seismic monitoring. Indeed, once the injection begins, seismic survey will be made at regular intervals to monitor the CO2 injection. Fluid simulations allow us to work on synthetic models, but yet are close to what we expect in the reality.

We use here Gassmann fluid substitution to obtain the elastic parameters (VP, Vs and ρ) for different time of injection (1 year after the beginning of the injection and 1 year after the end of the injection), for a 300m depth CO2 reservoir. In those models, synthetic data are generated then processed. This work give us a good approximation of the feasibility of a time-lapse seismic monitoring, considering the conditions of CaMI.FRS project.

a) b) c)

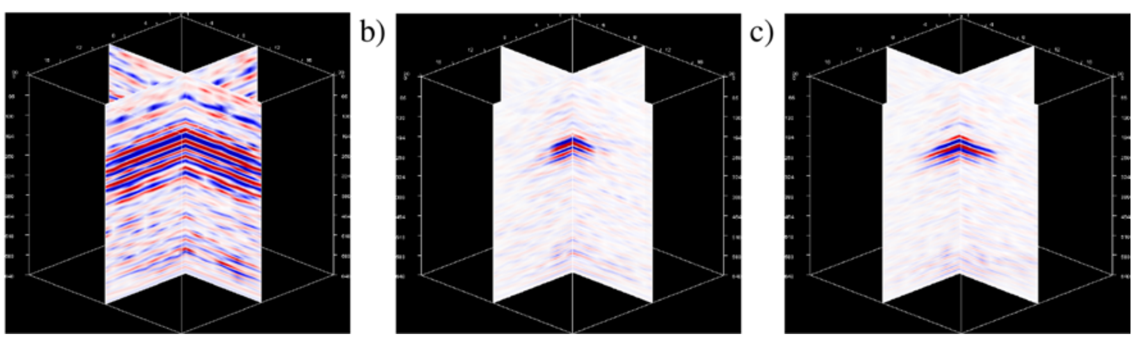

FIG. 1. Results of processing on the seismic data. a) Baseline 3D volume. b) Monitoring for 1 year after the beginning of the injection (3D volume at t = 1 year - baseline 3D volume). c) Monitoring for 1 year after the end on the injection (3D volume at t = 6 years - baseline 3D volume).

Towards seismic moment tensor inversion for source mechanism

Faranak Mahmoudian and Kristopher A. Innanen

ABSTRACT

We are working towards obtaining seismic moment tensor, M_{pq}, from amplitude inversion of multi-components microseismic data. M_{pq} describes source mechanism and can be decomposed into double-couple, isotropic and compensated-linear-vector-dipole (related to tensile fracturing) components - the tensile components might be correlated to hydrocarbon production rate. The retrieved M_{pq} is sensitive to the accuracy of source location, accuracy of the velocity model, and the receiver array geometry. While not examining the first two factors, we searched for the proper observation geometry for which the full moment tensor is resolvable. Having two vertical or surface receiver arrays, or any combination of them, the M_{pq} is fully resolvable using inversion of P- and S-wave first arrival amplitudes. This adequate configuration includes the receiver arrays located in the vertical and horizontal part of a single deviated well. Avoiding the cumbersome task of picking first-arrival amplitudes, we investigated a waveform inversion based on the method proposed by Vavryčuk and Kühn (2012). This method combines inversions in time and frequency domains. First, the source-time function is estimated in a frequency domain inversion. Second, a time domain inversion for M_{pq}, using the source-time function calculated in the first step, is applied. For this waveform inversion, we have not yet achieved the accurate retrieval of M_{pq}, but we were able to obtain an accurate source-time function estimate at this point.

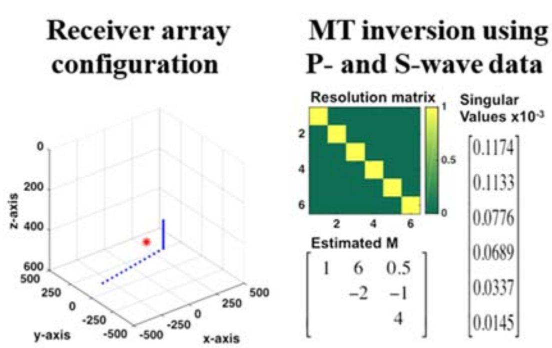

FIG. 1. Moment tensor inversion for a deviated well configuration.

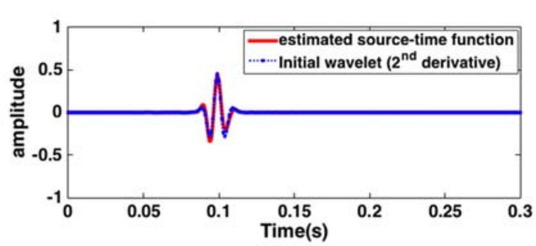

FIG. 2. Comparison of the estimated source-tim function with the initial wavelet

Attenuation and Deconvolution

Gary F. Margrave, Devon Canada Corporation

ABSTRACT

All seismic waves experience some degree of anelastic attenuation as they propagate because the earth is not a perfect, homogeneous, elastic solid. This causes the seismic wavelet to evolve as it propagates in a way characterized by progressive diminishment of high frequencies and progressive phase rotations. As a result, there is no single "wavelet" embedded in a seismic record, instead, there is a changing and evolving wavelet which has progressively lower bandwidth as traveltime increases. Mathematically, data with this property are said to be nonstationary. In contrast, the major wavelet shaping step in seismic data processing remains stationary spiking deconvolution, an algorithm that has changed very little since its introduction some 70 years ago. This algorithm explicitly assumes that seismic data are stationary, or equivalently, that the wavelet does not evolve. Data processors often cope with this conflict between physics and algorithmic assumptions by designing the deconvolution operator over a limited time window containing the exploration target. While this can optimize the image at target, the essential nonstationarity of the data is not addressed and the result is data with characteristic wavelet distortions at times outside the design window. I present a systematic study of this issue using a sophisticated synthetic dataset created with finite-difference modelling over a 2D earth whose stratigraphy comes from well logs and whose attenuation is prescribed by constant-Q theory. The study reveals the characteristic wavelet distortions that are present in real seismic data when the processing includes only stationary methods.

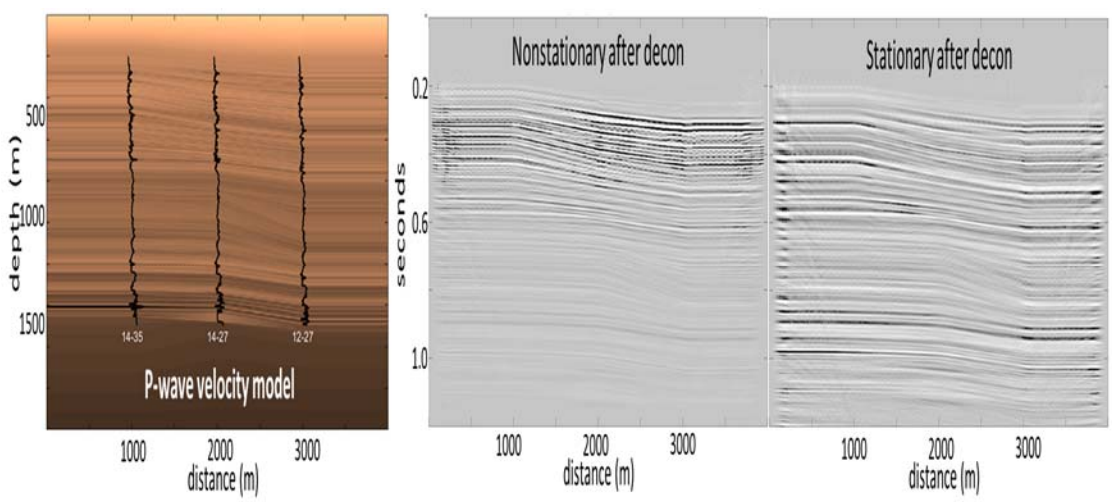

(Left) The stratigraphic velocity model used in the simulation. Stratigraphy was designed on a 2.5m grid directly from well logs. A similar density model was created. Sixty seismic shot records were simulated with and without attenuation ($Q = 50$). (Middle) The CMP stack on the nonstationary data after prestack decon using a design window roughly 0.8 to 1.1 seconds. (Right) The CMP stack of the stationary data after an identical deconvolution. The amplitude imbalance of the nonstationary data is obvious and is the tell-tale symptom of uncompensated attenuation. Although not obvious in this picture, the imbalance is frequency dependent and included both amplitude and phase errors.

Case study: measurement of Q and cumulative attenuation from VSP data

Gary F. Margrave*, Devon Canada Corporation

ABSTRACT

The measurement of attenuation in seismic data is described and analyzed. The measurement problem is defined as the estimation of the attenuation parameter Q or the estimation of the related quantity CA (cumulative attenuation) or both. Two very different estimation techniques are described: the spectral-ratio method (SRM), which is well-known, and the dominant-frequency method, which is mostly new here. The strengths and weaknesses of both methods are discussed and the extension to CA is given. It is demonstrated that CA estimates are more stable than Q estimates when attenuation is weak. The application of these techniques is demonstrated on a zero-offset VSP with a vibroseis source. Using the shallowest receiver (2185ft) as a reference, attenuation estimates were obtained for all receivers at depths equal to or greater than 5000ft. Consistent estimates were obtained from both the SRM and the DFM but it is demonstrated that any residual upcoming waves in the downgoing wave cause considerable error. The possibility of extending these measurements to the earth's surface by assuming the reference wave there is the Klauder wavelet is examined. The results are plausible and seem appropriate to apply to surface recordings for bandwidth enhancement.

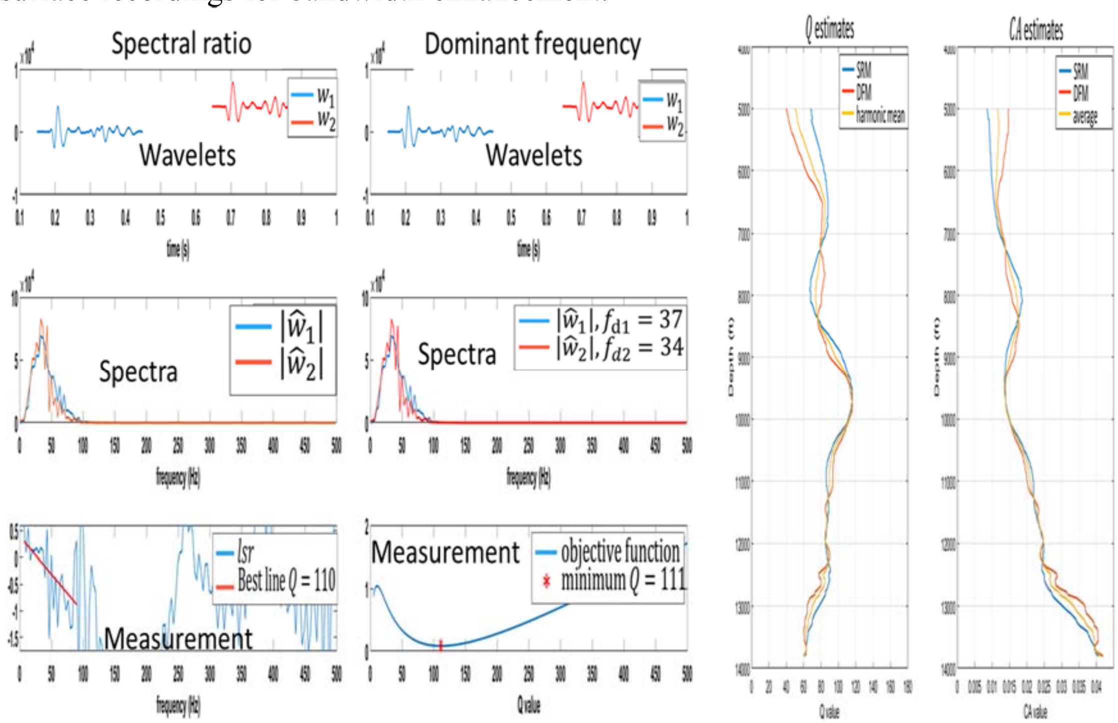

(Left) An example of the spectral-ratio method (SRM) showing the wavelets being compared, their spectra, and (bottom) the lsr (log-spectral ratio) plot. The best-fit straight line (red) has a slope which estimates Q. (Middle) A similar example for the dominant frequency method (DFM). The objective function (described in the paper) has a minimum at the estimated Q. (Right) Q and CA (cumulative attenuation) estimates from the VSP. Results from both methods are in close agreement.

Brute force analysis of residuals arising from the near surface

Andrew Mills and Kris Innanen

ABSTRACT

Variations in the elastic properties of the near surface are known to cause issues with seismic imaging and inversion, with velocity, density, and thickness variations resulting in statics problems. In particular, in contemplating FWI on land, the sensitivity of amplitude and phase information to changes in the near surface is known to be complex, but we have little quantitative information to guide us here. In this paper, an initial model with a complex near surface and deeper reflectors is studied. Piece by piece, a single characteristic (velocity, density, or thickness) is altered for a single layer or unit. The resulting shot record is compared to the original, to gauge the effect that that rock property change or geometry change has on the recorded events, for both surface waves and reflections. By subtracting the original shot record from the result, we can quantify this effect in a residual and ℓ_2 norm. Velocity changes in shallower layers are found to have the greatest effect, with changes in thickness having a lesser effect. With increasing depth, property changes have a reduced effect on the ℓ_2 norm. It is shown that a minor change in the near surface has an effect on the ℓ_2 norm orders of magnitude greater than the same change made at greater depth, demonstrating the importance of understanding the properties of the near surface.

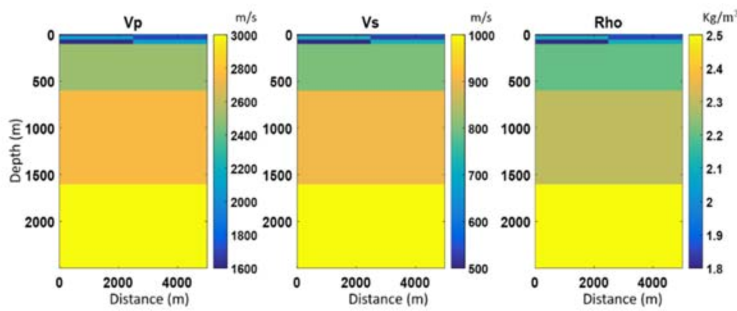

FIG. 1. Initial geologic models used for synthetic modelling.

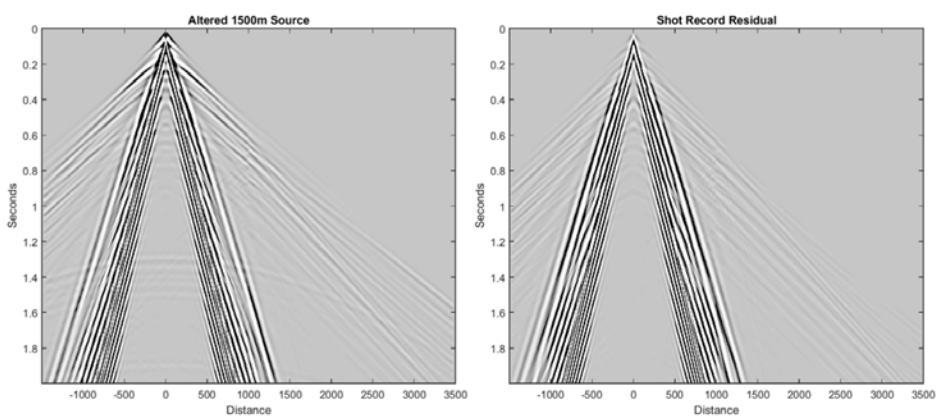

FIG. 2. Model Nsv1: Left: Shot record with second layer Vs increased by 100m/s. Right: Residual between this shot record and the original model. $\|r\|_2 = 0.0303$. This change had the greatest effect on the residual.

The effect of the near surface on internal multiples: a test of 1.5D prediction on synthetic examples

Andrew Mills, Scott Keating, Jian Sun, and Kris Innanen

ABSTRACT

Internal multiples occur in seismic data when incident energy reflects downwards within a geological layer, and are recorded at the surface as a unique reflection event. These multiples must travel at least twice (downward and upward) through a low velocity, unconsolidated near surface, possibly with different properties at each raypath location. In this paper, various geological models are tested, in which at least one internal multiple is produced from a deeper low velocity layer. These internal multiples are compared for different complexities of near surfaces, and a 1.5D multiple prediction in the plane wave domain is tested on the produced seismic data. For simple models, the 1.5D prediction is accurate, but for a laterally heterogeneous near surface, the 1.5D prediction is insufficient to correctly predict the multiples.

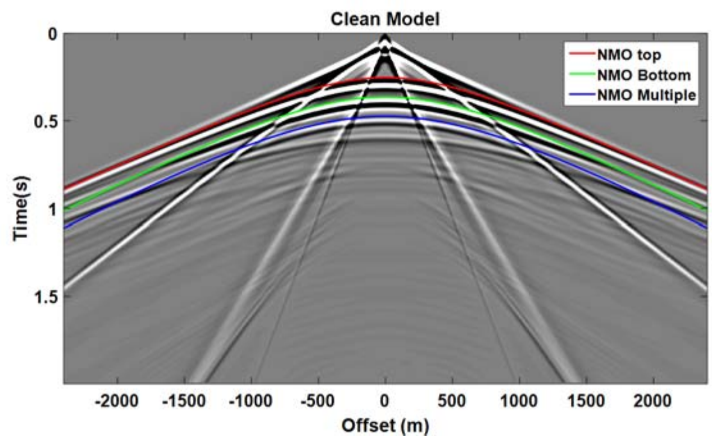

FIG. 1. Shot gather of Model 1 with NMO curves overlain of reflections from the internal multiple generator, and the first internal multiple.

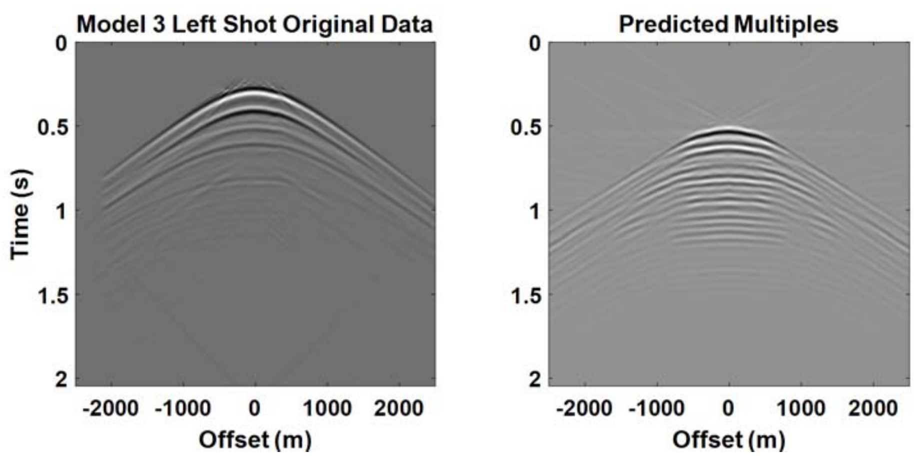

FIG. 2. Left (a): Original data for left shot of Model 3. Right (b): Predicted internal multiples from the data in FIG. 2a. Note differences in IM character at -1000m, 1000m offset.

Processing of ground roll for the study of near-surface Rayleigh wave dispersion

Andrew Mills* and Kris Innanen

ABSTRACT

In investigations of the generation of dispersion curves from shot records, it was noted that as receiver spacing increased, aliasing noise and other artefacts in the tau-p domain increased. This resulted in shear wave velocity dispersion curve “noise”, which masked the true dispersion curve. The purpose of this study is to test whether interpolation of ground roll in synthetic shot records can reduce the tau-p aliasing from sparsely sampled shot records, and as a result improve the generated dispersion curves. Synthetic shot records are generated at varying receiver spacings, then two methods of processing are tested and compared. FK filtering and muting of raw shot records to isolate ground roll followed by interpolation, and interpolation of raw shot records followed by FK filtering and muting to isolate ground roll. Dispersion spectrum noise is reduced or eliminated at low frequencies with both methods. However, when interpolation follows processing, the maximum detectable dispersion curve frequency is less than for the reverse process. This reverse process achieves an equivalent result to the original 10m receiver spacing dispersion spectra at frequencies below 35Hz.

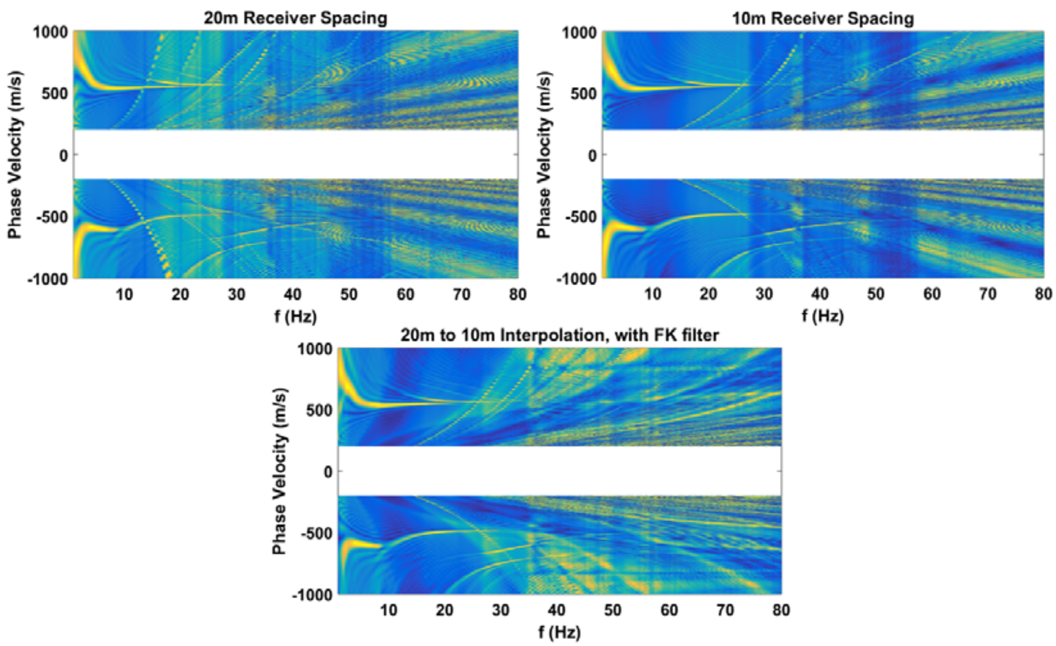

FIG. 1. Original 20m receiver spacing dispersion spectrum (upper left). Original 10m receiver spacing dispersion spectrum (upper right). Dispersion spectrum after interpolation and filtering of original 20m receiver spacing shot record (bottom); equivalent in quality to 10m spectra <35Hz.

Surface wave modelling and near surface characterization background

Andrew Mills, Raul Cova and Kris Innanen

ABSTRACT

Commonly, ground roll "noise" is removed from seismic data, and discarded. While inconvenient for reflection surveying, this apparent noise contains valuable information about the near surface. In this paper, near surface velocity and density models are constructed, and used to model elastic wave propagation of Rayleigh waves through the near surface. Existing near surface characterization techniques are briefly summarized, and used as the basis for this project. Through increasing the complexity or the near surface, issues or shortcomings in existing methods arise in Rayleigh wave dispersion analysis. These issues are identified, and methods of overcoming them are proposed.

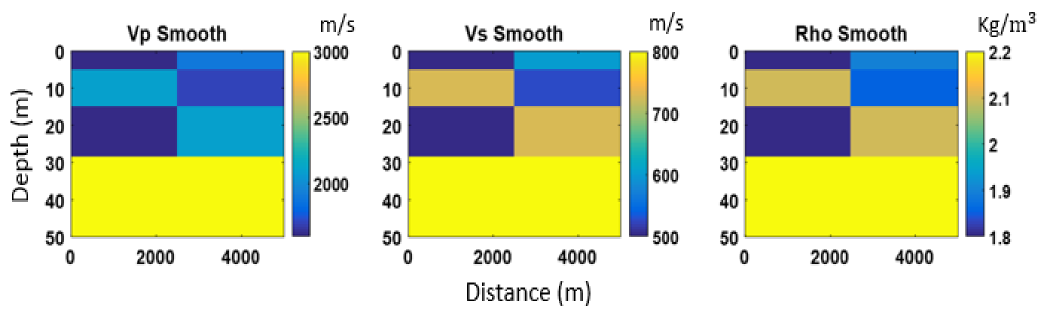

FIG. 1. Velocity and density geologic models used to generate dispersion spectra.

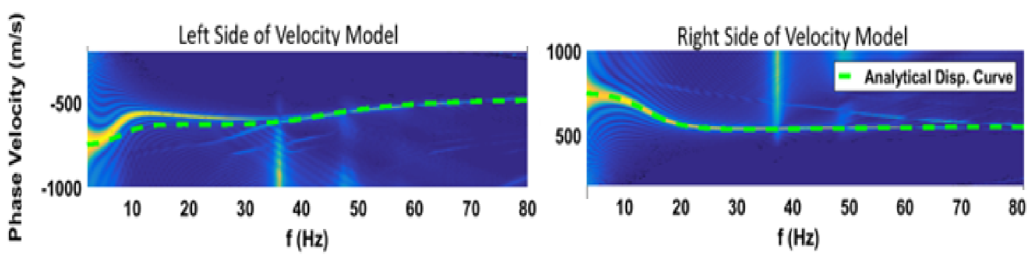

FIG. 2. Dispersion spectra generated when the source is on the vertical discontinuity of the model, at 5m depth. Left: Dispersion spectrum for the left side of the velocity model, with analytical curve overlain. Right: Dispersion curve for the right side of the velocity model, with analytical curve overlain. Note mismatch of curves in the left figure, due to surface wave reflections off of the vertical discontinuity.

Full waveform inversion sensitivities in anisotropic viscoelastic media

Shahpoor Moradi* and Kris Innanen

ABSTRACT

Scattering potentials based on the Born approximation describes the low contrast layered medium reflection coefficients for scattering of seismic waves from complex structures including the anisotropy and attenuation. The scattering of the seismic waves from a viscoelastic VTI media is well described by the scattering potential described by solutions by means of perturbation theory. The advantages of this approach is that it does not need the exact solutions of the wave equation. Our work is concerned with the scattering potential, relies on the perturbation theory, for scattering of viscoelastic waves in an anisotropic viscoelastic media. We employ the geometry of the Born approximation which provides a useful and simple language in which the amplitude variation with offset equations can be formulated effectively and clearly. The resulting expressions for scattering potentials are sensitivity kernels related to the Frechet derivatives which linearly link data and perturbations in medium properties.

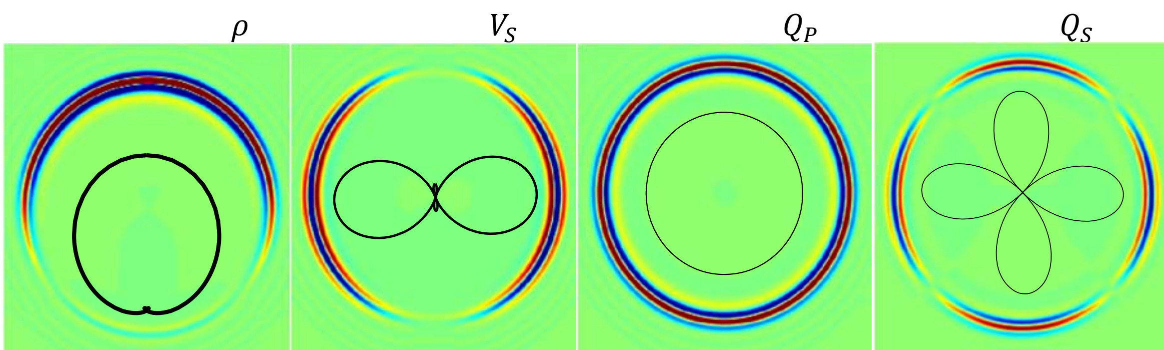

Fig. 1. Sensitivity kernels for full waveform inversion in anisotropic viscoelastic media. Black patterns refer to the theoretical results obtained from Born approximations matches with numerical modeling results.

Significance and behavior of the homogeneous and inhomogeneous components of linearized viscoelastic reflection coefficients

Shahpoor Moradi and Kris Innanen

ABSTRACT

The formulation of the amplitude-versus-offset equations for viscoelastic media is of increasing interest and importance, with quantitative interpretation of seismic data being deployed to characterize fluid presence, type, and viscosity in hydrocarbon reservoirs, CO_2 injection sites, and other exploration and monitoring settings. Properly formulated, these equations also provide insights into the character of eventual viscoelastic full waveform inversion algorithms. To date, investigations and analysis of anelastic reflection coefficients have been constructed on the assumption that the attenuation angle is unchanged across the boundary, which cannot be generally justified. We believe that a more fruitful approach approach is to apply an appropriate version of Snell's law in such way that transmitted and reflected attenuation angles are expressed in terms of the incident attenuation angle. This approach allows changes in attenuation angle to be expressed in terms of changes in velocity and quality factors, leading to new terms in the relevant AVO equations with a wider capture of anelastic reflection and transmission phenomena incorporated. We show how Snell's law can be put to work in order to learn about the homogeneous and inhomogeneous components of complex vertical slowness. We have presented a decomposition of the exact and approximate viscoelastic reflection coefficients to expose the above discussed of the attenuation angle, demonstrating the possibly significant errors resulting from its neglect, in particular in cases of for highly attenuative media.

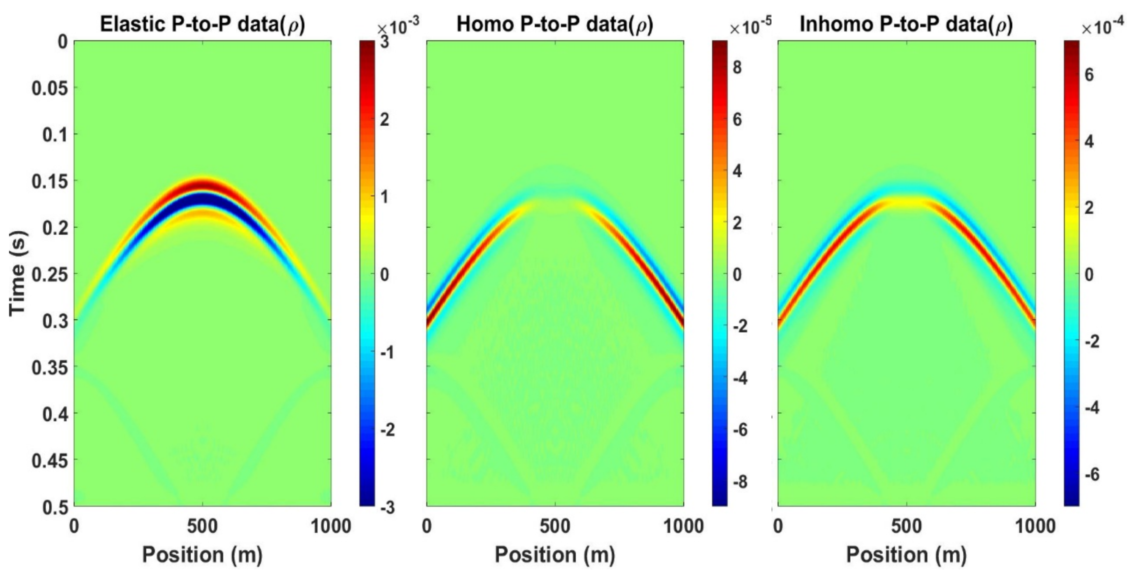

FIG. 1. Kirchhoff modeling of the elastic, homogeneous and inhomogeneous components of the linearized reflection coefficients for contrast in density.

Rock physics modeling of a bitumen saturated reservoir with unconsolidated sands

Evan Mutual*, David Cho and Kristopher Innanen

ABSTRACT

Time-lapse (4D) seismic monitoring of thermal heavy oil production represents a simple and cost-effective method of characterizing the spatial changes in reservoir conditions due to steam injection. Using 4D AVO inversion techniques, we can estimate the changes in elastic properties due to production. To understand these elastic property changes in terms of more meaningful petrophysical parameters, we must consider the rock physics associated with our reservoir. In shallow, heavy oil reservoirs such as the McMurray formation, the rock physics are complex and many standard relationships are insufficient. In this study, a 4D rock physics model is created that accounts for both the unconsolidated nature of our reservoir and the finite shear modulus associated with the quasi-solid bitumen.

Avseth et al. (2005), Bachrach et al. (2008) and Milovac (2009), among others, have noted that in such shallow, unconsolidated reservoirs we generally observe higher Vp/Vs than predicted by standard rock physics models due to a lower shear modulus. To account for this phenomenon, we apply the workflow described by Bachrach (2008) to estimate a value for fraction of non-slip contacts of 0.37 for this area. Bitumen in Alberta's oil sands behaves as a quasi-solid at in-situ conditions due to its high viscosity. As such, the bitumen has a finite shear modulus contributing to the rock's effective shear modulus. The bitumen must therefore be accounted for as a separate mineral in our rock physics modeling. To do this, we re-normalize our petro-physical logs to yield a bitumen volume that is considered as a third mineral end-member in addition to our sand and shale volumes. These re-normalized logs are used an input to a non-linear regression that estimates the bulk and shear moduli of each mineral end member. Finally, we consider the time-lapse response of the rock physics by evoking empirically derived relationships from Kato et al. (2008) to model the response of heated oil and the presence of steam. The resulting 4D rock physics model can be used to guide interpretation and if properly calibrated, as an input to a 4D rock physics inversion.

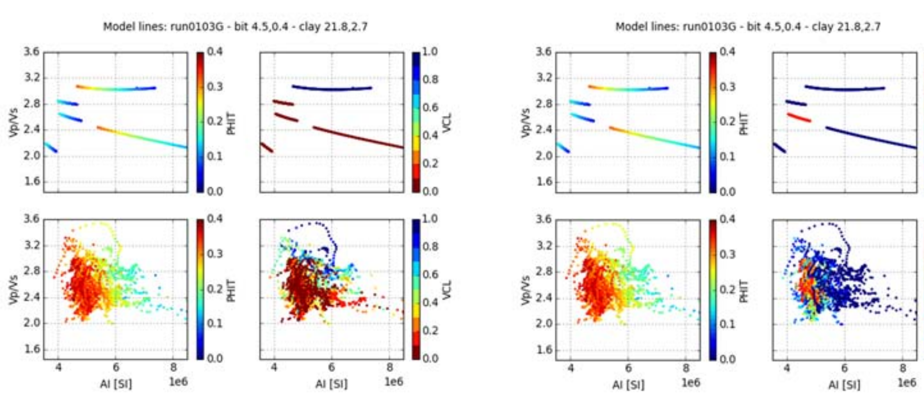

FIG. 1. Rock physics model with porosity trend lines for brine sand, brine shale, steam sand, bitumen sand and oil sand colour coded by porosity, volume of clay and volume of bitumen.

Time-lapse AVO inversion and rock physics analysis of thermal heavy oil production

Evan Mutual, David Cho, Byron Kelly and Kristopher Innanen

ABSTRACT

Time-lapse seismic monitoring of a heavy oil reservoir undergoing steam injection is a critical step in the evaluation of production efficiency, where pressure, temperature and fluid changes in the reservoir can be monitored remotely over a large spatial area without drilling costly observation wells. Seismic amplitude data can be used to image changes in the reservoir, providing a qualitative view of production related effects and their spatial extent, however, the physical cause of the changes cannot be determined from amplitude data alone. The use of pre-stack simultaneous AVO inversion of 4D seismic data, in conjunction with rock physics analysis, has the ability to quantify changes in reservoir conditions, bridging the gap between seismic amplitudes, elastic properties and reservoir parameters.

This study outlines the workflow implemented to quantify changes in reservoir conditions due to steam injection and production of an Athabasca Oil Sands bitumen reservoir. A holistic approach to interpretation was implemented, encompassing unconsolidated rock physics analysis, pre-stack 4D simultaneous AVO inversion to quantify elastic changes in the reservoir, and subsequent rock physics driven probabilistic lithology classification to separate our elastic changes into steam or gas, water, and mobile oil. Ultimately, the identification of various production related effects such as steam chamber development and mobile oil leads to improved reservoir optimization opportunities, allowing for an increase in bitumen production. Quantitative interpretation using insights from rock physics analysis provides insight into changes in actual reservoir parameters and conditions, as a function of deviations of in-situ pressures and temperatures due to steam injection.

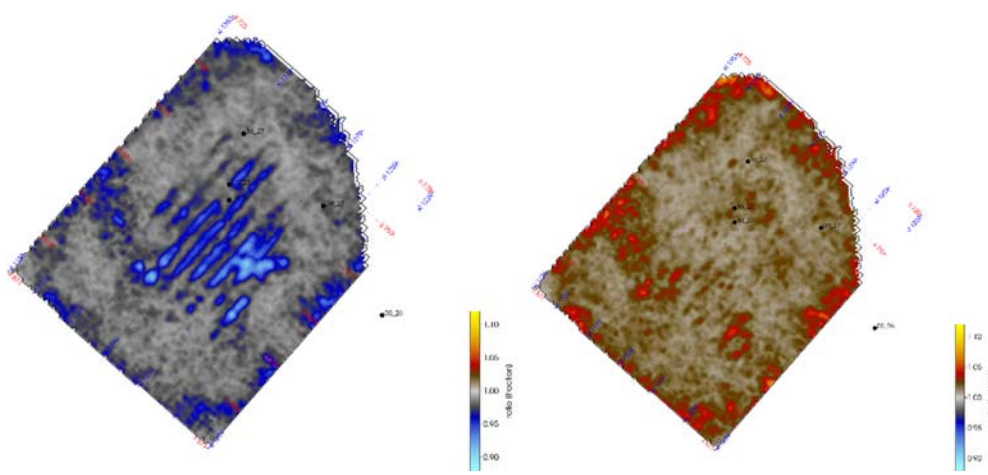

FIG. 11. Horizon slices of elastic property changes through the reservoir zone. Left figure shows decrease in Vp/Vs indicating the presence of steam and right figure shows increase in Vp/Vs, characterizing the phase change from bitumen to heated oil.

The seismic interpretability of a 4D data, a case study: The FRS project

Davood Nowroozi*, Donald C. Lawton and Hassan Khaniani

ABSTRACT

The Field Research Station (FRS) is a project developed by CMC Research Institutes, Inc. (CMC) and the University of Calgary. During the injection CO_2 in the shallow target layer (300 m depth), dynamic parameters of the reservoir as pressure and brine/CO_2 saturation will change, and they can be derived from the fluid simulation result. The injection is in the shallow target to monitor possible gas leakage and detection by geophysical methods. For the project, the injection strategy is five years' CO_2 gas phase injection with a constant bottom hole pressure equal to 49.4 bar.

In the first part of the seismic modeling, we used synthetic velocity models to compare seismic responses of a reservoir with different saturation, pressure, and plume size. Based on the synthetic models, there is an amplitude change in the reservoir and a time delay in the deeper levels because of velocity change. The effect of time delay is removed after migration with the realistic velocity model. The seismic models include VSP and cross well surveys and show high amplitudes due to gas injection, and because of lower noise content in these methods, we expect to map the reservoir properties in the early injection step by well seismic acquisition.

The surface seismic models show lower amplitudes than the well seismic methods after injection. Considering the surface related noises, the monitoring by surface seismic may not be possible in the first years when saturation and plume size are small, but the surface seismic should generate better images after several years of injection.

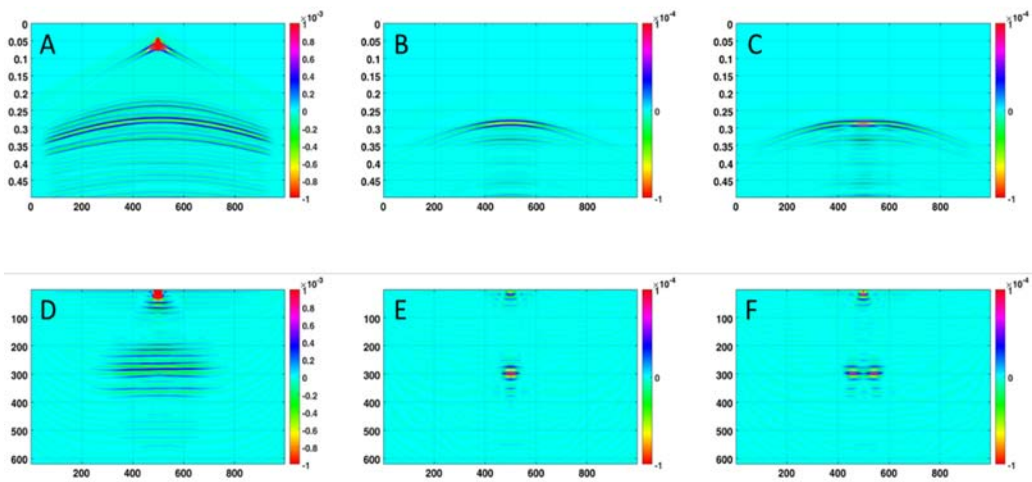

FIG. 1. The time lapse seismic models: A: The seismic model for one-year injection. B: The difference between the baseline and A. C: The difference between seismic models after five years' injection and one-year injection. D: Migrated section of A. E: Difference of migration sections between the baseline and one year's injection data. F: Difference of migrated data between five years and one-year injection data.

Elastic full-waveform inversion: density effects, cycle-skipping, and inter-parameter mapping

Wenyong Pan, Kristopher Innanen

ABSTRACT

In this research, we studied the problems when recovering elastic parameters (P-wave velocity, S-wave velocity and density) including cycle-skipping problem, density effect, and inter-parameter crosstalk issue. We find that elastic wave equation trave time method with a cross-correlation misfit function can be employed to build long wavenumber components for P-wave velocity and S-wave velocity, which helps to overcome the cycle-skipping problem in elastic FWI. Then elastic wave equation waveform inversion can be used to provide high resolution estimates of the model parameters. Density is quite difficult to be recovered, which may be caused by its insensitivity to travel time or the inter-parameter trade-off. We also propose to quantify the parameter trade-off by probing the multi-parameter Hessian. The multi-parameter point spread functions, which is proportional to one column of the multi-parameter Hessian, measure the parameter trade-off between different physical parameters more completely compared to traditional studies based on scattering patterns. The studies are verified using numerical examples with reflection survey and transmission survey.

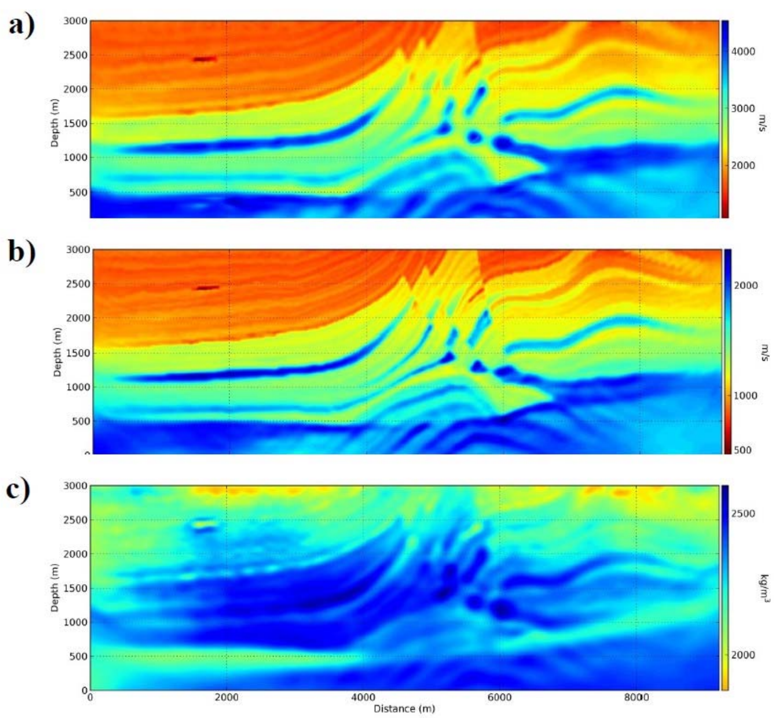

FIG. 1. (a), (b) and (c) show the inverted P-wave velocity, S-wave velocity and density respectively.

Multi-parameter acoustic full-waveform inversion: a comparison of different parameterizations and optimization methods

Wenyong Pan, Kristopher Innanen, Yu Geng

ABSTRACT

Full-waveform inversion methods allow to provide high-resolution estimates of subsurface elastic properties, which are very important for reservoir characterization. However, multi-parameter FWI suffers from parameter crosstalk artifacts arising from the inherent ambiguities (or coupling effects) among different physical parameters, which significantly increase the non-linearity of the inverse problems. For multi-parameter acoustic FWI, density is difficult to be inverted, which maybe caused by the strong parameter trade-off from velocity. Different parameterizations have different resolving abilities. An appropriate parameterization in multi-parameter FWI can help avoid parameter crosstalk and reconstruct the model parameters efficiently. Scattering patterns due to different physical parameters have been employed to study the resolving abilities of different parameterizations. In this research, we will illustrate the scattering patterns for different parameterizations in acoustic media. It has been proved that the second-order derivative (namely Hessian operator) is capable to suppress the parameter crosstalk artifacts. The Hessian-free optimization methods are generally employed for avoiding construct the multi-parameter Hessian explicitly. In this research, we compare the inversion efficiencies of different parameterizations with different optimization methods for multi-parameter acoustic FWI.

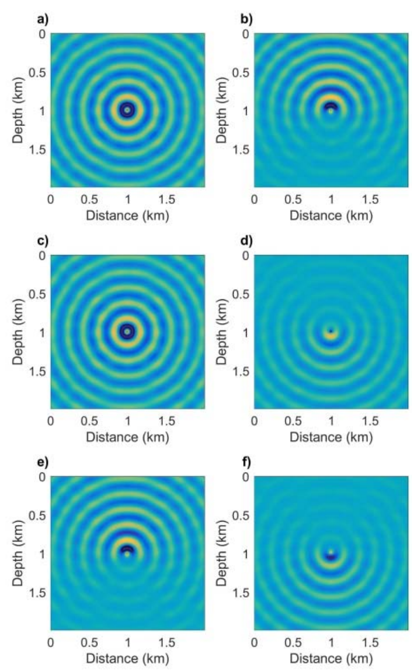

FIG. 2. (a) and (b) show the scattering patterns of velocity and density for the velocity-density parameterization; (c) and (d) show the scattering patterns of impedance and density for the impedance-density parameterization; (e) and (f) show the scattering patterns of impedance and velocity for the impedance-velocity parameterization.

Quantify parameter resolution for 3D elastic and anisotropic full-waveform inversion via multi-parameter Hessian probing

Wenyong Pan*, Kristopher Innanen, Junxiao Li

ABSTRACT

Estimating multiple physical parameters in subsurface using full-waveform inversion (FWI) methods suffers from parameter crosstalk challenge. The inherent ambiguities among different physical parameters make the inverse problems much more non-linear. The parameter resolution is highly influenced by the parameterization selected for describing the subsurface elastic and anisotropic medium. Quantify the parameter resolution for determining the optimal parameterization in multi-parameter FWI becomes essential for reducing the parameter crosstalk difficulty. In recent years, researchers devote significant effort for evaluating the resolving abilities of different parameterizations for elastic and anisotropic full-waveform inversion based on the analytic solutions of the Fréchect derivative wavefields (so called "scattering" or "radiation" patterns). However, these studies may not be able to evaluate the resolving abilities of different parameter classes completely because of the inherent defects of the scattering patterns. The goal of this research is to develop new strategies for quantifying the parameter resolution for multi-parameter elastic and anisotropic full-waveform inversion. We find that the multi-parameter Hessian, the second-order derivative of the misfit function, provides direct and complete measurements of the inter-parameter trade-off. The investigations based on scattering patterns can be interpreted as an asymptotic approximation of the multi-parameter Gauss-Newton Hessian. With the block-diagonal approximation of the multi-parameter Gauss-Newton Hessian, we are able to assess the parameter resolution by taking the geometrical spreading and complex model into consideration. Furthermore, with the adjoint-state technique, we are able to calculate one column of the multi-parameter Hessian (multi-parameter point spread function), defined as parameter resolution kernel in this research, with which we can evaluate the inter-parameter mapping of different parameters at adjacent positions locally by considering finite-frequency effects.

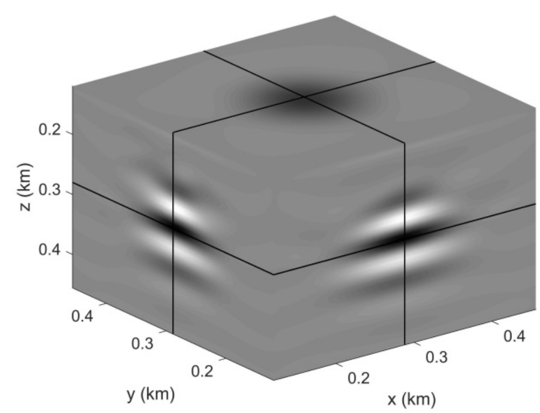

FIG. 1. Multi-parameter point spread function $\mathbf{H}_{\alpha\alpha}(\mathbf{x})$ for parameter resolution analysis in 3D elastic and anisotropic media.

IMMI's performance with different seismic acquisition parameters and random noise

Sergio Romahn and Kris Innanen

ABSTRACT

IMMI stands for iterative modelling, migration and inversion. It proposes to incorporate standard processing techniques into the process of full waveform inversion (FWI). Following IMMI's philosophy, we use a phase shift plus interpolation (PSPI) migration with a deconvolution imaging condition to obtain the gradient, and well velocity to scale the gradient into a velocity perturbation. The above contrasts with the use of a two-way wave migration method (such as reverse time migration RTM), and the use of an approximation of the inverse Hessian matrix or a line search to find the scale, as is done in standard FWI. We show the suitability of estimating the subsurface velocity model by applying IMMI's approach using a synthetic example. The results confirms that the gradient obtained with PSPI provides an adequate direction to minimize the objective function, and that well calibration produces an efficient scale to convert the gradient into a velocity perturbation. We evaluated the performance of the inversion when the maximum offset and the source interval are changed with and without the presence of random noise. Generally speaking, larger offsets and higher shot density generate better results, specially in the presence of noise. Higher folds, produced by large offsets and small source interval, improve the inversion result because the gradient is obtained by stacking the migrated data residuals.

RI (m)	SI (m)	Max offset (m)	Fold	Channels	Number of shots
10	100	2000	20	401	81

No noise

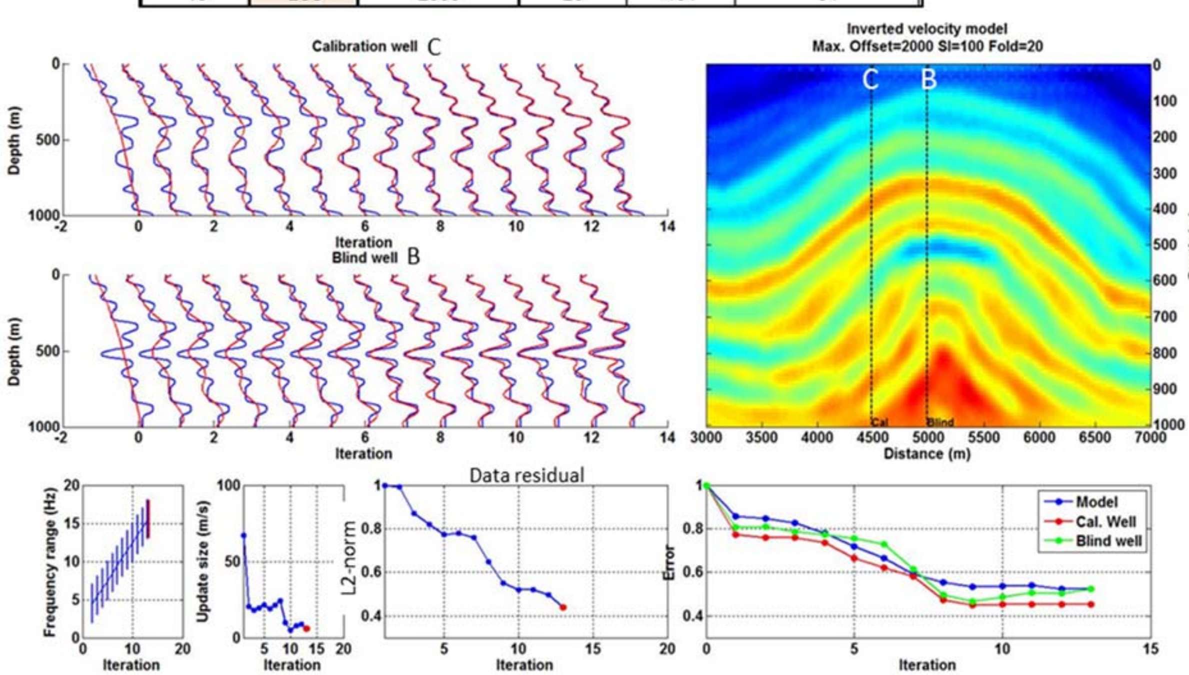

FIG. 1. Inversion performance with no noise.

IMMI: the role of well calibration in the context of high geological complexity

Sergio Romahn* and Kris Innanen

ABSTRACT

Iterative modelling, migration and inversion (IMMI) aims to incorporate standard processing techniques into the process of full waveform inversion (FWI). IMMI proposes the use of any depth migration method to obtain the gradient, while FWI uses a two-way wave migration, commonly reverse time migration (RTM). IMMI uses well calibration to scale the gradient, instead of applying a line search to find the scalar or an approximation of the inverse Hessian matrix. We used a phase shift plus interpolation (PSPI) migration with a deconvolution imaging condition that works as a gain correction. We show the suitability of estimating the subsurface velocity model by applying IMMI's approach using synthetic examples with increasingly geological complexity. We found consistently low errors in the well calibration location, even in the most complex settings. This suggests that the gradient obtained by applying PSPI migration points to the correct direction to minimize the objective function, and that well calibration provides an optimal scale. This is promising in the context of reservoir characterization, where we may have many control wells. We found that IMMI satisfactorily performs in the presence of moderate lateral velocity changes. The results indicate that well calibration is a worthy option under scenarios of strong lateral velocity changes, providing that the well is representative of the geology in the zone of interest.

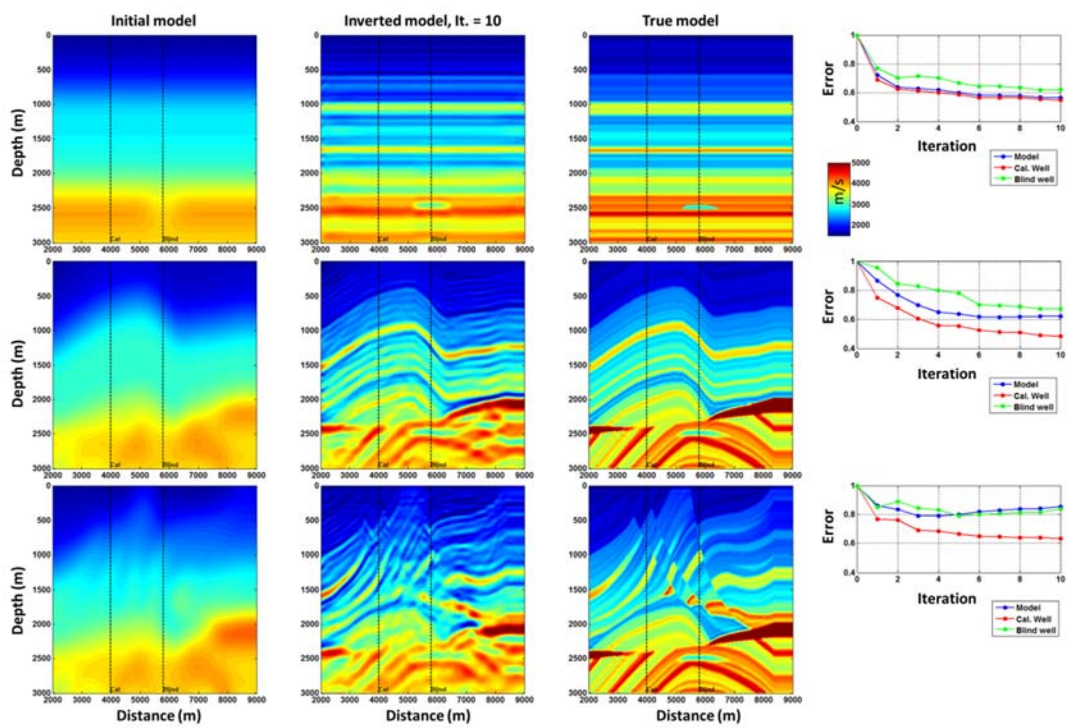

FIG. 1. IMMI's performance under three different geological settings. The error in the calibration well is consistently small in the three scenarios.

Predicting oil sands viscosity from well logs, NMR logs, and calculated seismic properties

Eric A. Rops* and Laurence R. Lines

ABSTRACT

This study is an expansion of the work from last year where it was demonstrated that oil sands viscosity could be predicted directly from standard well logs within 13% error (or 0.72 of one standard deviation) using a real viscosity dataset from Donor Company. This work has been expanded by: normalizing the well logs, using seismic properties calculated from well logs to predict viscosity, adding NMR logs as predictors, improving the viscosity training model, and including reservoir depth as a predictor.

Multi-attribute analysis enables a target attribute (viscosity) to be predicted using other known attributes (the well logs). The top well logs for predicting viscosity were: *resistivity, gamma ray, SP, NMR Total Porosity, NMR Free Porosity, and S-wave sonic.* They successfully predicted viscosity with an average validation error of 69,000cP (or 0.69 of one standard deviation). The top seismic properties for predicting viscosity were: *P-wave velocity* and *P-Impedance*. They predicted viscosity with an average validation error of 94,000cP (or 0.94 of one standard deviation). Figure 1 shows the prediction results for an example well, which models two increasing viscosity gradients from 440m to 460m, seen from well logs. The seismic properties see less viscosity variations than the well logs do.

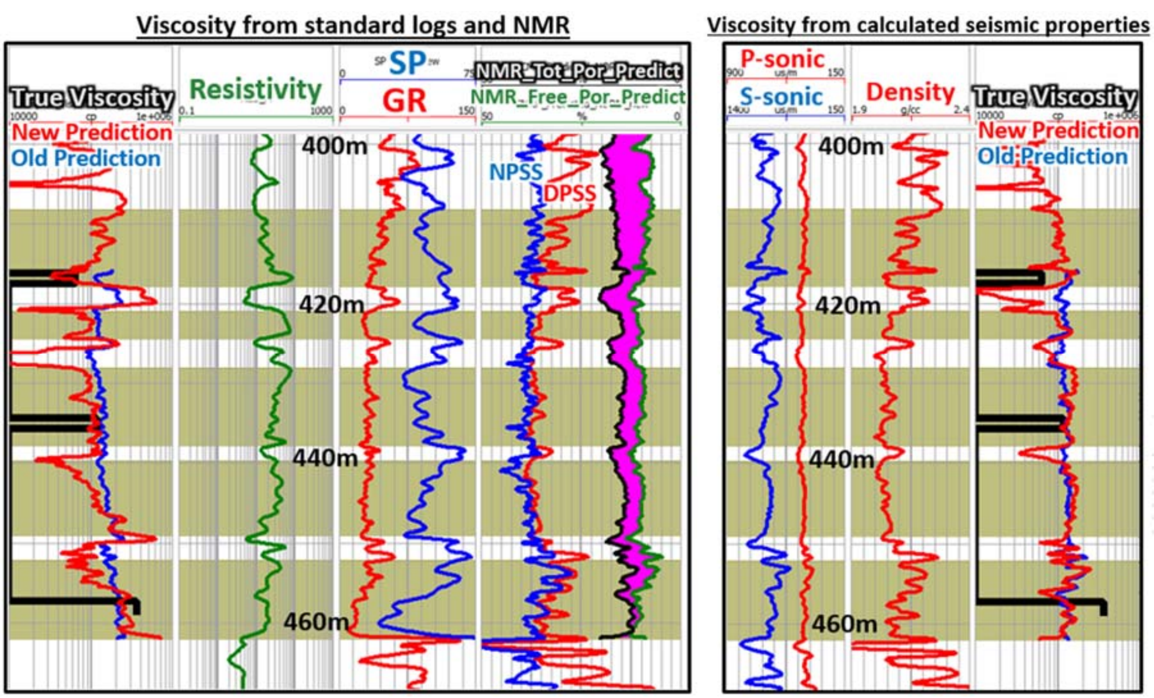

FIG. 1. Predicting viscosity from standard logs and NMR (left side), and calculated seismic properties (right side). Validation results for an example well are shown. The two outermost tracks show the true viscosity measurements (35^{0}C) in black, with the new prediction in red overtop the old prediction in blue (presented on logarithmic scales from 10,000cP to 1,000,000cP). The gold zones highlight the bitumen intervals. The magenta colored area is the separation between the NMR Total and NMR Free porosity logs, which was one of the top viscosity predictors.

Jean Morlet and the Continuous Wavelet Transform

Brian Russell*[1] and Jiajun Han

ABSTRACT

Jean Morlet was a French geophysicist who proposed a new method of time-frequency analysis based on his knowledge of seismic processing algorithms. Geophysicists did not recognize the originality of Morlet's work, but mathematicians did, and his method was re-named the Continuous Wavelet Transform, or CWT, introducing a new branch of mathematics. Morlet introduced five key ideas. First, he used the Gabor wavelet, a Gaussian multiplied by a complex sinusoid. Second, he used the Heisenberg uncertainty principle to keep the product of the time and frequency widths of the wavelets constant. Third, he defined the width of the of the wavelet envelope as an integer times the dominant period of the sinusoid, introducing the concept of shape. Fourth, he used a logarithmic increment in the frequency domain, introducing what is now called scale. Finally, he cross-correlated each of his wavelets with each input seismic trace to analyze the frequency content of the traces. This report will re-examine the ground-breaking work of Morlet.

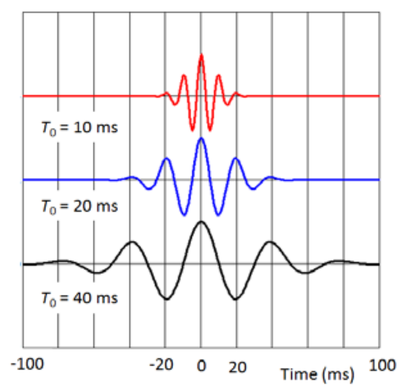

FIG. 1. Three Morlet/Gabor wavelets that preserve shape.

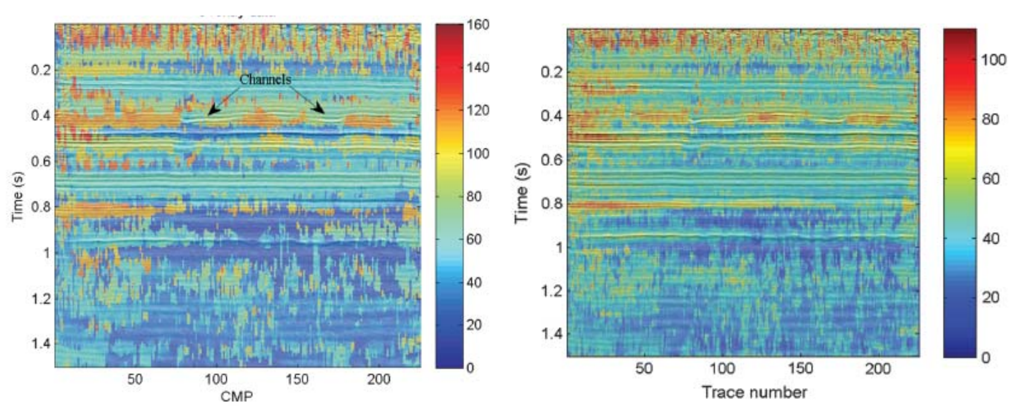

FIG. 2. The application of: (a) the short time Fourier transform (Han and van der Baan, 2013) and (b) the CWT (Herrera et al., 2014) to a seismic section from Alberta. Note the improvement in the resolution of the channels

[1] Hampson-Russell, A CGG GeoSoftware Company, Calgary, Alberta, brian.russell@cgg.com

Instantaneous frequency estimation using weighted least squares Tikhonov regularization with box constraints

Ahmed H. Sigiuk , Matthew J. Yedlin

ABSTRACT

In this report, we begin with a brief introduction into the concept of instantaneous frequency, where we use the complex analytical signal to obtain the time dependent signal phase, and differentiate the phase with respect to time to obtain the instantaneous frequency. We reformulate our problem into a weighted least squares Tikhonov regularization with box constraints, and explain the advantages of the added terms in helping to smooth and stabilize our results. We conclude with some synthetic and real data simulation results and compare the proposed algorithm results with a well-established time-frequency distribution method.

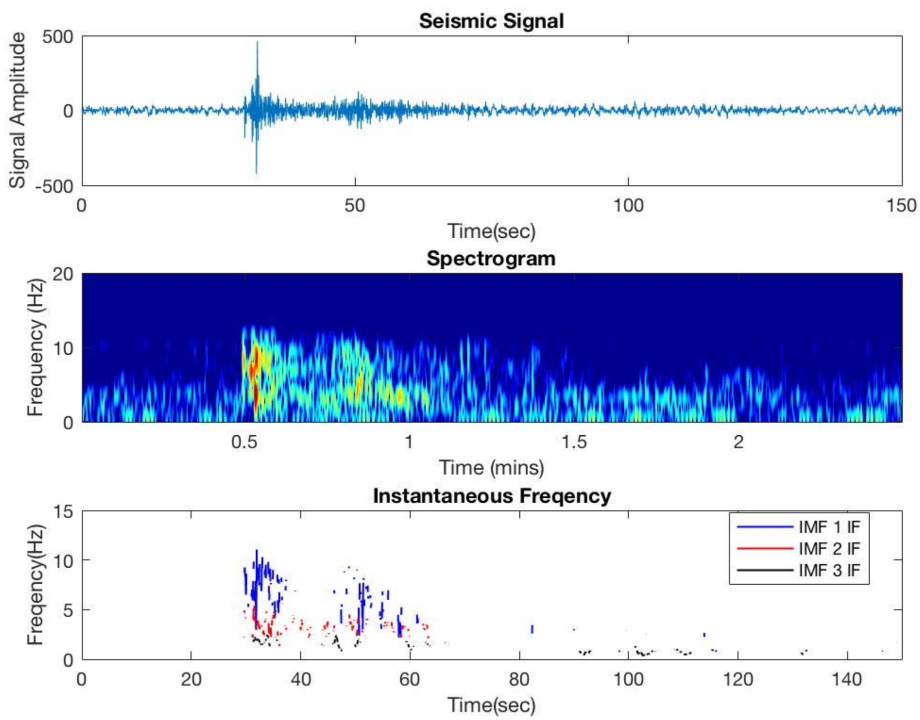

FIG. 1. Instantaneous Frequency Estimation using Empirical Mode Decomposition (EMD) and Tikhonov regularization

Implementation of predicting elastic internal multiples based on inverse scattering series: synthetic results

Jian Sun, Kristopher A.H. Innanen

ABSTRACT

Prediction and removal internal multiples is an increasingly high priority task in seismic data processing, due to the increased sensitivity with which primary amplitudes in quantitative interpretation are now analyzed, however, remains to be a big challenge. The more geological model we build approach to real, the more precise the prediction algorithm can be achieved. In a companion paper (Sun and Innanen, 2016d), we proposed a theoretical framework of elastic internal multiples prediction using inverse scattering series, which works for an elastic isotropic medium. In this paper, we investigate how to prepare the input, and concentrate on how to implement the elastic internal multiples prediction algorithm, using the seismic data generated from an elastic isotropic synthetic model. The analysis of the estimated result is also being examined.

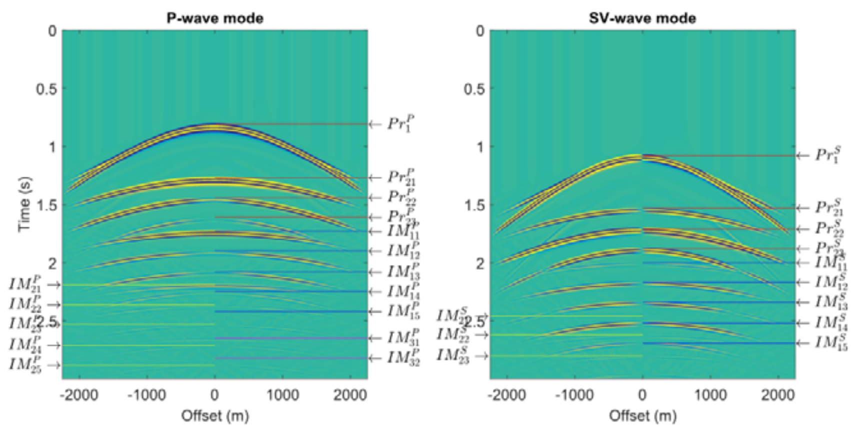

FIG. 4. Decomposed P- and SV-wave components of seismic record.

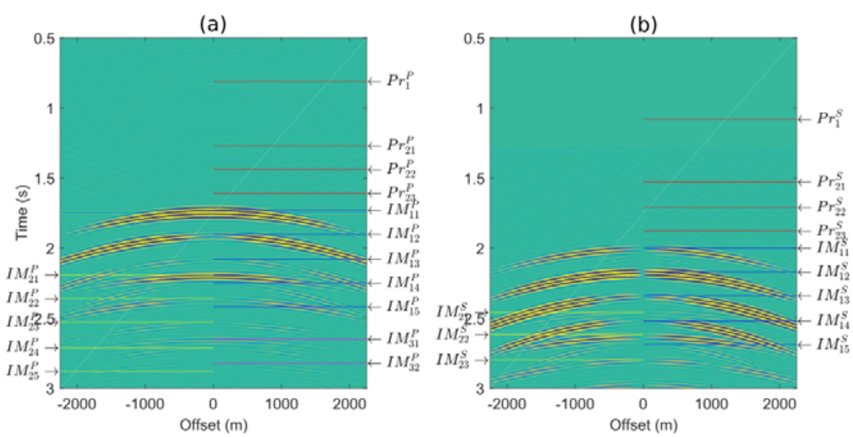

FIG. 8. Predicted elastic internal multiples occurred in Figure 4. (a) predicted elastic internal multiples in decomposed P-wave component, corresponded to data shown in left panel of Figure 4; (b) predicted elastic internal multiples in decomposed SV-wave component related to data shown in right panel of Figure 4.

Literature review and discussions of inverse scattering series on internal multiple prediction

Jian Sun*, Kristopher A.H. Innanen

ABSTRACT

Internal multiple attenuation is an increasingly high priority in seismic data analysis in the wake of increased sensitivity of primary amplitudes in quantitative interpretation, due to more information intend to be squeezed from seismic data. Removal of internal multiple is still a big challenge even though several various methods has been proposed. Inverse scattering series internal multiple attenuation algorithm, with great potential, developed by Weglein and collaborators in the 1990s, indicated that all internal multiples can be estimated by combining those sub-events satisfying a certain schema, which is the lower-higher-lower criterion. Many considerable discussions of internal multiple attenuation have been made based on inverse scattering series algorithm. In this paper, start with forward scattering series, we comprehensive review inverse scattering series internal multiple attenuation algorithm both in theoretical and its applications.

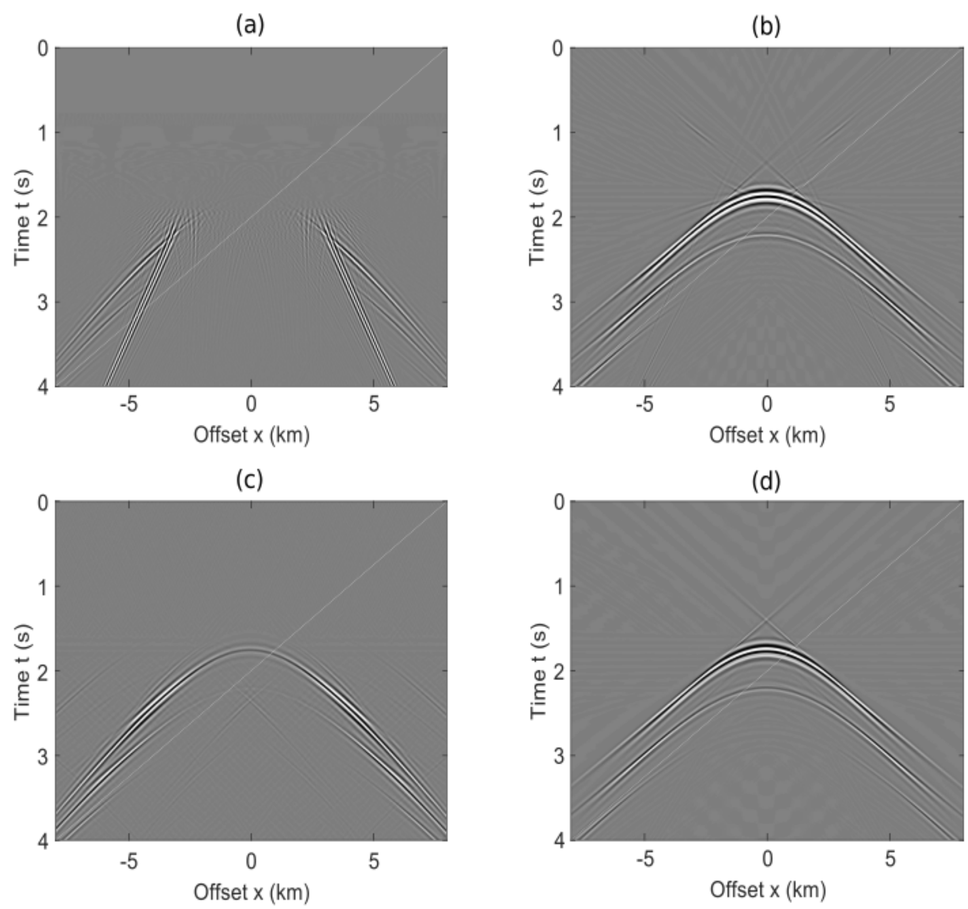

FIG. 10. The predictions of internal multiples using corresponded inputs shown in Figure 4. (a) predictions using input b1(kg,z) with a constant ϵ=0.3km; (b) predictions using input b1(pg,z) with a constant ϵ =0.3km; (c) predictions using input b1(kg,t) with functioned limits α (t,t1, ϵ_2(kg)) and β (t, ϵ_1(kg)); (d) predictions using input b1(pg, τ) with a constant ϵ =0.3s.

Theoretical framework of elastic internal multiples prediction based on inverse scattering series

Jian Sun, Kristopher A.H. Innanen

ABSTRACT

Inverse scattering series has been revealed in extremely powerful capabilities of seismic data processing and inversion, such as full waveform inversion (FWI), direct nonlinear AVO inversion, and surface-related or internal multiples attenuation, due to its property of model independence. Significant benefits have been achieved by performing internal multiple prediction using inverse scattering series in several different domains. Nevertheless, elastic internal multiples remain a significant hazard as multi-component acquisition technology has been widely applied. Unfortunately, for an elastic media, the off-the-shelf internal multiple attenuation is either inadequate or non-existent. By considering an elastic, isotropic and homogeneous media as background, this paper presents a theoretical framework of elastic internal multiple prediction using inverse scattering series.

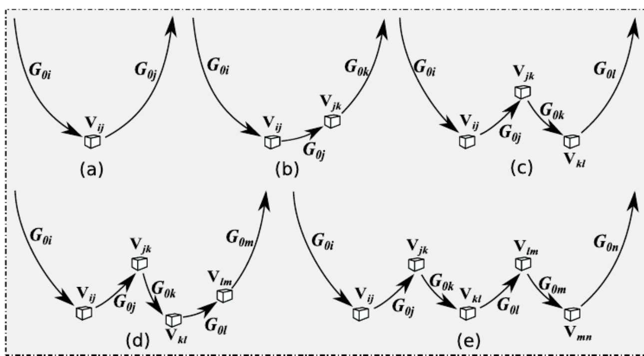

FIG. 1. Wave propagation in perturbation mode. The subscripts (i,j,k,l,m,n) denote the wave mode: { P,SH,SV }.

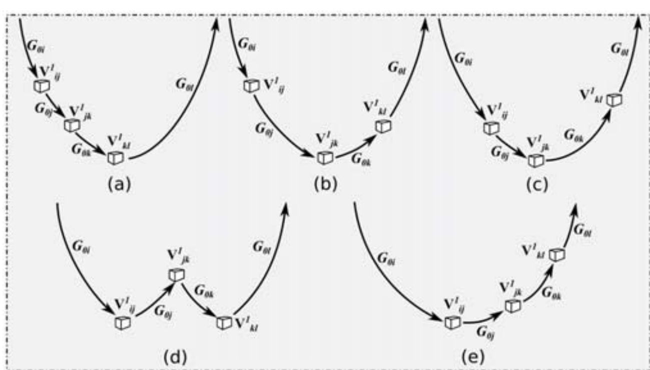

FIG. 2. Contributions of $G_{0i}V_{ij}^{33}\varphi_{0j}$ depending on variant depth (z1, z2, z3) relations between perturbations. (a) z1 < z2 < z3 (b) z1 < z3 < z2 (c) z3 < z1 < z2 (d) z2 < z1 and z2 < z3 (e) z3 < z2 < z1.

RefMod: software program for reflectivity modeling

Todor I. Todorov and Gary F. Margrave

ABSTRACT

RefMod is a software program designed to generate body-wave synthetic seismograms based on the reflectivity method. The model consists of flat elastic isotropic layers, with a point source (explosion) on the surface and receivers on the surface. The software generates two-component seismograms: vertical and horizontal components. The reflectivity method of modeling has a number of advantages. It generates high-frequency synthetics, incudes inter-bed multiples and mode-conversions. Attenuation is easily incorporated by using complex velocities. The method allows the user to turn ‘On’ and ‘Off’ the effects of multiples and mode-conversions, allowing easier interpretation of different contributions. The current implementation does not include free-surface effects.

The software is developed in JAVA programing language, which makes it platform independent: Windows, Mac OS, Linux, and UNIX. In order to run the software, the user must install Java Virtual Machine (JVM) from the Oracle website. It is multi-threaded, i.e. one can use the power of multi-core processors. The generated vertical and horizontal component shot gathers can be exported as a SEGY file.

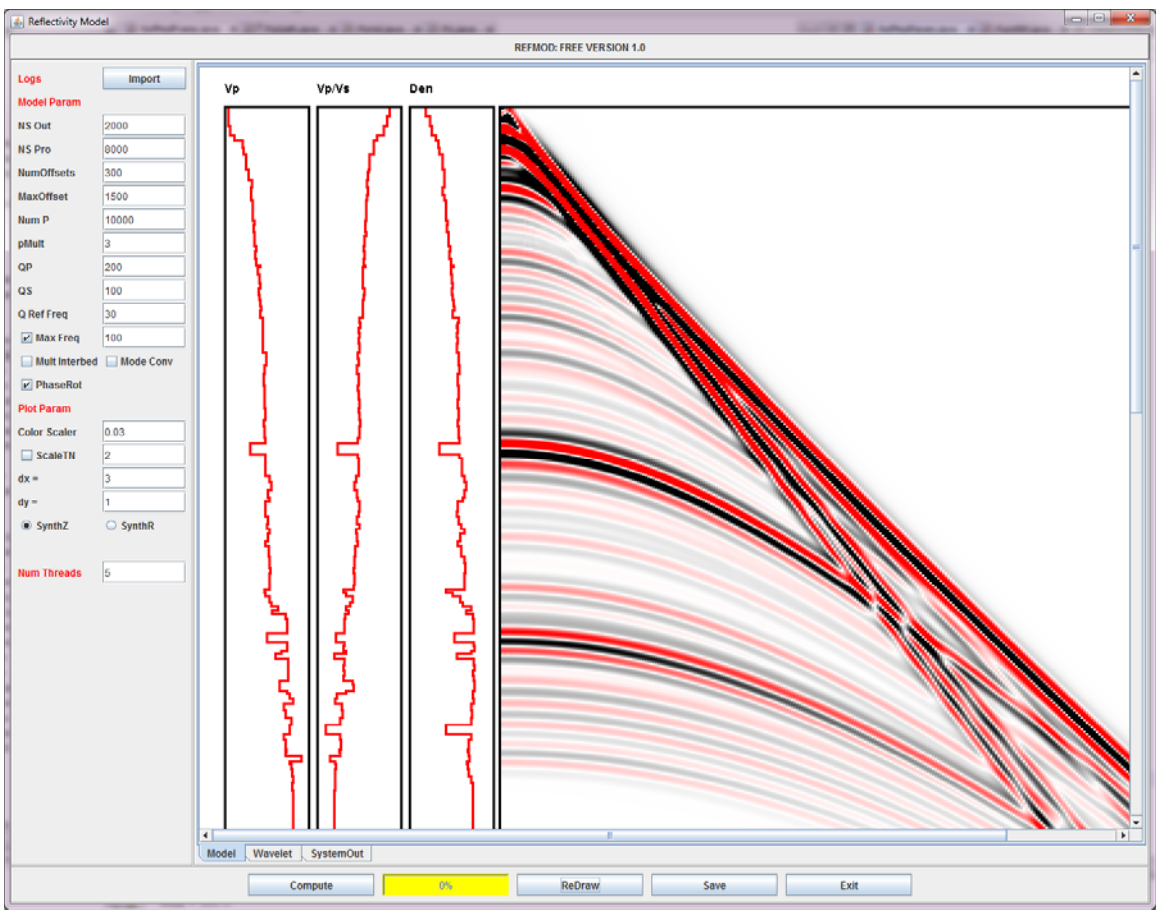

FIG. 1. RefMod: software program to generate seismograms based on the reflectivity method.

Five-Dimensional Interpolation: exploring different Fourier operators

Daniel Trad*

ABSTRACT

Five-Dimensional interpolation has become a very popular method to pre-condition data for migration. Many different implementations have been developed in the last decade, most of them sharing a similar dataflow and principles, which is applying sparseness to a transform calculated by inversion, and mapping back to a new seismic geometry. In this report, I explore three different ways to implement the mapping between data and model in the context of Fourier transforms. These three methods are multidimensional Fast Fourier transform, Discrete Fourier Transforms, and Non-Equidistant Fast Fourier transforms. I incorporate the three operators inside the same inversion algorithm, to be able to perform a fair comparison between them. The main difference between these three transformations, one that affects their efficiency and flexibility is whether they use exact input spatial locations or some approximation achieved by multi-dimensional binning, either direct or with some intermediate interpolation. When using exact locations, these transformations become computationally expensive to invert. When using binning these transformations are efficient and can handle large window sizes and gaps, but lose precision and flexibility to adapt to narrow azimuths and long offsets. What is interesting about Fourier transforms, and maybe the reason why they are still used the most in industry, is that they seem to adapt well for either approach. The subject of this paper is to explore how Fourier interpolation performs in one or the other case.

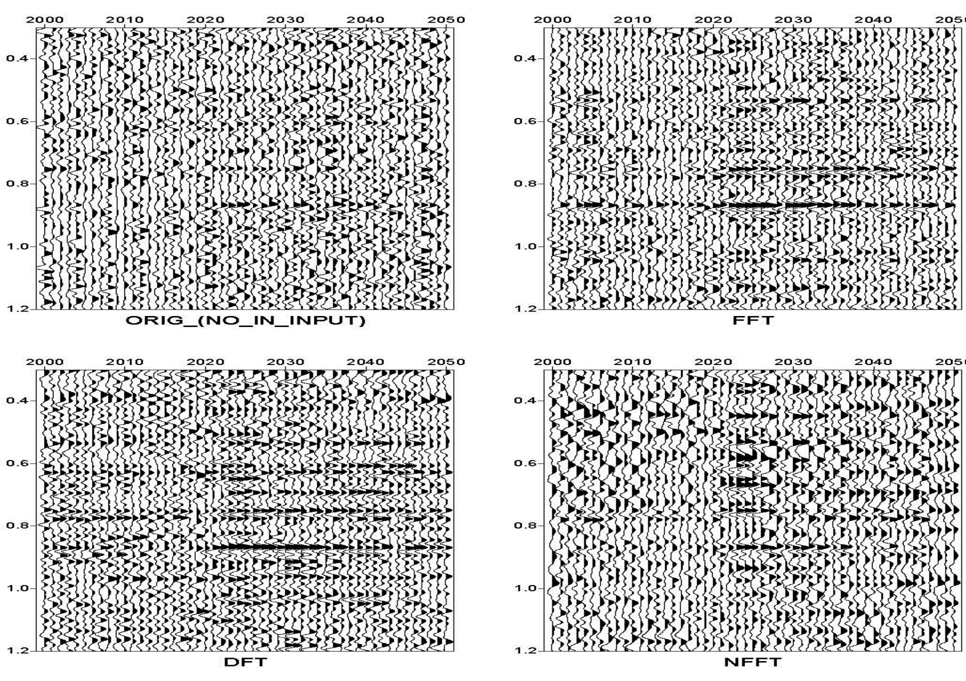

FIG. 4. Decreasing receiver line spacing in Brooks data set. a) Original receiver line, not in input. b) Predicted by FFT algorithm, c) Predicted by DFT, d) Predicted by NFFT.

Nuts and bolts of least squares Kirchhoff migration

Daniel Trad*

ABSTRACT

Least squares migration has been an important research topic in the academia for about two decades, but only recently it has attracted interest from the industry. The main reason is that from a practical point of view its ratio of benefit/cost has not been sufficient for its use in seismic exploration. Another problem is that these benefits are mixed with effects from the filtering techniques used to regularize the inversion, which are computationally much cheaper. In this report, I discuss some challenges with least squares Kirchhoff depth migration. This algorithm, although less precise than the more popular least squares reverse time migration, has the advantage of being fast enough to be applied in a production environment, and flexible enough to be applied without data regularization. This last characteristic makes it a good candidate to understand benefits in terms of footprint acquisition and aliasing. In addition, its limitations in terms of modelling/imaging accuracy make more evident some problems that exist but are often ignored when using reverse time migration with synthetic data. This work focuses on some implementation issues that are not often mentioned in other papers. First I discuss the effects of amplitude weights: by testing on a flat synthetic reflector I compare spectra, amplitude preservation and convergence when using different weights and imaging condition. Second I apply least squares migration to the Marmousi data set, and compare the previously discussed effects. Also, I show the impact of traveltime tables on the convergence and the predictions. Finally, I explore some connections with seismic data interpolation, and show examples of data prediction using time and depth migration.

Depth Migration

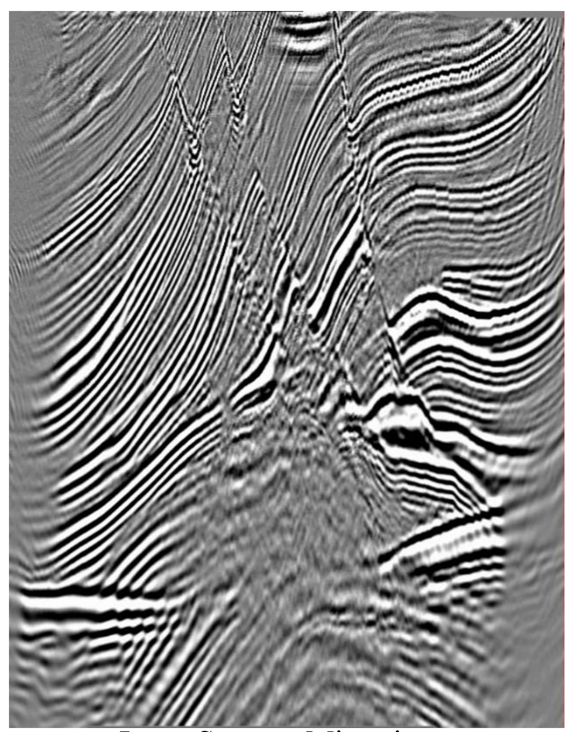

Least Squares Migration

Integrating Seismic Derived Rock properties with Horizontal Well Induced Fractures in the Duvernay

Ronald Weir, D. Eaton, L Lines, D. Lawton

ABSTRACT

The Duvernay formation is a major zone of interest for unconventional oil production. It is the stratragraphic equivalent of the lower Leduc, and is commonly believed to be the source rock for most of the Devonian age production in Alberta. Microseismic Techniques have been used to evaluate the efficiently of hydraulic fracture stimulations. The Duvernay has been drilled horizontally, and hydraulic fracking has been deployed to enhance oil production. Microseismic surveys have been carried out in a number of areas to determine fracture length, height, and general efficiency of the completion. In this paper, a method of using seismic attributes is proposed to optimize drilling programs. Seismically derived geological attributes can be used in the well placement and fracture stimulation intervals to optimize recovery. To date, most Duvernay drilling patterns have been laid out in a uniform pattern, orthogonal to the regional stress, or parallel to the boundaries of the oil lease. localized geological rock properties are used in the initial planning stage, but not in well placemen; a common assumption is the rock is uniform, and fractures will occur governed by the regional stress regime. Seismic derived attributes can provide valuable information with respect to well placement, and what facies are favorable to hydraulic fracture stimulation, fracture length, and direction. Seismic attributes can and should be used to direct horizontal well placement, as well as completion programs. Some completions perform well, whilst others fail. Fracture patterns and induced seismicity may preferentially follow geologic depositional patterns; this should be considered in well planning.

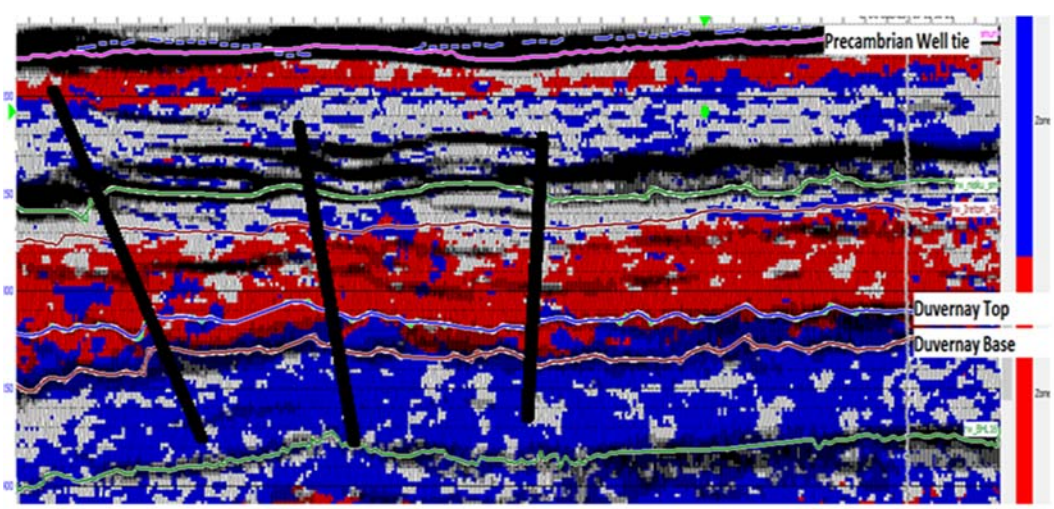

FIG. 1. Seismic display of Young's Modulus Vs Poisson`s Ratio. The colours are derived from the E (Young's Modulus) vs. Poison Ration Cross Plot. The zone of interest, The Duvernay is marked at 1325 ms. Note the variance from NE to SW. in the Duvernay interval. The Blue zone indicates more brittle rock, the red, less. According to this, a hydraulic fracture at the well bore would perform well; an induced fracture at 5426 (red colour) would perform poorly. (three deep seated faults have been interpreted on this 2-D line cutting the Duvernay).

Prestack seismic analysis of the Rangeland Basal Belly River gas pool, Alberta

Ronald Weir, D. Lawton, L Lines

ABSTRACT

The Basal Belly River is a member of the Belly River Formation (BBR), and is the lowermost member, deposited as a marine or tidal sequence. It is a known oil and gas producer throughout Alberta. In the Rangeland area, the Basal Belly River is at a depth of 725 meters, and has a pay thickness of up to 7 meters. Seismic analysis was performed by using forward modeling, and comparing it to actual seismic data. Poststack, and pre stack seismic models were generated, based on the parameters of the 2-D data, and petrophysical parameters derived from well logs. The seismic data was reprocessed, correlated and interpreted using conventional methods. The results indicate the Basal Belly River gas play is a viable seismic The Basal Belly River pool in Southern Alberta is Upper Cretaceous in age. It is a exploration and development target using pre stack data analysis.

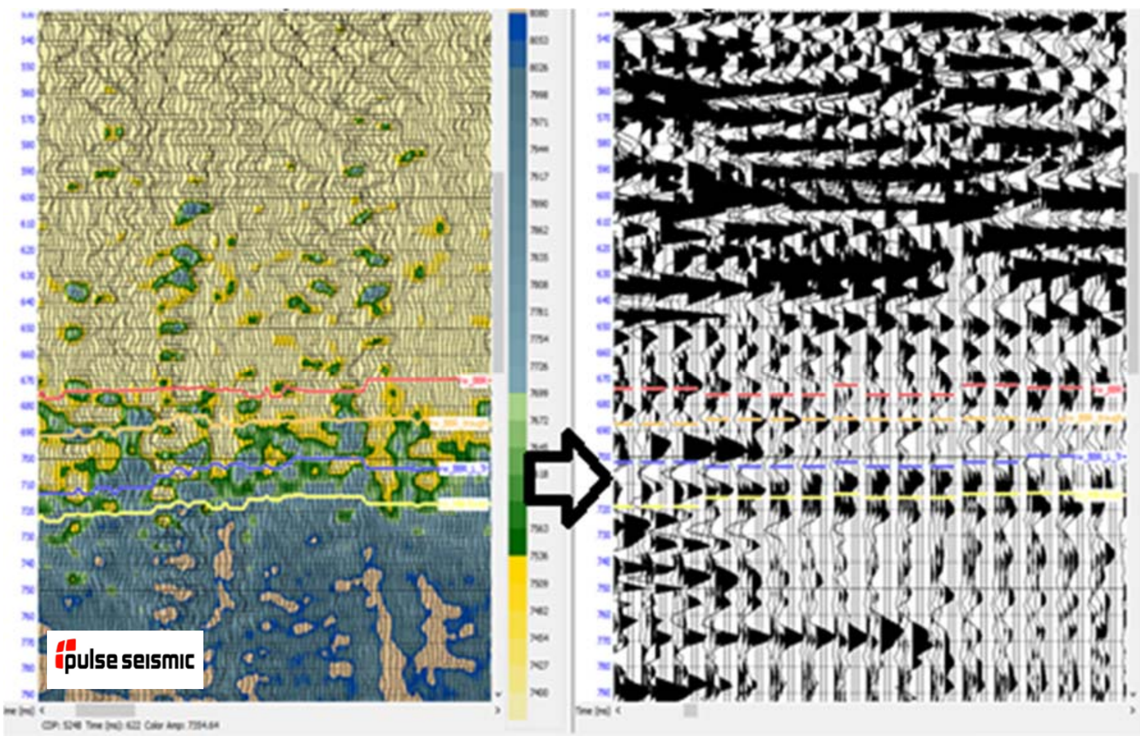

100/04-12-038-22W4, CDP 5254, SP 2627. The location is projected into the line from 150 meters north. The arrows show the projection of the well bore and the target zone. The CMP super gathers show a strong increase in AVO, the Zp inversion shows a weak low impedance anomaly. This is the thickest BBR gas well in the area, 7 to 8 metres of pay. This is a strong direct correlation between AVO effect and gas pay.

Enhancing reflection SNRs on seismic field data acquired using multiple vibrators driven by m-sequence pilots

Joe Wong and David Langton

ABSTRACT

In field tests using filtered m-sequence as quasi-orthogonal pilots to drive two or four vibrator sources simultaneously, we have found that reflections on the deblended common-source gathers are somewhat degraded by vibrator-to-vibrator crosstalk and by weak artifacts with moveouts running parallel to direct arrivals. Deeper analysis of the results lead us to conclude that crosstalk can be minimized by keeping the distance between adjacent vibrators to 100m or less. Also, judicious application of localized slant stacking to the deblended common-source gathers reduces the artifact amplitudes and increases the signal-to-noise ratios of reflections. We conclude that, by following these operational and processing steps, it is possible to efficiently conduct high-resolution 3D surveys with four vibrators controlled by m-sequence pilots and running simultaneously.

Figure 1 shows the common-source gather (CSG) for vibrator V1 extracted from blended field data by crosscorrelation with the appropriate m-sequence pilot. The blended field data were acquired with four vibrators V1-V4 spaced 50m apart, controlled by m-sequence pilots, and running simultaneously. The figure exemplifies the gain in reflection signal-to-noise ratios after artifact reduction and slant stacking.

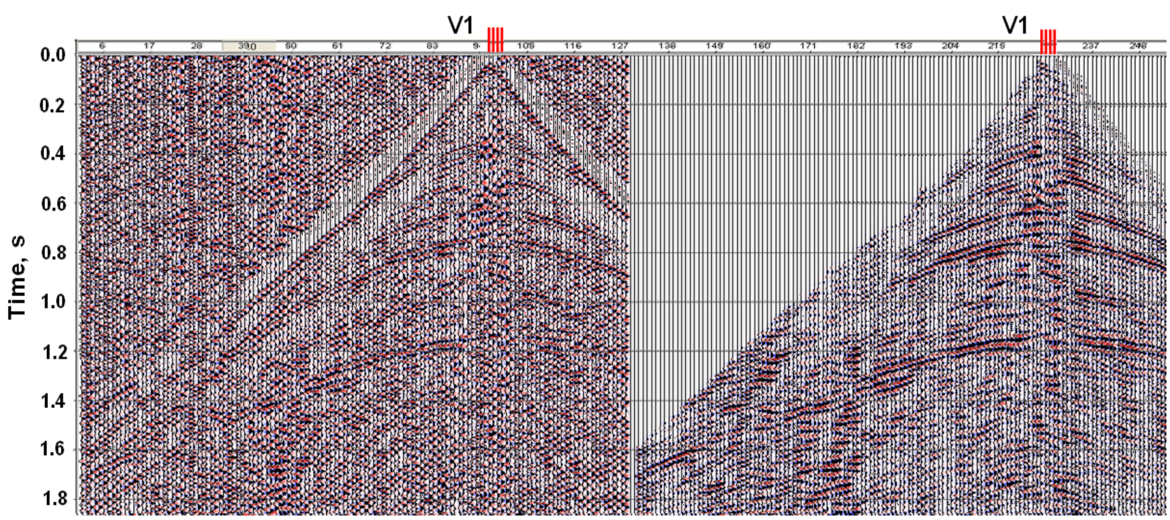

FIG. 1. AGC plot of common-source gather deblended for vibrator V1. The left plot is the CSG after bandpass filtering to remove ground roll. The right plot is the filtered CSG after artifact cancellation and local slant stacking to enhance reflection amplitudes. Vibrator spacing and trace separation are 50m.

Physically–modeled 3D survey over a channel structure

Joe Wong, Kevin Bertram, and Kevin Hall

ABSTRACT

We set up a physical model consisting of a PVC slab overlying an acrylic slab with a cut channel with both immersed in water. A 3D marine survey was conducted over an area with scaled X-Y dimensions of 5000m by 5000m. Both source and receiver lines were along the Y direction, with line separations of 100m. Source and receiver intervals along the lines were 50m. The thickness of the water layer was 500m.

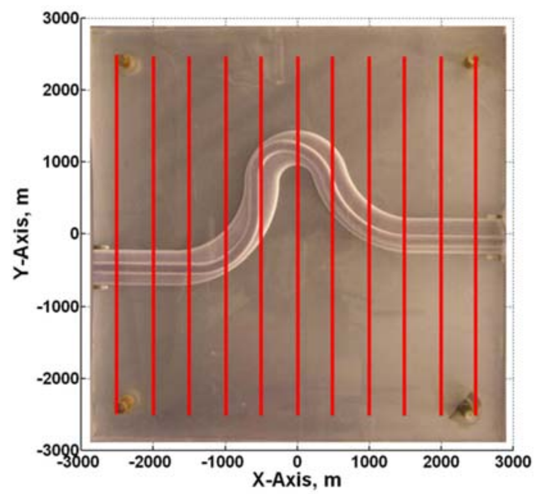

FIG. 1. The channel model with a few survey lines shown in red.

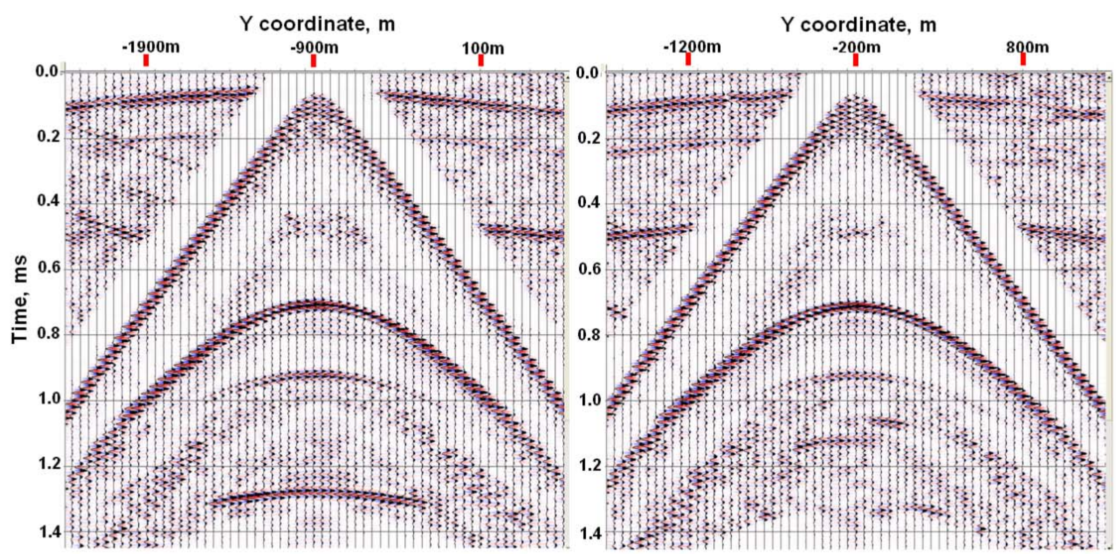

FIG. 2. Common source gathers, for line with X = -1500m. Left: source is at Y = -900m, well away from centre of channel. Right: source is at Y = -200m, almost at centre of channel.

Picking far-offset arrival times on common-source gathers

Joe Wong

ABSTRACT

A processing flow that uses a modified energy ratio (MER) attribute is effective for automatically picking first-arrival times near the hyperbolic apexes of common-source gathers. At the flanks of the hyperbolas, where the source-receiver offsets are large and the signal-to noise ratios of the first arrivals are small, a signal-enhancement technique using a three-trace summation along a range of time-space slopes must be used to increase signal-to-noise ratios before MER picking.

Even after signal enhancement, many of the MER picked times at far source-receiver offsets will be outliers. However, when source-receiver offsets are large, arrivals on common-source gathers tend to have time moveouts that are almost linear with receiver position. A Radon transform helps to identify slowness and time-intercept values that most closely match the observed linear trends.

Outlier MER picked times will have large deviations from the linear trends identified by the Radon transform. These outliers can be eliminated, and the remaining times and their receiver positions can be fitted with least-squares straight lines. The fitted lines provide interpolated times for those receivers with missing or rejected MER times.

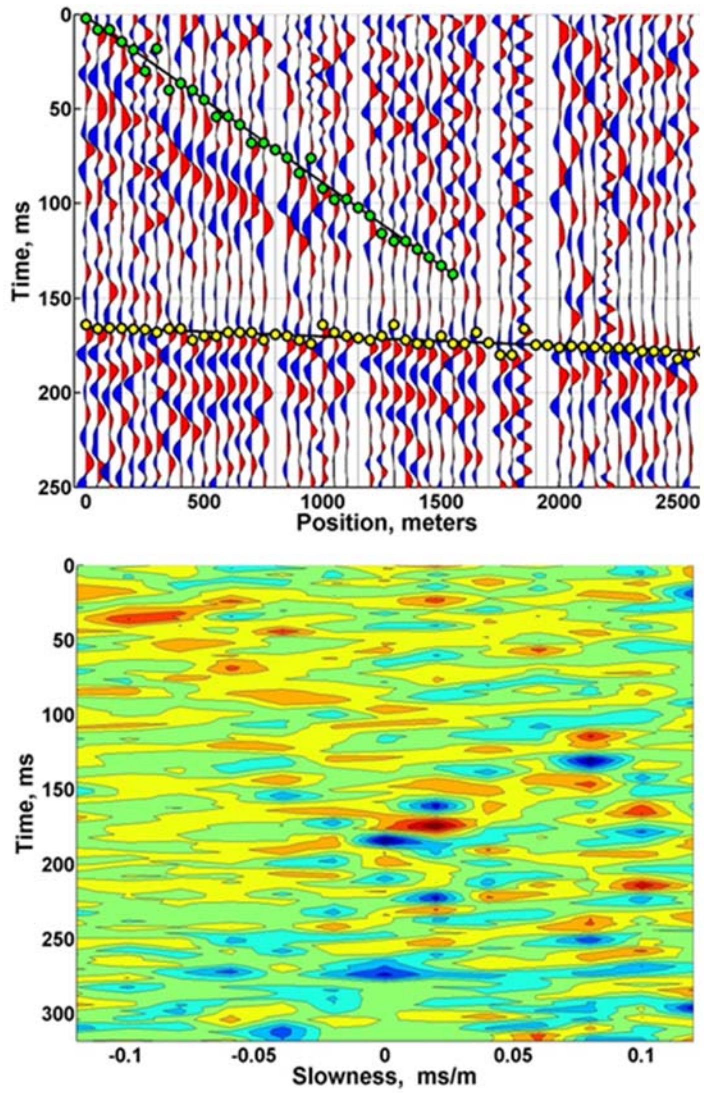

FIG. 1. (a) First-break picks for two linear events on the far-offset seismograms from a common source gather. (b) Radon transform of the data of (a); the two strongest transform responses are tied to the two linear events.

Sequential Gaussian simulation using multi-variable Cokriging

Kiki (Hong) Xu*, Jian Sun, Brian Russell, Kristopher A.H. Innanen

ABSTRACT

Uncertainty analysis is a key element in reservoir properties prediction, and many techniques have been developed, such as simulation, which is usually performed by least square method. Least square estimation is a classic and well known approach as a best fit solver, which is equivalent to simple kriging or cokriging system in case of geostatistics filed. Inspired by the distinction of simple and ordinary system in geostatistics and benefited from the extended cokriging system, for reservoir properties prediction, we propose an approach to implement sequential simulation with multiple priori information using the extended cokriging system. As it implies, the conditional mean and variance in the posterior distribution are obtained by performing the extended cokriging system. Comparison between this approach and traditional sequential simulation using least square method are discussed in sense of semi-variogram. The advantage are further analyzed through the estimated error map, which indicates that simulation using the extended geostatistics method can produce an more an accurate map, especially dealing with the data has the dramatical changes.

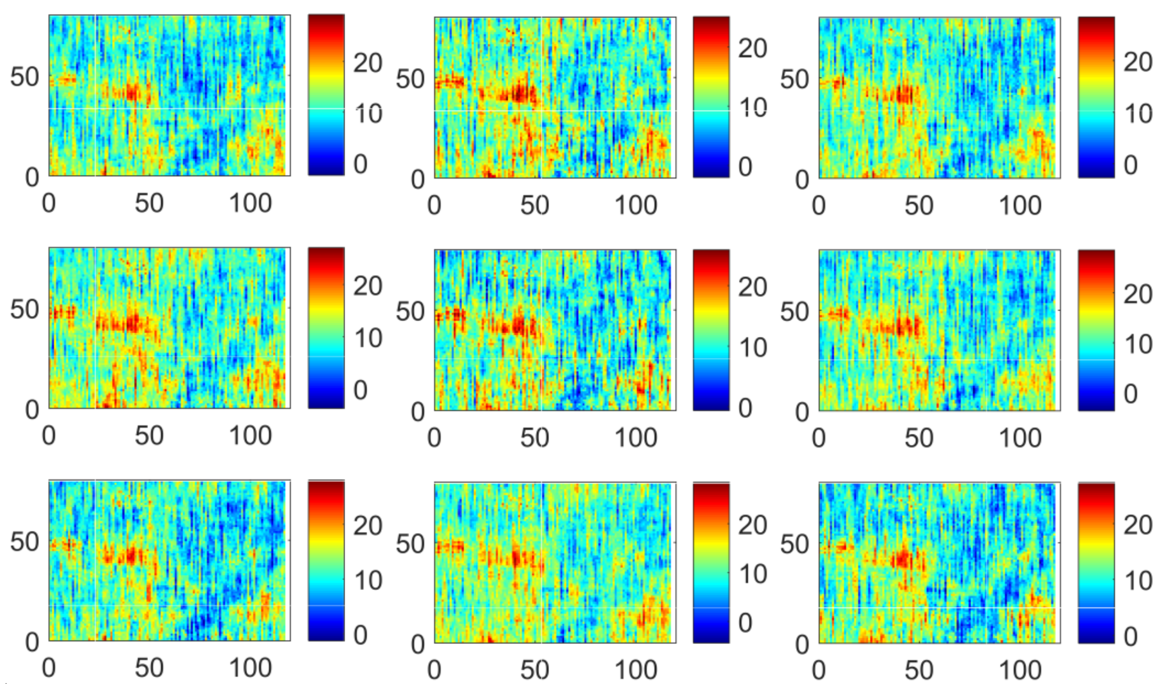

FIG. 1. All 9 of 1000 realizations using sequential conditional Gaussian simulation with extend rescaled ordinary cokriging (ROCK) system.

Elastic wave equations in modified patchy-saturated media and its numerical simulation

Huixing Zhang, Kristopher A. Innanen

ABSTRACT

Based on the modified patchy-saturated porous model, according to the method Biot used for the foundation of elastic wave equations in porous media, we established the stress-strain relations and obtained the dissipation function and kinetic energy in patchy-saturated porous media. By applying the Lagrange's equations, we derived the elastic wave equations in modified patchy-saturated media. Through changing the equations to first-order stress-velocity equations, we deduced the 3D high-order finite difference schemes and numerically solved the equations in the complex domain. Numerical results show that there are two kinds of P-waves and one S-wave in patchy-saturated media. The energy of the slow P-wave is very weak in the "solid" phase of the patchy-saturated porous media, and can hardly be seen, even though it is stronger in the fluid phase. The fast P-wave and S-wave are clear both in the solid phase and the fluid phase. The slow P-wave has a high dispersion. The velocities of the three waves are consistent with the theoretical results.

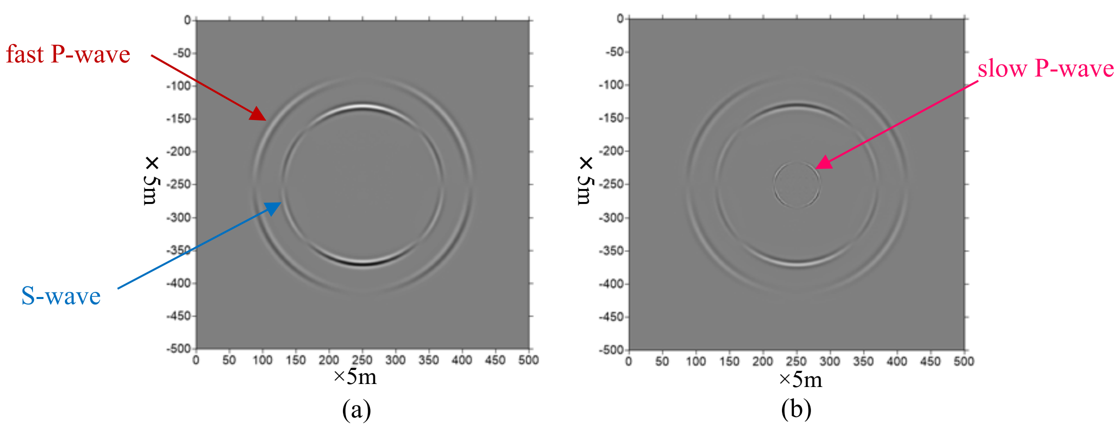

Snapshots of modified patchy-saturated porous medium (t=250ms): (a) x component in "solid" phase, (b) x component in fluid phase

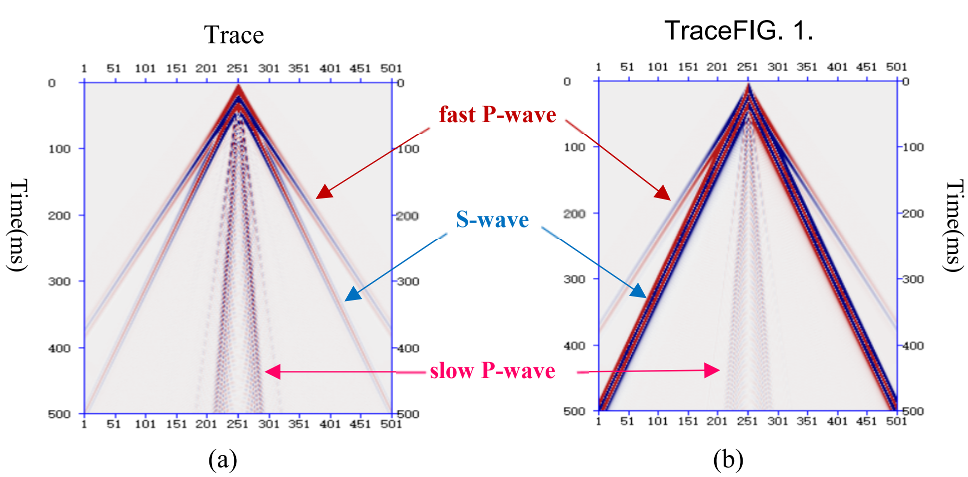

FIG. 2. Synthetic seismograms of modified patchy-saturated model: (a) x component, (b) z component

Frequency dependent attenuation and dispersion in patchy-saturated porous rocks

Huixing Zhang, Kristopher A. Innanen

ABSTRACT

From seismic wave equations in a modified patchy-saturated model established on the basis of the White model, we derive the formulas of reciprocal quality factors and velocities of the two kinds of P-waves and analyze the seismic attenuation and velocity dispersion of the two kinds of P-waves in patchy-saturated rocks within the seismic band. Through comparison of seismic attenuation in modified patchy-saturated, Biot and BISQ models, we find that seismic attenuation in modified patchy-saturated model is much higher than that in the other two models---about 1000 times higher. Therefore, a modified patchy-saturated model can describe seismic propagation more accurately in the seismic band and can be used in seismic exploration. Owing to the importance of porosity, permeability and fluid saturation, we also study and analyze the effects of the three factors on seismic attenuation and velocity dispersion of P-waves in patchy-saturated rocks within the seismic band. The conclusions are: Seismic attenuation of the fast P-wave increases with increasing frequency while attenuation of the slow P-wave decreases with increasing frequency within seismic band. As rock porosity goes up with other parameters constant, seismic attenuation and velocity dispersion of the fast P-wave increases with porosity. When the porosity is very low, velocity dispersion is not obvious within seismic band due to insufficient fluid in the pores. As for the effect of permeability to the fast P-wave, the attenuation peaks move to high frequency as rock permeability increases. Moreover, at low frequencies (below about 10Hz), attenuation at low permeability is greater than that at high permeability, and velocity dispersion is also more obvious at low frequencies than at high frequencies. When water saturation becomes high or gas saturation becomes low with other parameters constant, seismic attenuation and velocity dispersion of the fast P-wave increase within the seismic band. For the slow P-wave, attenuation increases with increasing porosity and gas saturation and decreasing rock permeability. Velocity dispersion is always apparent no matter what porosity, permeability or fluid saturation is, within seismic frequency band.

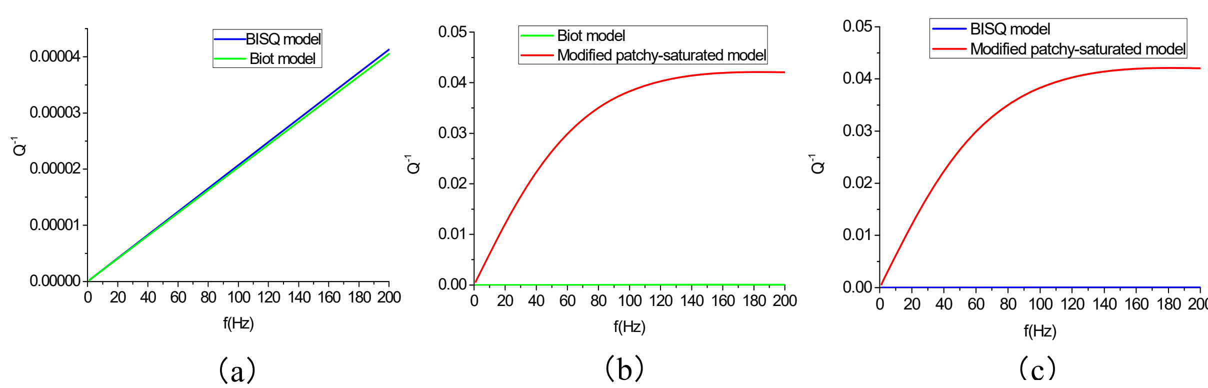

FIG. 1. Comparison of reciprocal quality factors in three models: (a) Attenuation comparison of the Biot and BISQ models. (b) Attenuation comparison of the Biot and modified patchy-saturated models. (c) Attenuation comparison of the BISQ and modified patchy-saturated models.